PLATINUM COORDINATION TO RNA

by

ERICH G. CHAPMAN

A DISSERTATION

Presented to the Department of Chemistry
and the Graduate School of the University of Oregon
in partial fulfillment of the requirements
for the degree of
Doctor of Philosophy

December 2010

"Platinum Coordination to RNA," a dissertation prepared by Erich G. Chapman in partial fulfillment of the requirements for the Doctor of Philosophy degree in the Department of Chemistry. This dissertation has been approved and accepted by:

_____

Michael M. Haley, Chair of the Examining Committee

_____

Date

Committee in Charge: Michael M. Haley, Chair
Victoria J. DeRose, Advisor
David R. Tyler
Andrew J. Berglund
Eric A. Johnson

Accepted by:

_____

Dean of the Graduate School

An Abstract of the Dissertation of

Erich G. Chapman for the degree of Doctor of Philosophy

in the Department of Chemistry to be taken December 2010

Title: PLATINUM COORDINATION TO RNA

Approved: _____
Victoria J. DeRose

Since discovery of its biological effects in the late 1960's, cisplatin (*cis*-diamminedichloroplatinum(II)) has become one of the most broadly-prescribed cancer drugs in use today. A majority of efforts to understand the metallobiochemistry of this drug have focused on describing the interactions of cisplatin-derived Pt(II) complexes with DNA. Drug binding to this "high value" cellular target is believed to trigger the apoptotic pathways that underlie cisplatin's cytotoxic effects. Although RNA is chemically similar to DNA and responsible for accurately transferring, regulating, and transforming the same genetic information that is stored within the DNA genome, surprisingly little is known about platinum(II) drug binding to RNA. Accordingly, the first three chapters of this dissertation describe efforts to address questions regarding cisplatin coordination to RNA on the molecular scale. Chapter I reviews fundamental aspects of how metal complexes interact with nucleic acids, highlighting the bioinorganic chemistry of platinum(II) antitumor drugs. This chapter also introduces the idea that drug binding to RNA may form an important part of how these complexes work in the cell. Chapter II describes cisplatin crosslinking between RNA nucleobases located on opposite sides of the internal loop of an RNA subdomain derived from the catalytic core of the spliceosome. Chapter

III describes how platinum adducts disrupt the activity of RNA processing enzymes similar to those that are necessary for maturation, maintenance and recycling of the transcriptome. Chapter III also describes the reversal of RNA platination using thiourea.

The chemistry of platinum(II) is also characterized by preferential coordination to sulfur ligands, or thiophilicity. Incorporating this property into RNA chemistry, Chapters IV and V describe the reaction of platinum(II) complexes with phosphorothioate-substituted RNAs. Chapter IV describes engineering platinum(II) crosslinks in the Hammerhead ribozyme through the targeting of a platinum(II) complex to a specific phosphorothioate substitution installed in the active site of this catalytic RNA. Chapter V outlines efforts to characterize the cleavage and isomerization reactions promoted by platinum(II) coordination to phosphorothioate-substituted RNAs. Finally, Chapter VI summarizes the insights gained throughout the course of our studies and provides an outlook on the future of platinum-RNA chemistry.

This dissertation includes co-authored material and previously published results.

CURRICULUM VITAE

NAME OF AUTHOR: Erich G. Chapman

GRADUATE AND UNDERGRADUATE SCHOOLS ATTENDED:

University of Oregon, Eugene, Oregon

University of Idaho, Moscow, Idaho

DEGREES AWARDED:

Doctor of Philosophy, Chemistry, 2010, University of Oregon

Bachelor of Science, Chemistry, 2004, University of Idaho

AREAS OF SPECIAL INTEREST:

RNA Structure, Function, and Catalysis

The RNA World

Viral RNAs

PROFESSIONAL EXPERIENCE:

Graduate Teaching Fellow, University of Oregon, Eugene, Oregon 2005-2010

Teaching Assistant, University of Idaho, Moscow, Idaho 2004

GRANTS, AWARDS AND HONORS:

Harris Lectureship, “Platinum Anticancer Drug Binding to RNA", University of Oregon, 2008

PUBLICATIONS:

Chapman, E.G.; DeRose V.J. “Site-Specific Platinum(II) Crosslinking in a Ribozyme Active Site” *submitted.*

Chapman, E.G.; Hostetter, A; Osborn, M.; Miller, A.; DeRose, V.J. “Binding of Kinetically Inert Metal Ions to RNA: The Case of Pt(II)” In *Metal Ions In Life Sciences: Structural and Catalytic Roles of Metal Ions in RNA;* Sigel, A.; Sigel, H.: Sigel, R.K.O. Eds. Royal Society of Chemistry, Cambridge, UK, **2011** *in press.*

Chapman, E.G.; DeRose, V.J. “Enzymatic Processing of Platinated RNAs” *J. Am. Chem. Soc.* **2010** *132*, 1946–1952.

Hostetter, A. A.; Chapman, E. G.; DeRose, V. J. “Rapid Cross-linking of an RNA Internal Loop by the Anticancer Drug Cisplatin” *J. Am. Chem. Soc.* **2009**, *131*, 9250-9257.

ACKNOWLEDGMENTS

Late one afternoon in the lab conference room, following a conversation about “what’s next”, Dr. Victoria DeRose turned to me with a sagacious grin and said, “I think you will have an interesting life.” I will always be grateful to Vickie, and an entire community of teachers and friends here in Eugene, for making her prediction for my future already so wonderfully true.

Foremost, I would like to express my deep gratitude to Dr. Victoria DeRose for her mentoring and friendship. Vickie has consistently challenged me by setting high expectations, only to match them with her dedicated support. I will always consider myself indebted to her for sharing her time, patience, wisdom and understanding. I hope our paths stay interwoven over many years of scientific endeavor and life adventures.

Secondly, I’d like to thank several other members of the outstanding faculty of the Chemistry Department at the University of Oregon. In the early years of my graduate career Dr. Mike Haley focused the exuberance of a young scientist and taught me about the art involved in balancing professional responsibilities with a love of the Northwest’s wild places. Dr. Andy Berglund has always encouraged my sense of scientific curiosity, teaching and sharing ideas with an ever-welcoming smile. Prof. Dave Tyler, Prof. Darren Johnson and Prof. Shih-Yuan Liu have all given me meaningful guidance and shaped the ways in which I think about chemistry. I am grateful to these exceptional people and the entire community of faculty and staff that work together to create a feeling of “home” within the Chemistry Department.

I am blessed to have a wonderful family who have unwaveringly supported my education. My Pa ends every conversation we have with the phrase “I’m proud of you,” and is my best friend and chief counsel on the workings of the world at large. My mom has forever been as devoted to my success, both as a scientist and as a person, as mother grizzly is to her cubs on the tundra. For over twenty years my stepdad Mike has taught me about tinkering with things, being “squared-away” and the value of personal integrity. Finally, my brother Ryan has stood next to me through blizzards on the tops of the highest mountains in the Cascades and will forever be my closest companion in life’s journeys.

I am lucky to have been surrounded by the world’s best friends. So many people here in Eugene have touched my life that there is no reasonable way for me to mention everyone at the beginning of this dissertation. Instead, I’d like to say “thank you” to a few who I know will read

this introduction and simply have it known that, in true Oregon fashion, I hope to thank everyone else over pints of hoppy beer. Luke Ward and I have shared many adventures in science and life that I will always happily remember. He is a wonderful friend. While I have participated in different types of missions, quests, and crusades with each one of them, Eric Abbey, Ian Moody, Charlie Swor and Zack Mensinger have been great comrades and have formed the core of an exceptional cadre of friends I've had in the Chemistry Department. I am very grateful for having had a chance to live and learn with the amazing people who have called Janet Smith Student Cooperative "home" over the past three years. I will always remember sharing the field with the Specific Heat and floating the river with Adam Unger and Dan Morris. Finally, Lenny Stewart, Hailey McAllister and Stacy Armstrong have made Alder St. one of my favorite places on Earth.

I am grateful to all of these people and wish to express my heartfelt gratitude to them for enriching my life while I've pursued the science that is written about in this dissertation.

This dissertation is dedicated to my friends in Eugene.

Thank you for sharing this place on Earth with me.

TABLE OF CONTENTS

Chapter Page

Chapter Page

Chapter Page

LIST OF FIGURES

Figure Page

Figure Page

LIST OF TABLES

LIST OF SCHEMES

Scheme Page

CHAPTER I

PLATINUM COORDINATION TO RNA

Introduction and Recognition of the Contributions of Others in This Dissertation:

This dissertation describes platinum(II) coordination to ribonucleic acid (RNA) and includes contributions from a number of individuals who have helped me explore this interesting type of chemistry. Dr. Victoria DeRose initiated this line of research while at Texas A&M University and has overseen its development since, shaping many aspects of the studies described in subsequent chapters. In addition to her ongoing scientific guidance, Dr. DeRose has provided extensive assistance in editing the following chapters for their inclusion in this dissertation. Alethia Hostetter has worked along side me for the past five years and has shared many important ideas that have influenced how our research group thinks about the biological effects of Pt(II) antitumor drugs. Studies she performed, characterizing the rate of Pt(II) coordination to various RNA and DNA constructs, are included in Chapter II. Maire Osborn, a recent addition to the DeRose group, has similarly provided us with new ideas and interesting hypotheses about how Pt(II) complexes may influence cellular function. Several of her ideas are introduced in Chapter I as part of building the case that Pt(II) coordination to RNA may be important component of the biological activity of Pt(II) antitumor drugs. Chapter IV describes Pt(II) crosslinking in the core of the Hammerhead ribozyme. Here, Luke Ward taught me about the structure of an all-RNA active site and about how RNAs folds. Chapter V, which describes a series of phosphoryl transfer reactions initiated by Pt(II) coordination to a phosphorothioate substitution, includes data from a trio of exceptional rotation students. Emma Downs, Josiah Vincek and Alex Kendall all contributed ideas and experimental data that have helped us form the mechanistic hypothesis presented within this chapter. I am grateful to these individuals and to many others who have shared in the scientific pursuits described in this dissertation and hope that I will be able to reciprocate in kind.

Parts of this chapter have been adapted from: "Binding of Kinetically Inert Metal Ions to RNA: The Case of Pt(II)" Chapman, E.G.; Hostetter, A; Osborn, M.; Miller, A.; DeRose, V.J. In *Metal Ions In Life Sciences: Structural and Catalytic Roles of Metal Ions in RNA;* Sigel, A.; Sigel, H.: Sigel, R.K.O. Eds. Royal Society of Chemistry, Cambridge, UK, **2011** *in press.*

The Antitumor Drug Cisplatin:

"I've just cured cancer!" are reportedly the words Dr. Barnett Rosenberg first exclaimed after discovering that *E. coli.* cells grown in the presence of an electric current did not divide as normal, but instead elongated to 50-60 times their normal length.[1,2] Immediately realizing the enormous therapeutic potential for whatever was causing this behaviour, researchers at Michigan State University conducted a series of careful control studies demonstrating that a soluble Pt salt produced by hydrolysis reactions occurring at the electrodes used in these experiments was responsible for these astonishing effects.[2] Follow-up studies revealed that the square-planar Pt(II) complex *cis*-$Pt(NH_3)_2Cl_2$, (cisplatin, *cis*-diamminedichloroplatinum(II), **1**) potently inhibited *E. coli* cell division.[3] The discovery of the biological activity of this molecule marked a new era in bioinorganic chemistry.[4] The ensuing development and successful clinical application of Pt(II) antitumor drugs has transformed the treatment of many cancers[5] and inspired vigorous research[6,7] into the molecular basis of how relatively simple Pt(II) complexes are able to treat a disease as notoriously complex as cancer.[8] Over 40 years of research have now been invested in developing a model in which neutral Pt(II) drug complexes accumulate[9] in a cell, subsequently becoming 'activated' by the loss of anionic ligands. The cationic Pt(II) species that result can coordinate to a variety biomolecular targets.[10] Currently, the activity of Pt(II) antitumor drugs is ascribed to their ability to form kinetically-inert adducts with adjacent purine nucleotides within regions of genomic DNA, distorting the double helical structure of the genetic code.[10-12] Sensing of these types of Pt(II) lesions by proteins responsible for ensuring the fidelity of the information stored within the genome[13] can go on to trigger programmed cell death, or apoptosis.[14,15] Because drug binding to DNA is considered to be the determining factor in initiating apoptosis many of the basic principles that govern Pt(II) coordination to DNA have been elucidated.[16] Despite RNA's chemical similarity to DNA and its critical roles in accurately transferring, regulating and transforming the very same genetic information that is contained within the DNA genome, relatively little is known about how cisplatin coordinates to RNA. This chapter reviews the fundamental chemical principles of how Pt(II) antitumor drugs coordinate to nucleic acids, using cisplatin as the primary example to illustrate how Pt(II) complexes coordinate in complex RNA architectures. This chapter also introduces the idea that this type of coordination, when occurring in the cell, may disrupt important cellular processes dependent on RNA fidelity. Combined, these topics form the basis for the studies presented in subsequent chapters.

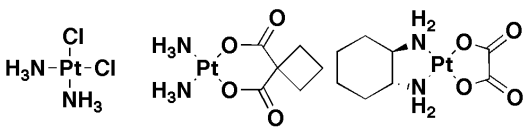

1 2 3

Figure 1.1. Structures of Pt(II) antitumor drugs: 1) Cisplatin 2) Carboplatin 3) Oxaliplatin.

Platinum(II) Coordination Chemistry:

Compared to the scaffolds of many chemotherapeutics the structure of cisplatin, an 11-atom square-planar Pt(II) metal complex, is remarkably simple. Kinetically-labile chloride ligands are arranged opposite to relatively exchange-inert ammine ligands in a *cis*- geometry around a d^8 Pt(II) center. This basic geometry is characteristic of the Pt(II) antitumor drug family (**Figure 1**). The bioactivity of these compounds is based on a series of ligand exchange reactions occurring around Pt(II). Because these types of reactions are central to the biological activity of Pt(II) complexes it is useful to review basic principles of Pt(II) coordination chemistry prior to proceeding to a discussion of the reactivity of Pt(II) antitumor drugs in the cell.

The coordination chemistry of Pt(II) is highlighted by the propensity of the metal to form kinetically-inert complexes with "soft" σ-donating ligands. This class of ligands is represented by cyanato, thiocyanato, sulfido, thiolate, thiol, and phosphine ligands as well by more intermediate σ-donors such as ammines and imines.[17] Other types of ligands are observed to form more kinetically-labile complexes with Pt(II) that undergo ligand substitution reactions through an associative mechanism, common to $16e^-$ transition metal complexes. The preference of Pt(II) to form stable complexes with strong σ-donating ligands has made the metal a classical platform for experiments demonstrating the "*trans* effect".[17,18] This effect describes the observation that certain classes of ligands strongly labilize ligands located on the opposite side of a metal center. This "effect" is actually the combination of both kinetic and thermodynamic influences on ligand substitution reactions. Strong σ-donating ligands, observed to demonstrate large *trans* effects, weaken the strength of the metal-ligand bond opposite to their position and decrease the ground state stabilization associated with ligand coordination to this site. Conversely, strong π-accepting ligands demonstrate large *trans* effects based on their ability to accept electron density from metal based d_{xz} molecular orbitals during the trigonal bipyramidal transition state that is passed through during ligand substitution. This stabilization decreases kinetic barrier involved in ligand substitution and in turn increases the rates of these types of reactions.[17,18] Combined with Pt(II)'s preference for soft ligands, the *trans* effect is characteristic of coordination chemistry of square-

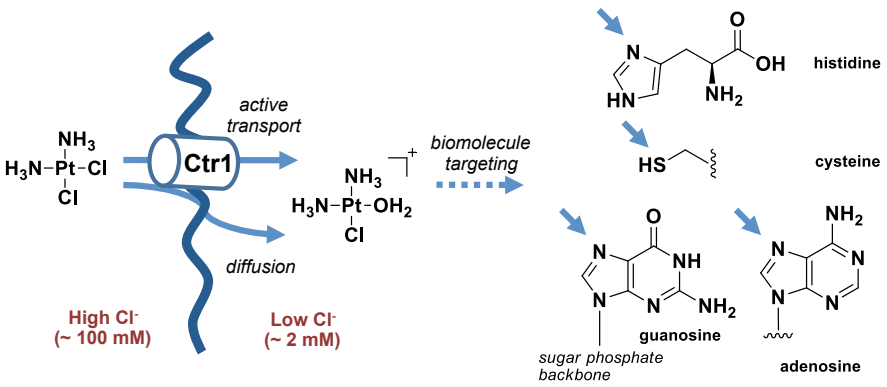

Figure 1.2. Uptake and biomolecular targets of Pt(II) antitumor drugs.

planar Pt(II) complexes and has a large effect on how these complexes work in biological settings.

Cisplatin Chemistry in the Cell:

Typically, cisplatin and other Pt(II) antitumor drugs are administered intravenously into the bloodstream where a high chloride concentration (~100 mM) is believed to prevent loss of the molecule's chloride ligands until it enters a cell either by active uptake through copper transport proteins[19] or by passive diffusion (**Figure 1.2**).[9] Once inside the cell, a lower chloride concentration (~2mM) facilitates the exchange of cisplatin's chloride ligands, giving rise to the equilibria depicted in **Scheme 1.1**.[20] Many factors, including the identity and orientation of the Pt(II) ligand set, pH and the surrounding ionic environment, influence the rates and mechanisms these reactions.[21]

Once positively charged, cationic Pt(II) complexes undergo further ligand substitution reactions to coordinate and form kinetically inert adducts with 'soft' biomolecular nucleophiles (**Figure 1.2**). Appropriate Pt(II) coordination sites are found in a variety of small molecules, protein residues and on RNA and DNA nucleobases.[10] In proteins and small molecules thiol, thioether, and imidazolic functionalities (on cysteine, methionine, and histidine residues respectively) seem to be particularly targeted. Pt(II) coordination to the small, cysteine-containing tripeptide glutathione has long been implicated in attenuating the effects of Pt(II) anticancer compounds.[22] A recent crystal structure depicting Pt(II) coordination to cysteine residues in a human copper chaperone protein[23] similarly highlights the propensity of Pt(II) compounds for coordinating to these types of ligands. The reaction of Pt(II) species with DNA and RNA is subsequently considered, however the significant body of research that has been

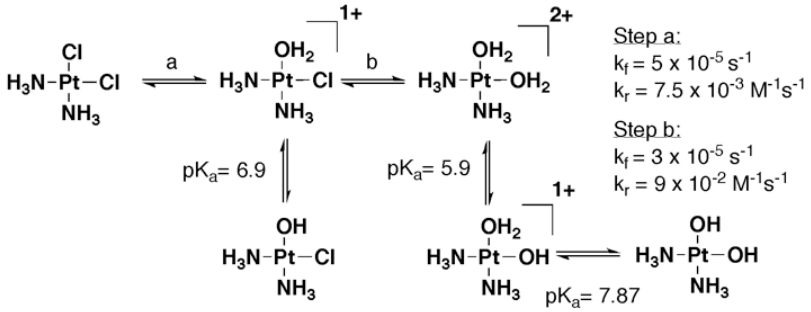

Scheme 1.1. Cisplatin equilibria in water. Kinetic and pK_a values at 25 °C taken from reference 20.

devoted to discovering new bioactive Pt(II) complexes[24] bears mention here as the majority of these efforts have focused on tuning the reactivity of Pt(II) complexes to increase their cellular and molecular level selectivity.

Cisplatin Analogues:

Despite the synthesis and screening of thousands of Pt(II) centered molecules,[25] in addition to cisplatin, only two of these have been approved by the U.S. Food and Drug administration[26] for use in chemotherapy: carboplatin (*cis*-diammine (cyclobutanedicarboxylato) platinum(II), (**2**)), and oxaliplatin (*cis*-oxalato-(trans-1)-1,2-(diaminocyclohexane)platinum(II),(**3**)) (**Figure 1.1**). The variation of Pt(II) ligands in the compounds represents two parameters that have been found to be important in determining efficacy of Pt(II) antitumor complexes. The dicarboxylate ligand of carboplatin is believed to slow hydration of the Pt(II) center[27] and tune the pharmokinetics of the drug *in vivo*. It is interesting to note that despite different *in vivo* activity, coordination of carboplatin to biomolecular targets results in the same types of $Pt(NH_3)_2$-biomolecule adducts as the parent compound cisplatin. In contrast, the chiral ammine ligand of oxaliplatin is kinetically inert and expected to remain bound to Pt(II) following coordination to a targeted biomolecule. The activity of this drug in cisplatin-resistant cell lines[28] is believed to result from the formation of DNA lesions that are differentially recognized than those formed by cisplatin.[29] Combined, the efficacy of carboplatin and oxaliplatin demonstrate that simple changes in the Pt(II) ligand set can give rise different activity profiles for Pt(II) antitumor drugs. Synthetic attempts to tune the reactivity of Pt(II) chemotherapeutics through simple changes in the primary ligand sphere have now given way to the pursuit of more advanced strategies, primarily focused on drug delivery. The conjugation of Pt(IV) prodrugs to nanoscale sized "longboats"[30] and "warheads"[31] for selective delivery into cancer cells exemplify modern efforts.

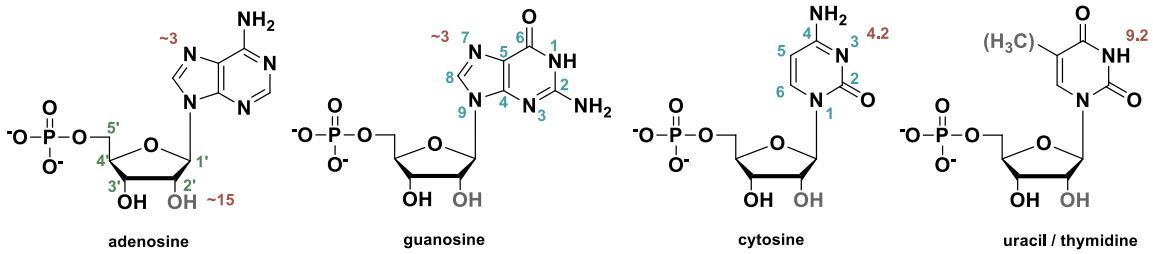

Figure 1.3 Structures of RNA and DNA nucleotides. Nucleobase numbering conventions are indicated in blue. Ribose numbering conventions are indicated in green. Approximate pK_a values of positions on the nucleobases are indicated in red. Chemical differences between RNA and DNA are highlighted in gray.

Platinum(II) Coordination to Nucleic Acids:

Pt(II) coordination to DNA to has been linked to the induction of apoptosis,[32] making an understanding of this process critical to the development of a comprehensive description of the biological activity of Pt(II) antitumor drugs. Accordingly, extensive research efforts have been directed toward describing the metallobiochemistry of Pt(II) and DNA.[33] Significantly less research has been performed describing the reactions of Pt(II) species with RNA, however the chemical similarity between the two biopolymers allows many aspects of the chemistry involved to be considered simultaneously. Here, it is useful to consider the interaction of Pt(II) complexes with DNA and RNA hierarchally, proceeding from the basic chemical structure of these biopolymers up to secondary and tertiary structural parameters that effect Pt(II) coordination to nucleic acids.

The Influence of Primary Structure on Platinum(II) Coordination to RNA and DNA:

Both DNA and RNA are polyanionic biopolymers formed by nucleotide monomers.[32] The chemical structure of these nucleic acids consists of three main components: i) a *phosphodiester backbone* forming linkages between 3' and 5' positions on ii) a *β-D-ribose-* or *2'-deoxy-ribose* rings substituted at the 1' position with a iii) *purine* or *pyrimidine nitrogenous base*.[34,35] Together these components define the primary structure of a nucleic acid. The numbering conventions used in describing the structure of these biopolymers along with the pK_a values of various functionalities are indicated in **Figure 1.3**.[36] The primary chemical difference between RNA and DNA is the presence of the hydroxyl group at the 2' position of the RNA ribose ring. While not directly involved in coordinating Pt(II), this functionality is critical to many of the biological roles of RNA.

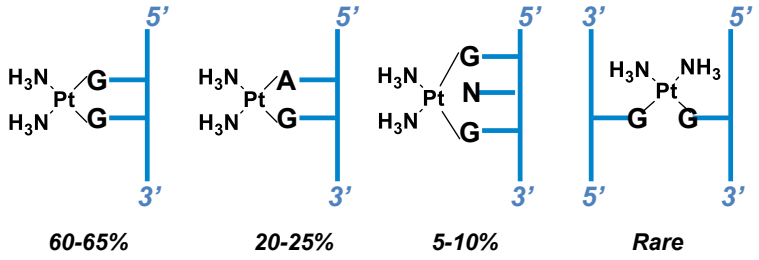

Figure 1.4. Major Pt(II)-DNA adducts. The relative abundance of these adducts occurring in DNA isolated from cisplatin treated cells is indicated below each adduct.

Because Pt(II) preferentially coordinates to 'soft' nucleophiles, only a limited subset of the positions on RNA and DNA are typically considered to be targets for Pt(II) binding. These include the N7 positions of both adenine and guanine as well as the N3 position of cytosine and N1 position of adenine.[37] Typically, Pt(II) complexes with two open coordination sites are observed to form macrochelate complexes between the N7 atoms of adjacent purine nucleotides.[38] Kinetic preference for initial, monofunctional Pt(II) coordination to the N7 of guanosine over the N7 of adenosine has recently been proposed based on the ability of a Pt(II) NH_3 ligand to form hydrogen bonds with the O6 keto oxygen of guanosine.[39] Differences in the electronics of the N7 atom of each purine base have also been proposed to help rationalize the observation that G nucleotides are included in each of Pt(II) adducts observed in DNA isolated from Pt(II)-treated cells (**Figure 1.4**).[33] As described below, the secondary and tertiary structure of DNA and RNA also play an important part in determining where Pt(II) will coordinate to these molecules.

The Influence of Secondary Structure on Platinum(II) Coordination to RNA and DNA:

Folding of RNA and DNA biopolymers is driven by a combination of hydrophobic effects and the stabilization associated with the formation of hydrogen bonds between complementary purine and pyrimide nucleobases. In DNA, folding most typically results in the formation of a double helical structure. In RNA similar helical structures are formed but are accompanied by a myriad of other motifs (**Figure 1.5**).[40] While principles that govern Pt(II) coordination to the diverse range of secondary structures adopted by RNA have not been developed, many aspects of how cisplatin coordinates to DNA double helices have been described (**Figure 1.6**).[10]

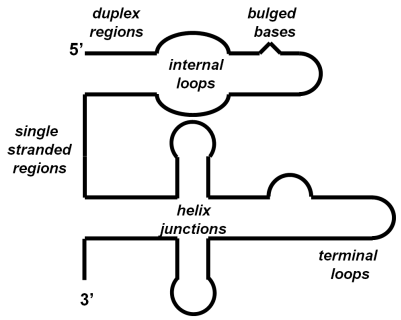

Figure 1.5. Schematic representation of RNA secondary structures.

Helix	Orientation	Bases Per Turn	Helical Turn per Base Pair (°)	Rise per Base Pair (Å)	Sugar Pucker	Groove Width (Å) Minor	Groove Width (Å) Major	Groove Depth (Å) Minor	Groove Depth (Å) Major
A-DNA	Right	11	37.2	2.9	C3'-*endo*	11.0	2.7	2.8	13.5
B-DNA	Right	10	36	3.3-3.4	C2'-*endo*	5.7	11.7	7.5	8.8
Z-DNA	Left	12	-9, -51	3.7	C3'-*endo*	2.0	8.8	13.8	3.7
A-RNA	Right	11	32.7	2.8	C3'-*endo*	10.9	3.8	3.3	12.9
A'-RNA	Right	11	30	3.0	C3'-*endo*	10.8	8.0	3.4	14.4

Table 1.1. Structural parameters of helical nucleic acids. Values from reference 35.

Differences between the major helical conformations of RNA and DNA may influence how Pt(II) coordinates to each biopolymer. As shown in **Table 1.1** the structural parameters of the A-form helix adopted by RNA are significantly different that those of the B-form structure adopted by DNA.[35] In DNA, Pt(II) coordination typically takes place to the N7 atoms of neighboring purine nucleotides. These positions are located in the wide, relatively shallow major groove of the B-form double helix. In RNA, the equivalent positions are significantly more buried in the narrow and deep major grove of the A form helices (see **Table 1.1**). As described in the following sections this structural feature may preclude the formation of the same types Pt(II) adducts observed in DNA.

The Influence of Tertiary Structure on Platinum(II) Coordination to RNA and DNA:

In cells, DNA that is not actively being transcribed or replicated is typically coiled around nucleosomes and packaged in chromatin. Few studies have addressed the platination of DNA in this structural context. Recent findings, that site-specific Pt(II) adducts installed prior to DNA winding around nucleosomes disrupt nucleosome positioning,[41,42] represent the first inroads made toward understanding platination in these situations. Accordingly, the influence of tertiary structure in determining Pt(II) adducts formed with DNA remains to be explored.

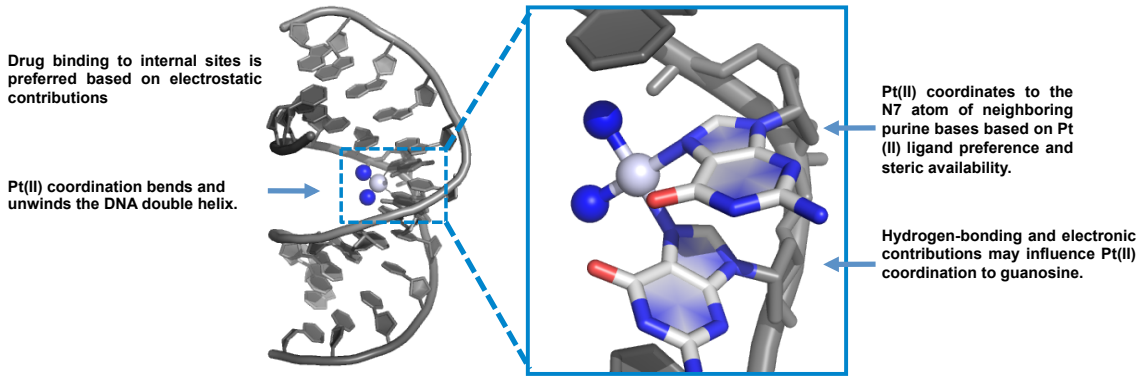

Figure 1.6. Structure of the major cisplatin adduct formed with DNA and factors affecting Pt(II) coordination to DNA. Structure generated using coordinates in reference 47.

In contrast to DNA, RNA folding results in the formation of incredibly complex molecular architectures which include specific and pre-oreganized metal binding sites[34,43,44] as well as solvent-excluded folds where nucleobase pK_a's can be significantly different from those observed in free solution.[45,46] Consequently, these structures greatly expand the chemical space in which Pt(II) complexes may find appropriate coordination geometries to form drug-biomolecule adducts. The following section describes the studies that have characterized Pt(II) coordination to RNA to date.

Examples of Platinum(II) Coordination to RNA:

A number of recent studies have described the formation of Pt(II) adducts formed with isolated RNAs (**Figure 1.7)**. These investigations have examined cases ranging from the platination of relatively short, single-stranded RNAs[48] to studies involving cisplatin coordination to intact bacterial ribosomes.[49] In accordance with the observations above, an emerging feature of this research seems to be ability of Pt(II) complexes to coordinate in non-Watson-Crick base-paired regions of RNA.

Several preliminary studies, conducted shortly after the discovery of cisplatin's antitumor properties, sought to identify Pt(II) binding sites within $tRNA^{Phe}$ by soaking the compound into pre-formed RNA crystals or by reacting Pt(II) complexes with the RNA in high ionic strength conditions similar to those used in crystallization.[50-52] In the earliest of these studies, Clark and coworkers reacted both *cis*- and transplatin with $tRNA^{Phe}$ at 4°C for 3 days in solutions containing high concentrations of Mg^{2+}, spermine and 1,6-*n*-hexane-diol.[50] Using thin-layer chromatography to characterize RNA fragments produced by nuclease digestion of platinated $tRNA^{Phe}$, the authors

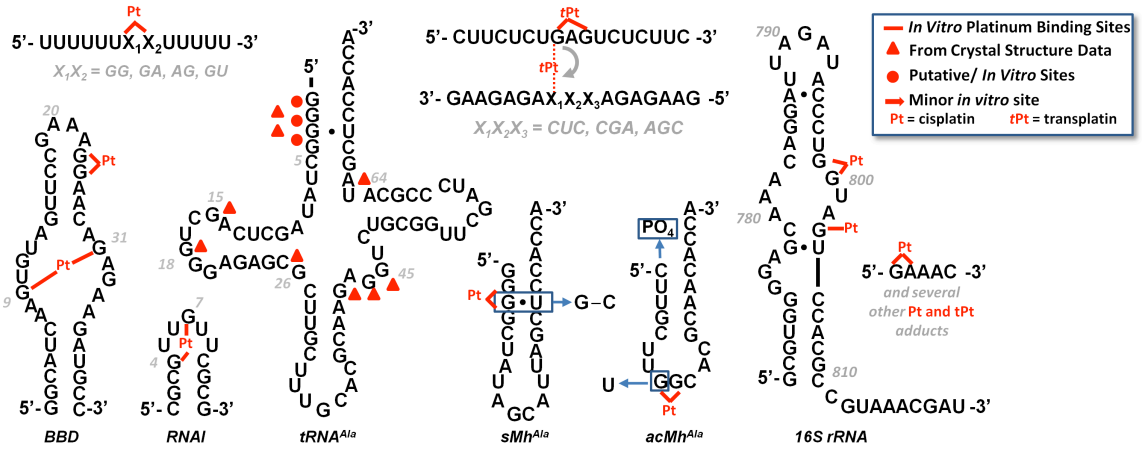

Figure 1.7. Examples of platinated RNAs. RNA structures that have been studied include the model 5'-U_5XXU_5-3' (X1/2 =A or G),[48] a purine-rich internal loop derived from the spliceosome (BBD),[53] an RNA hairpin (RNAI),[54] tRNA,[50,52-54] hairpin models for the tRNA acceptor stem (sMh^{Ala})[54,55] and anticodon loop ($acMh^{Ala}$),[55] intrastrand-to-interstrand cross-linking in RNA duplexes,[56-58] a site on the ribosomal small subunit,[49] and a small purine-rich strand.[59] Pt(II) adduct identification has relied on mapping techniques with the exception of low-resolution crystallography of tRNA mentioned in the text. While $tRNA^{Ala}$ is shown, several of the crystallographic studies mentioned in the text were performed using $tRNA^{Phe}$. The binding sites identified in these studies are indicated using triangles and are overlayed on the $tRNA^{Ala}$ sequences.

identified a major transplatin binding site within the purine-rich anticodon loop of the RNA and a second, minor Pt(II) binding site within loop III. Surprisingly, under the conditions used in this study, cisplatin was not observed to coordinate to the RNA. A second investigation carried out by soaking Pt(II) complexes into pre-formed $tRNA^{Phe}$ crystals produced somewhat different results.[51] While only relatively low-resolution $tRNA^{Phe}$ structures were obtained (5.5Å), the authors identified both transplatin adducts described previously and additional Pt(II) binding sites at G18 in the dihydrouridine loop and at A73 located in the molecule's acceptor stem. Contrasting the earlier report however, this study also identified cisplatin adducts formed at both G15 and G18 in the D arm of the tRNA. In an independent, but very similar study, Dewan later reported a 6Å Pt(II)-soaked $tRNA^{Phe}$ structure with four cisplatin binding sites.[52] The low resolution of these crystals, reportedly unavoidable due to the structural distortions caused by Pt(II) binding, prevented a detailed analysis, however electron density indicative of Pt(II) binding is apparent at

G3-G4, C25-mG26, G42-G43-A44-G45 and at A64-G65. The combined results of these three studies are overlaid on the secondary structure of $tRNA^{Ala}$ in **Figure 1.7**.

More recent biochemical studies conducted by Elmroth and co-workers have employed full length $tRNA^{Ala}$ as well as hairpin models of the molecule's anticodon loop and acceptor stem to provide several interesting insights regarding the sequence and structural specificity of Pt(II) binding to these RNAs.[54,55] By monitoring shifts in the dPAGE mobility of platinated RNAs, it was found that in the hairpin model of the $tRNA^{Ala}$ acceptor stem ($sMh^{Ala,}$ **Figure 1.7**), replacement of a native G•U wobble pair with a fully-complementary G-C base pair inhibits platinum binding to this RNA. Additionally, attachment of a 5'-terminal phosphate within the same region of the RNA alters the distributions of products observed upon platination. In the hairpin model of the $tRNA^{Ala}$ anticodon stem, substitution of a natural UG sequence in the terminal loop for a GG sequence increases the rate of platination observed for this RNA and suggests that, similar to what is observed in DNA, Pt(II) complexes target neighboring purine sequences in RNA. Combined, these results highlight the influence of sequence and local structure in determining *in vitro* Pt(II) interactions with RNA.

Because non-Watson-Crick base-paired regions of RNA form the core of many functional RNAs, understanding how Pt(II) complexes coordinate to these structures is important in determining how Pt(II) antitumor drugs may affect RNA processes. The spliceosome is an incredibly complex RNA-protein machine responsible for removing intronic sequences from pre-mRNAs. The catalytic core of the spliceosome is proposed to be comprised of the U2-U6 snRNA complex.[60] In efforts to understand how cisplatin coordinates to structured regions of RNA, our lab has recently characterized how the drug binds to a 41nt RNA subdomain of the U2-U6 complex, termed 'BBD' for 'branch-bulge domain' (Chapter II).[53] BBD RNA consists of a hairpin structure in which base-paired regions flank a purine-rich, asymmetric internal loop (**Figure 1.7**). Reaction of this RNA with an aquated form of cisplatin results in the formation of a novel, Pt(II)-induced intramolecular crosslink. While the structure of this RNA is currently unknown, the nucleotides involved in forming this crosslink have been proposed as metal ion binding sites in the full U2-U6 snRNA complex.[61,62] In light of this information, it is thought-provoking to speculate that cisplatin may compete with native metal ion binding sites in RNA. This type of mimicry would be particularly interesting as metal ions often mediate important tertiary contacts between interacting RNA domains[63] where crosslinking could potentially disrupt the dynamic function of these structures.

In another recent example of cisplatin coordination to a complex RNA structure, Rijal and Chow have reported how Pt(II) complexes may be used as a chemical probes for identifying

solvent-exposed purine nucleotides in intact bacterial ribosomes.[49] Stable platinum adducts resulting from both *in vivo* and *in vitro* platination were identified in helix 24 of *E. coli* ribosomes using primer extension to detect Pt(II)-dependent halts in reverse transcription. Using this method, it was found that several G nucleotides located in non-Watson-Crick base-paired regions of the RNA were targeted by cisplatin. Pt(II) coordination to these nucleotides provides another example of platination occurring within regions of complex RNA structure, notably even in the presence of competing GG sequences in nearby helical regions of the same RNA.

RNA Crosslinking by Transplatin and Platinum(II)-Drug Conjugates

The nucleic acid coordination properties of Pt(II) complexes have inspired research seeking to use these types of compounds as sequence-specific RNA crosslinking reagents and as scaffolds upon which to construct new RNA-targeting drug conjugates.

In studies aimed at determining how transplatin adducts distort nucleic acid structure it was discovered that pre-formed 1,3 G*pNpG* transplatin adducts (where "*" denotes a platinated nucleotide) in DNA readily rearrange into intermolecular crosslinks when annealed to complementary oligonucleotides.[56-58] Subsequent mechanistic studies have shown that isomerization reactions between 1,3 G*pNpG* transplatin adducts and complementary oligonucleotides are sequence-specific,[64] can result in unusual G-N7* to C-N3* crosslinks,[57] and are also observed using 2'-OMe[65] and other chemically modified RNAs. Further work has shown that transplatin- modified 2'-OMe RNAs[66] and cisplatin-modified RNAs[67,68] can be used as anti-sense oligos for attenuating gene expression in cell lysates and in living cells.

Work in advancing RNA as a drug target[69] has prompted synthesis of a pair of Pt(II)-drug conjugates. Tethering neomycin B and guanidinoneomycin B to a square planar Pt(II) complex, Tor and coworkers[70] have shown that Pt(II)-drug conjugates can demonstrate substantial selectivity in targeting RNA over DNA as well as can form intramolecular crosslinks in RNA. Similarly, a Pt(II)-estradiol conjugate has also recently been shown to coordinate to tRNA.[71]

Platinum(II) Coordination to RNA on the Molecular Scale:

The preceding sections describe how Pt(II) complexes coordinate to RNA on the molecular scale. Cumulatively, the largest differences displayed in how Pt(II) species coordinate to RNA versus DNA seems to be that platination is favored in non-helical regions of RNA, perhaps due to the steric inaccessibility of purine N7 targets within A-form helices. As Pt(II) coordination to increasingly complex structures is explored it seems likely that drug binding to non-Watson-Crick base-paired regions of RNA structure will emerge as a theme in these studies. Because such

regions are critical in forming RNA-RNA and RNA-protein contacts, drug binding within these regions could be envisioned to disrupt the function of important cellular machines. The following sections describe the limited number of reports that have examined this type of disruption. Combined, these studies portray the potential of Pt(II) treatment to interfere in almost every stage in the lifecycle of cellular RNAs.

Platination of RNA in the Cell:

An important aspect in determining how Pt(II) targeting of RNA may factor into the biological activity of Pt(II) antitumor drugs is the extent to which RNA is platinated *in vivo*. Surprisingly, while many aspects of the biology of Pt(II) antitumor compounds have been extensively characterized, only a limited number of studies have quantified drug binding to RNA and DNA simultaneously.

In the earliest of these studies Pascoe and Roberts quantified Pt(II) binding in HeLa cells following treatment with 5-400 uM cisplatin.[72] After fractionation of DNA, RNA and protein components by phenol chloroform extractions and selective precipitations, the authors quantified the amount of Pt(II) bound to each type of macromolecule using atomic absorption spectroscopy. Interestingly, the results of these experiments show that when considered on a Pt(II) per gram biomolecule basis, significantly more Pt(II) is bound to RNA than DNA. These authors also pursued similar experiments with the less bioactive transplatin isomer and show that despite higher levels of cellular accumulation and more extensive binding to RNA, DNA and protein fractions, the *trans* complex is significantly less cytotoxic.

A more recent study, which similarly assessed levels of Pt(II) coordination to different types of biomolecules in HeLa cells, measured the extent of incorporation of metastable ^{195m}Pt(II) complexes into the DNA, RNA and protein components in drug-treated cells.[73] In these experiments ^{195m}Pt(II) was found to accumulate to a large extent in protein fractions, and while RNA and DNA are both significantly less platinated, they are found bind Pt(II) in an approximately equal ratio. Interestingly, this ratio changes over time with drug binding to DNA leveling off by 4 hr following drug treatment while cellular RNAs continue to accumulate Pt(II).

Combined these studies raise important questions about which types of cellular RNAs are targeted by Pt(II) antitumor drugs and whether additional factors such as cellular localization or cellular lifecycle may effect these distributions.

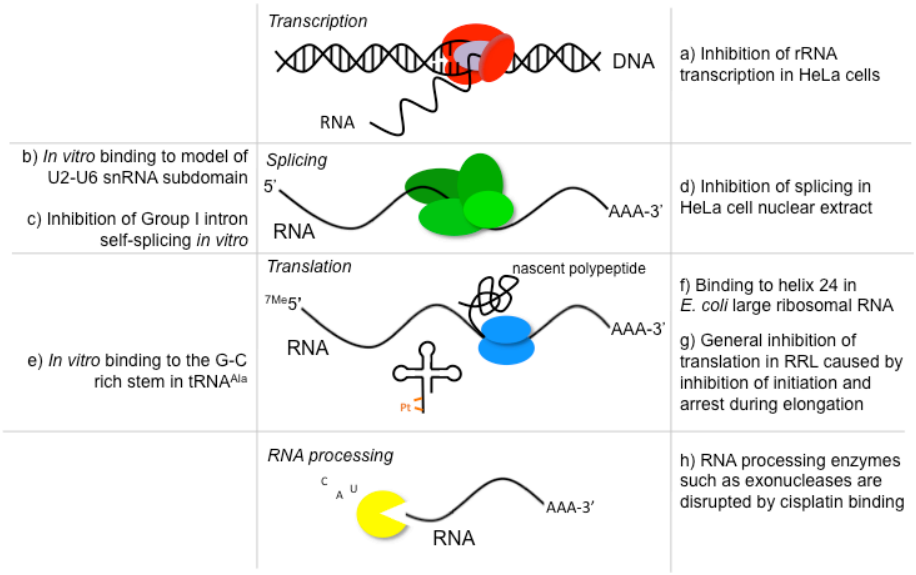

Figure 1.8. RNA processes inhibited by Pt(II) compounds as determined from studies in cells, cell extracts, and *in vitro*. References: a) 74, 76-78 b) 53 c) 81 d) 80 e) 54,55 f) 49 g) 79, 82-83 h) 48. Figure created by Maire Osborn.

Platinum(II) Antitumor Drugs Influence Transcription, Translation, and Splicing:

In addition to RNA's role in ferrying genetic information, RNA and RNP machines catalyze many critical reactions within the cell. It is interesting to imagine how structural damage inflicted by Pt(II) drug binding might affect the function of these intricate machines. Indeed, several reports have shown that platination can interfere with critical points in the lifecycles of cellular RNAs. These studies are, by necessity, carried out in chemically complex systems where it is challenging to ascribe a loss in function to a specific instance of drug binding, however the effects that have been described motivate detailed examination in future studies.

The earliest point at which platination has been observed to interfere with the function of RNA is during its synthesis. Several high resolution studies have shown that a single and specific Pt(II) adduct synthetically installed on a plasmid template blocks RNA synthesis by RNA polymerases *in vitro*,[74] in cellular extracts,[75] and recently in living cells.[76] The structural basis behind this disruption was recently reported showing that a platinated DNA template is unable to gain access into the active site of RNA polymerase II.[77] On the cellular level, platination has been shown to interefere preferentially with rRNA synthesis in HeLa cells accompanied by a redistribution of transcriptional machinery.[78,79]

Following its synthesis, the majority of RNA in a cell is processed in some way before being used. One critical component of RNA processing involves the removal of non-coding, intronic sequences from pre-mRNAs by the spliceosome. Platination has been observed to interfere with this process in HeLa cell nuclear extracts by disrupting the assembly of spliceosomal intermediates.[80] The impact of platinating RNA components of the splicing machineries is further suggested by similar results showing the disruption of self-splicing by the *Tetrahymena* Group I Intron which takes place in the absence of protein cofactors.[81] Interestingly, this study suggests that RNA crosslinking is responsible for the loss of activity.

The ribosome relies upon the concerted function of mRNA, rRNA, and tRNA. Platination of any of these types of RNA could foreseeably act as a wrench thrown into the cogs this cellular factory. Accordingly, *in cellulo* studies using rabbit reticulocyte lysate have demonstrated that platination of either pre-mRNA or rRNA components interferes with translation.[82,83] Subsequent studies have suggested that this disruption is a combination of cisplatin's ability to disrupt both initiation and elongation.[78,82,83] Recent studies in both yeast and *E. coli.* demonstrating the formation of specific Pt(II) adducts on the ribosomes of Pt(II) treated cells complement these findings.[49] It still remains very challenging however to assess if single Pt(II) adducts affect the function of a 2.5 MDa machine.

Platinum(II) Coordination to RNA Disrupts RNA Processing:

RNA is processed in a number of ways throughout its cellular lifetime. Exonucleases work both to mature mRNA's as well as dispose of them once they are no longer needed by the cell. Endonucleases cut at specific points within an RNA and act in a number of critical regulatory pathways including RNA interference pathways, and have recently been discovered to cleave tRNA in response to cellular stress. As Chapter III describes, each of these types of RNA-processing enzymes are disrupted by platination of a substrate RNA.

Determining the Effects of Platinating Cellular RNAs- A Daunting Task:

A cell is a complicated place. Cisplatin's selectivity is largely based on relatively simple coordination chemistry, making soft nucleophilic sites on proteins, DNA and RNA all viable targets for Pt(II) antitumor drugs. Determining how drug targeting of only one of these types of molecules effects cellular function is a challenging task. Adding to this complexity, both proteins and RNA are critical components of many pathways that are monitored by the cell to ensure its own health. Pt(II)-interference with one of these processes could influence secondary signaling pathways, magnifying the effects of platinating just a single target. A growing appreciation of the

complex roles played by RNA in post-transcriptional gene regulation motivates future studies aimed at determining how platination may influence these processes. These investigations may simultaneously provide useful insight into many fundamental questions such as how the cell handles general RNA damage or how RNA regulatory pathways are used to respond to cellular distress.

Summary and Bridge to Chapter II:

Chapter I provides a summary of the coordination chemistry of Pt(II) antitumor drugs as well as a survey of the limited number of studies that have suggested that platination of RNA may disrupt important processes within the cell. In line with this, Chapter II describes how cisplatin coordinates to a 41-nucleotide RNA subdomain derived from the spliceosome. These studies show rapid targeting of RNA by cisplatin and the formation of intramolecular, Pt(II)-induced crosslinks spanning an RNA internal loop.

CHAPTER II

RAPID CROSSLINKING OF AN RNA INTERNAL LOOP BY THE ANTICANCER DRUG CISPLATIN

Introduction:

This chapter includes contributions from Alethia A. Hostetter and Prof. Dr. Victoria J. DeRose. Alethia Hostetter characterized RNA and DNA platination kinetics, isolated the RNA used in mass spectrometry experiments and co-wrote the corresponding manuscript. I identified the locations of platinum crosslinks in BBD and the SBBD construct, performed mass spectrometry experiments and also co-wrote the resulting manuscript. Prof. Victoria DeRose conceived the original focus of this research, guided experimentation, as well as edited and shaped the resulting article. The RNA subdomain used in this work was originally characterized by Sarah Tate and Dr. Janell E. Schaak as part of studies aimed at understanding the role of metal ions in RNA splicing. This chapter includes work published in the *Journal of the American Chemical Society* (**2009**, *131*, 9250-9257, © 2009 American Chemical Society).

Cisplatin Coordination to RNA:

Cisplatin (*cis*-diamminedichloroplatinum(II)) is the flagship compound for a series of platinum(II) anti-tumor agents employed in the treatment of a wide range of cancers.[1-3] Cisplatin activity involves intracellular exchange of the labile chloride ligands and ultimate coordination to "soft" biomolecular donor sites. *In vivo*, cisplatin is known to bind to multiple targets including DNA, RNA, proteins, and small-molecule ligands. Drug binding to adjacent purines on genomic DNA has been linked to the induction of apoptosis, a foundation of antitumor activity. Despite their prevalent use, a comprehensive understanding of additional drug-related biological processes is still forming for the platinum antitumor compounds.

Early studies that are often cited in identifying DNA as a target for cisplatin reveal that, on a per nucleotide basis, drug binding to DNA and RNA is roughly equivalent.[4,5] Additional studies have shown that platinum drug treatment is capable of interfering with transcription,[6-8] and that critical RNA-dependent activities such as splicing[9] and translation[5,10,11] are inhibited when measured in cell extracts. Combined, these studies suggest that the binding of cisplatin-derived species to RNA may contribute to the drug's *in vivo* effects. A limited number of studies have revealed further details concerning the interactions of cisplatin with RNA. Elmroth, Chow, and coworkers have previously communicated enhanced reactivity and more pronounced dependence of reaction rate on ionic conditions for the reaction of a 13nt RNA hairpin in comparison with a DNA analog.[12] Elmroth and coworkers have additionally suggested binding locations for cisplatin near the G•U wobble pair in a $tRNA^{Ala}$ acceptor stem,[13,14] and have explored platinum-RNA adducts for directing RNA silencing.[15] Cisplatin has been shown by Danenberg and coworkers to inhibit *in vitro* activity of a Group I intron ribozyme.[16] Very recently, Rijal and Chow have reported cisplatin as a structural probe to identify accessible purine nucleobases in bacterial ribosomes.[17] These studies suggest intriguingly selective cisplatin-RNA reactivity, and call for more detailed kinetic analyses and comprehensive characterization of the nature of the platinated products in complex RNAs.

A common characteristic of naturally-occurring metal sites in RNA is the involvement of ligands that are distant in primary sequence but brought into proximity in the folded RNA structure.[18-20] By crosslinking two such ligands, cisplatin-induced chelation, whether in naturally occurring metal sites or novel target sites, has the potential to inhibit activities that depend on the dynamic nature of RNA. The spliceosome is an example of an RNA machine that is dependent on dynamic rearrangements for function.[21,22] One key step in spliceosomal function is the formation of a complex between the U2 and U6 snRNAs that is implicated in the first step of pre-mRNA splicing.[23] This chapter provides an *in vitro* analysis of the reaction between aquated cisplatin and a 41 nt RNA construct termed BBD (*b*ranch-*b*ulge-*d*omain) that contains the purine-rich internal loop formed from U2 and U6 snRNA strands (**Figure 2.1**).[24] It shows that platinum forms a novel intrastrand cross-link across the internal loop of BBD and an interstrand cross-link in an analogous two-piece construct. Additionally, this chapter describes that, under biologically pertinent ionic conditions, platination of both BBD and a related 40 nt RNA hairpin is ~5-fold faster than for a DNA hairpin analogue. MALDI-MS data are presented that complement the conclusions from corresponding biochemical studies. Taken together, these results indicate facile cisplatin-induced adduct formation across an RNA internal loop and fast platination kinetics of RNA oligonucleotides.

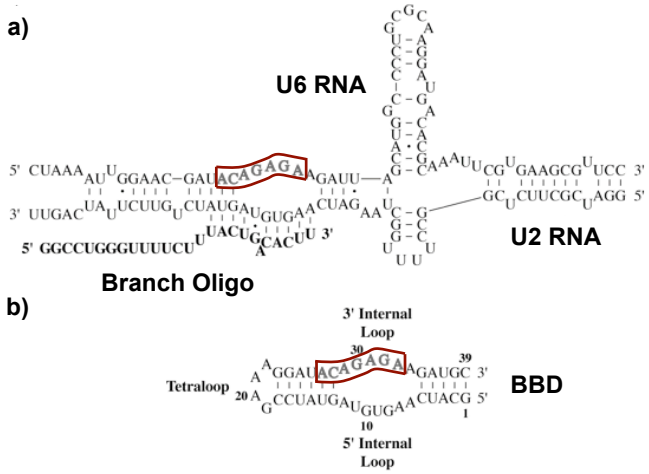

Figure 2.1. Derivation of the BBD RNA Sequence. a) Proposed secondary structure of the human U2:U6 snRNA core complex indicating the branch oligonucleotide.[18] Conserved nucleotides are outlined in maroon. b) Predicted secondary structure of the BBD RNA subdomain used in this study, with invariant nucleotides again highlighted by maroon outline.

Evidence of Platinum(II)-Induced RNA Crosslinking:

RNA and DNA oligonucleotides used in this study are shown in **Figure 2.2a**. The BBD RNA subdomain contains a purine-rich internal loop flanked by helical regions, whereas the RNA and DNA hairpin sequences (RNA HP and DNA HP) are fully base-paired. In previous studies, reaction of RNA or DNA with cisplatin has resulted in product species that are typically observed to migrate more slowly when analyzed by denaturing polyacrylamide gel electrophoresis (dPAGE).[25,26] Slower migration of platinated oligonucleotides is likely due to added molecular weight and a decrease in the overall charge of the nucleic acid through binding of a $[Pt(NH_3)_2]^{2+}$ fragment. By contrast, cisplatin reaction with BBD results in a product species with higher mobility (**Figure 2.2b**). Faster mobility under denaturing conditions may be caused by intrastrand crosslinking,[27,28] which was hypothesized to occur across the purine-rich internal loop region of the BBD RNA. In order to test this hypothesis, the BBD internal loop sequence was embedded between two new duplex sequences, creating a two-piece "split" BBD construct (SBBDs, **Figure 2.2a**). Platination of SBBD results in crosslinking of the two strands, as observed unambiguously by dPAGE (**Figure 2.2c**). Platination of the individual upper or lower SBBD strands does not result in a crosslinked species, although the presence of secondary platination sites is indicated by the dispersion of the dPAGE product bands (**Figure 2.2c**). These data indicate that cisplatin creates a crosslink across the internal loop of BBD RNA.

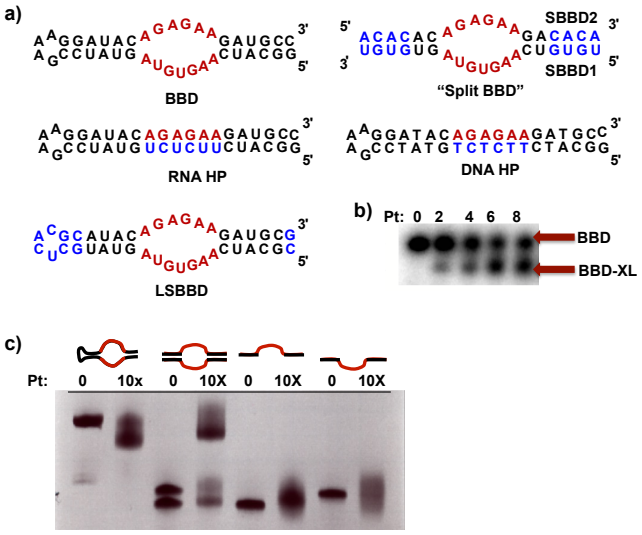

Figure 2.2. Crosslinking across the BBD internal loop. (a) Oligonucleotide sequences and predicted secondary structures. The BBD internal loop is highlighted in red. Differences in sequence relative to BBD are shown in blue. (b) Formation of a higher-mobility BBD product upon platination of BBD. (c) Confirmation of cisplatin-induced crosslinking in BBD internal loop sequence, showing products of platinum treatment with (i) BBD, (ii) SBBD, (iii) single strands of SBBD. Conditions: (b) 0.2 μM 5'^{32}P-labeled BBD treated with indicated concentrations of cisplatin for 1.5hr in deionized water, analyzed by 18% denaturing PAGE, and visualized by autoradiograph; (c) 20 μM (0.2 nmol) RNA reacted with 10x cisplatin in 5 mM TEA (pH 7.8), 12-15 hrs, 37 °C, analyzed by 20% denaturing PAGE, and visualized by staining with methylene blue.

Identification of Crosslinked Nucleobases:

In order to identify the specific bases involved in formation of an intrastrand crosslink, the proposed crosslinked product (BBD-XL) was isolated following dPAGE and mapped by partial alkali hydrolysis. Using 5' end-labeled RNA, normal hydrolysis products are expected to be observable up to the 5' side of the crosslinked site.[28-30] Hydrolysis products that contain the crosslinked site will result in significantly higher molecular weight species with unusual gel mobilities, leaving a gap in the hydrolysis ladder following the 5' crosslinked site.[28-30] As displayed in **Figure 2.3**, clear BBD-XL hydrolysis products are observed for nucleotides 3' to A_8, but not at G9, identifying G_9 as the major 5' site involved in the internal crosslink. An additional faint band at U_{10} suggests G_{11} as a minor secondary site for platinum-induced crosslinking. In the

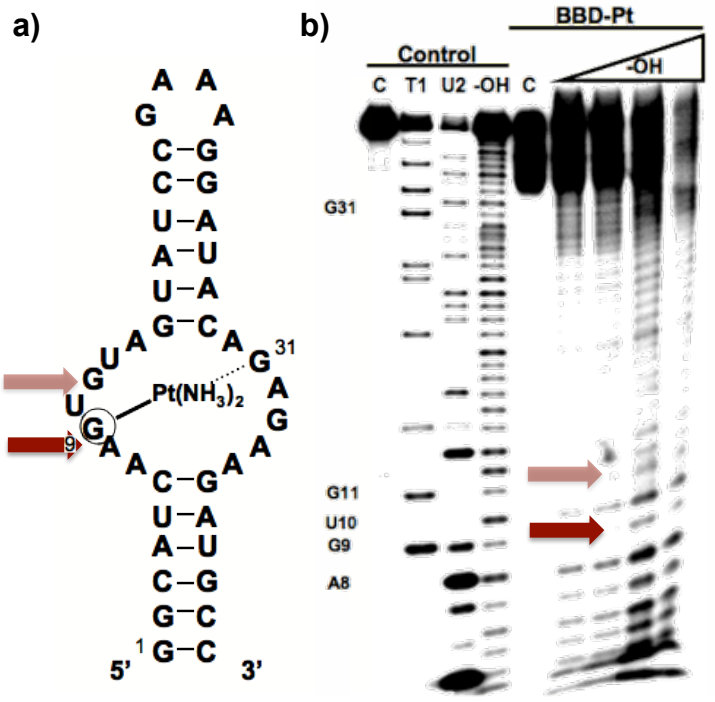

Figure 2.3. Location of platinum crosslinks formed in BBD RNA. (a) The secondary structure of BBD representing the location of the cisplatin-induced crosslink found in BBD-XL. (b) Cleavage products produced by the alkali hydrolysis of isolated BBD-XL. Lanes from left to right. Control lanes (untreated BBD) C: Control 5'-end-labeled untreated BBD. T1: G-specific sequence ladder generated by partial nuclease digestion by RNase T1. U2: A-specific sequence ladder generated by partial nuclease digestion by U2 RNAse. OH^-: Reference alkali hydrolysis ladder. BBD-XL lanes C: dPAGE-isolated BBD-XL. OH^- Lanes: dPAGE-isolated BBD-Pt treated under alkali hydrolysis conditions for increasing amounts of time (see Materials and Method in Appendix A). Arrows indicate major (bold arrow, G9) and minor (faded arrow, G11) sites of platinum coordination.

crosslinked species generated using the two-piece SBBD complex, the site equivalent to G_9 was again identified as one major adduct site (**Figure A.1, Appendix A**). Using this SBBD construct, hydrolysis mapping also identified the site corresponding to G_{31} as the crosslinking partner on the other side of the internal loop (**Figure A.2, Appendix A**). The identification from dPAGE-isolated products of the intrastrand crosslink in BBD and the analogous interstrand crosslink in the SBBD duplex strongly suggests that internal loop crosslinking is a major structural determinant for altered gel mobility upon platinum coordination to BBD.

Cisplatin-RNA Reaction Rates:

The *in vivo* relevance of cisplatin-RNA reactions, including the internal loop crosslinking reaction observed here, depends in part on their rates relative to adduct formation with DNA or other cellular targets. In evaluating the reaction rates of cisplatin with the oligonucleotides of **Figure 2.2a**, kinetic studies were performed at 37 ^{0}C and in a background of 0.1 M $NaNO_3$/1 mM $Mg(NO_3)_2$ in order to approximate cation competition *in vivo*. Nitrate salts were used instead of chloride salts to prevent bias of the observed reaction rates due to an increase in the cisplatin anation rate.[31] Because the aquation of cisplatin has been shown to be the rate-limiting step for reactions with oligonucleotides under similar conditions, cisplatin was aquated by reaction with $AgNO_3$ immediately before use.[32] RNA concentrations of 0.1 μM and platinum concentrations of at least 125-fold excess were used to ensure pseudo-first order conditions for the reaction (**Figure A.4, Appendix A**). Reaction products were analyzed following separation by dPAGE and autoradiography. Under these conditions, all data fit well to a single exponential function, indicating that a single rate-limiting step dominates the kinetics of product appearance in each case.

In addition to monitoring internal crosslink formation in BBD, reactions of cisplatin with two related hairpin structures were monitored. RNA HP and DNA HP (**Figure 2.2a**) retain the flanking helical and terminal loop sequences of BBD, but replace the internal bulge region with a fully base-paired sequence. These hairpin constructs provide control sequences having similar base composition, length, and terminal loops to those of BBD. Reaction of aquated cisplatin with both HP constructs results in products that migrate more slowly, in contrast to the faster-migrating crosslinked species produced with BBD (**Figure 2.4a**). As observed from **Figures 2.4a** and **2.4b**, both RNA sequences (BBD and RNA HP) react at similar rates of k_{obs} = 9.8(1.0) × 10^{-5} and 8.3(2) × 10^{-5} s^{-1} respectively in 50 μM CP, pH 7.8 (**Table A.1, Appendix A**). Product formation for the DNA construct is 5-6 fold slower, with an observed rate constant of 1.7(2) ×10^{-5} s^{-1} under identical conditions. The calculated second-order rate constants are k_{rxn2} = 2.0(2), 1.7(3), and 0.33(3) $M^{-1}s^{-1}$ for BBD, RNA HP, and DNA HP respectively. Reaction rates were also investigated, under identical buffer conditions, for the two-stranded SBBD hybrid substrate for which product formation results in a clearly-separated crosslinked species (**Figure 2.2c** and **A.3, Appendix A**). For SBBD, a pseudo first-order rate constant of k_{obs}= 5.2(3) × 10^{-5} s^{-1} and a calculated second-order rate constant of k_{rxn2}= 1.1(1) M^{-1} s^{-1} were obtained in 50 μM aquated cisplatin (**Figure A.3** and **Table A.1, Appendix A**). These values are approximately 50% of those determined for BBD, but still reflect faster reaction rates than observed for the DNA HP. A likely explanation for the slower reaction rate observed for intermolecular crosslinking of the

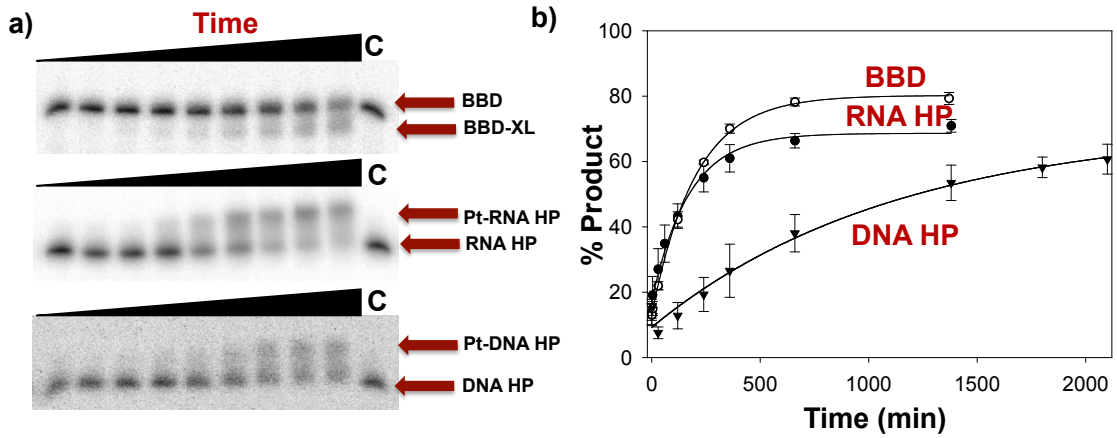

Figure 2.4. Platination kinetics. (a) Time-dependent product band appearance following treatment of radiolabeled RNA and DNA substrates with cisplatin and analysis by dPAGE. Oligonucleotide sequences are shown in Figure 2.2a. (b) Comparison of the reaction rates of cisplatin with BBD (open circles), RNA HP (filled circles), and DNA HP (triangles). Data are fit to a pseudo first-order rate expression as described in Materials and Methods, Appendix A. Conditions in (a): 0.1 μM oligonucleotide, 50 μM cisplatin, 100 mM $NaNO_3$, 1 mM $Mg(NO_3)_2$, and 5 mM TEA (pH 7.8) at 37 °C.

two-piece RNA SBBD construct in comparison with intramolecular crosslinking in BBD is the incomplete hybridization of the SBBD strands under these reaction conditions (see **Materials and Methods, Appendix A**). Nonetheless, the fact that similar values are observed for crosslinking in both BBD and the two-piece SBBD suggests that similar rate-limiting steps guide the internal loop crosslinking reaction regardless of RNA construct.

The reactions of aquated cisplatin with BBD and SBBD are pH-dependent, increasing in rate as the pH is lowered. At pH 6.8, second-order rate constants of 8.5(7) and 6.8(2) M^{-1} s^{-1} are measured for BBD and SBBD, respectively (**Table A.1, Appendix A**, data not shown). Based on known protonation equilibria for aquated cisplatin species, this rate enhancement likely reflects protonation of a cisplatin hydroxide ligand to aqua ligand on platinum(II), and is a closer approximation to rates that might be expected for *in vivo* conditions.

Analysis of Platinated RNAs by MALDI-MS:

As described above, platination of the RNA and DNA domains used in this study results in products that have distinctly altered mobilities when analyzed by dPAGE. To further analyze these products, MALDI-MS was used to identify platinum-oligonucleotide species[33] in samples isolated from the dPAGE gels. MALDI-MS data for the RNA and DNA HP sequences reacted for

5 hr at a ratio of 5:1 platinum:oligonucleotide are shown in Figure 5a. Products containing $[Pt(NH_3)_2]^{2+}$ adducts appear at the oligonucleotide mass plus increments of 229 amu. Additional lower-intensity peaks are often present at ~+17, +23 and +39 amu that are ascribed to residual $H_2O/OH/NH_4^+$, Na^+, and K^+, respectively. These features appear in untreated RNA as well as platinated RNA and their presence along with the breadth of the features preclude identification of $[Pt(NH_3)_2X]$ ($X=H_2O$, OH^-, or Cl^-) species. Although MALDI MS is not precisely quantitative, comparison of relative intensities within identically treated samples provides qualitative information on relative populations of the major RNA-platinum adducts. The data in **Figure 2.5** show that RNA and DNA HP samples, treated under the reaction conditions described above, separate into upper and lower dPAGE bands that both contain platinated oligomers. As expected from their slower electrophoretic mobility, samples isolated from the upper band of these gels show a higher extent of platination. At a ratio of 5:1 Pt:oligomer, species with 1-3 $[Pt(NH_3)_2]^{2+}$ are present in the lowest-running dPAGE bands, whereas the higher bands contain oligomers with 2-4 $[Pt(NH_3)_2]^{2+}$ bound (**Figure 2.5a**). Consistent with the observation that RNA exhibits a faster reaction time, a higher population of the +4 $[Pt(NH_3)_2]^{2+}$ species is observed for the RNA HP sample than is found for the DNA analogue at the same timepoint. Faster reaction kinetics with RNA are also evident from bulk analysis of samples that are reacted for 23 hr in the high platinum:oligonucleotide ratios used for kinetic studies. In this case, the bulk DNA HP sample shows an overall adduct distribution that has major populations of 2-3 bound $[Pt(NH_3)_2]^{2+}$, distinctly fewer than the 5-6 $[Pt(NH_3)_2]^{2+}$ in the highest amplitude MALDI-MS peaks for the RNA HP sample treated under identical conditions (**Figure 2.5b**). From these data, it is apparent that the cisplatin-treated HP products separated by dPAGE all contain multiple platinum adducts. In the case of the mainly helical hairpin samples, the major product quantified for kinetics analysis is separated as a lower-mobility species that also contains on average at least one more $[Pt(NH_3)_2]^{2+}$ ion (**Figure 2.5c**). Although not a complete study, these data are broadly consistent with a model in which one site on the HP sequence both reacts more quickly with cisplatin, and also causes a conformational change resulting in a distinctly lower-mobility species. Slower platination reactions occur at other sites, creating products that are not clearly separated by these dPAGE conditions.

The products of BBD platination were also analyzed by MALDI-MS. If a similar model holds in which one faster-reacting site results in altered gel mobility, then for the BBD reactions it is predicted that the higher mobility, cross-linked products will also contain an additional $[Pt(NH_3)_2]^{2+}$ ion. An alternative model for reactions of platinum with the BBD sequence is that

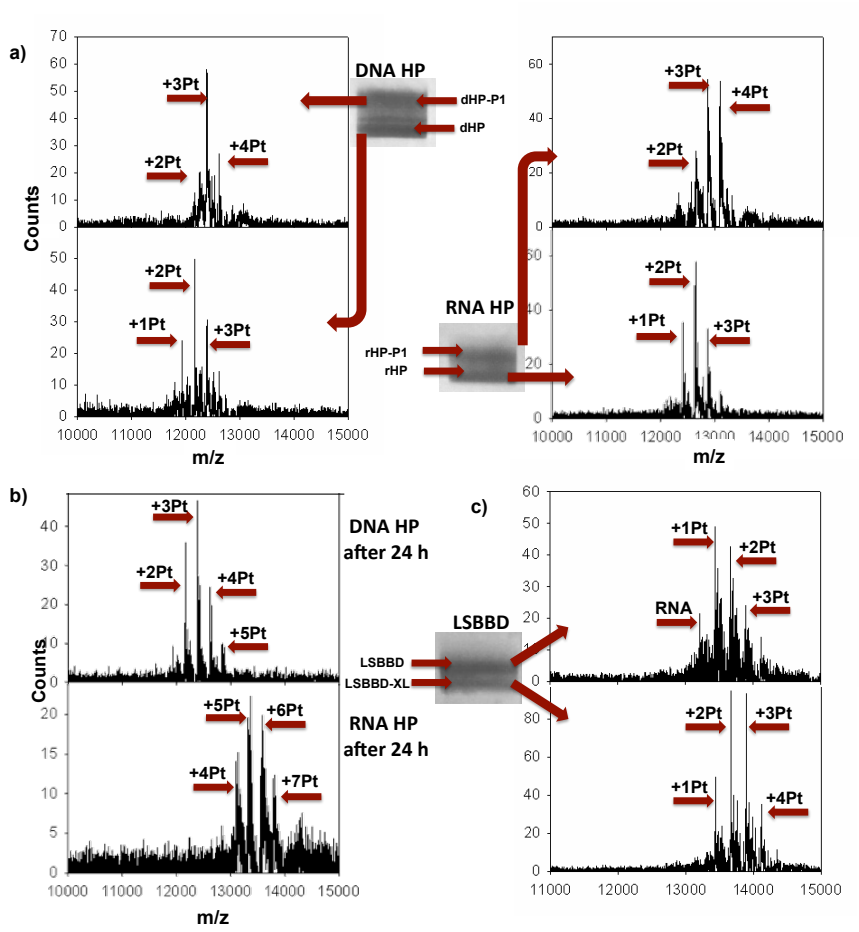

Figure 2.5. MALDI-MS analysis of platinated oligonucleotides. (a) Positive-ion mode MALDI mass spectra of products following cisplatin treatment of the RNA HP and DNA HP and isolation via dPAGE. Product bands are labeled rHP-P1 and dHP-P1 for RNA HP (rHP), and DNA HP (dHP) respectively. (b) Positive-ion mode MALDI mass spectra of the products of 23 hr reactions of RNA HP and DNA HP with cisplatin under the reaction conditions used for Figure 2.3. (c) The photograph and subsequent MALDI of the two main electrophoretic bands resulting from cisplatin treatment of LSBBD (sequence in Figure 2.2). The LSBBD (LS) product band is labeled LS-XL. Conditions: (a) Reactions were performed with 30 μM oligonucleotide, 150 μM cisplatin, 100 mM $NaNO_3$, 1 mM $Mg(NO_3)_2$, and 5 mM MOPS (pH 6.8) at 37 °C for 5 hr. The bands were separated by 20% dPAGE, stained with methylene blue, and then excised. MALDI-MS was performed in 3-hydroxypicolinic acid as a matrix. (c) Same as in (a), except that the reaction contained 90 μM cisplatin.

the crosslinking and non-crosslinking sites react at equal rates, which would result in an equal distribution of platinum in both dPAGE bands. To simplify the MALDI-MS data, a modified BBD sequence that maintains the internal loop but reduces the number of other purine sites was employed (**Figure 2.2a**). MALDI-MS spectra of platinated LSBBD shows that both dPAGE-isolated products contain multiple platinum adducts, but that peaks from the faster migrating product band are indeed shifted by approximately +1 $[Pt(NH_3)_2]^{2+}$ fragment (**Figure 2.5c**). Additional evidence that the gel bands observed for platinated BBD differ by one $[Pt(NH_3)_2]^{2+}$ fragment is provided by the dependence of reaction rates on platinum concentration. With platinum in large excess, the observed reaction rates vary linearly with a slope of 1.1 (r^2 = 1.0, **Figure S2.4, Appendix**), consistent with a 1:1 ratio between platinum and product.

The Significance of Cisplatin Binding to RNA:

Understanding of the biological roles of RNA has vastly expanded over the last three decades.[34] RNA is now recognized to regulate transcription and translation through gene silencing and RNAi pathways,[35.36] as well as through specific binding of small molecules in the structured regions of riboswitches.[37-40] Intricate RNA structures support catalytic active sites,[41] and dynamic RNA-protein rearrangements occur in complex cellular machineries such as the spliceosome.[22] These factors serve as the basis for the recent push in advancing RNA as a drug target and spur interest in understanding how existing nucleic acid-targeted drugs might act in previously unidentified pathways.[45,46] Cisplatin provides an example of a known DNA-binding compound that might have unique interactions with complex RNA structures. Factors that may be relevant to structurally diverse RNAs have been encountered in studies of platinated DNA hairpins, platinum-crosslinked quadruplex structures, and platinated DNA-protein complexes.[47-53] Additionally, preliminary investigations have already begun to address cisplatin's use as a structural probe and as drug conjugate for targeting RNA.[15,17,54,55]

This report describes cisplatin coordination to a 41-nucleotide RNA branch-bulge subdomain (BBD) that is derived from a U2-U6 snRNA complex proposed to form the active core of the spliceosome (**Figure 2.1**).[23,24] Cisplatin-induced intramolecular crosslinking takes place between G bases located in opposing sides of the BBD internal loop. In a cellular context, crosslinking of this type could be imagined to disrupt binding of the branch oligonucleotide or dissociation of the U2:U6 complex. It is interesting to note that the 3' side of the BBD internal loop corresponds to an invariant region of the U6 snRNA that is hypothesized to contain essential metal binding sites in the biological complex.[56,57] The ability of cisplatin to compete for pre-organized metal bind sites in RNA is unestablished and presents an interesting possibility for predicting *in vivo* drug

binding locations. Further studies will also focus on the sequence requirements and generality of cisplatin-based drug interactions with structured RNAs. Initial experiments indicate that this crosslinking reaction is tolerant of single base substitutions in the BBD internal loop, but that substitution of G31, the 3' partner in the major crosslink, with non metal-coordinating U results in a slightly different product as reflected by altered mapping data (data not shown). These limited studies indicate that platinum-induced crosslink formation is not strictly limited to internal loops with this exact BBD sequence, and is likely to take place in other structured RNAs. In general, cisplatin crosslinks in functional RNAs could disrupt a host of cellular processes that rely on RNA's dynamic structure.

Drug-binding kinetics may be an important factor governing the significance of cisplatin-RNA adducts *in vivo*. In this report we chose to compare the reaction rates of similar RNA and DNA oligomers *in vitro* in order to begin to address this question. Somewhat surprisingly, the RNA constructs exhibit reaction rates that are 5-6 times faster than those measured for the DNA construct. In a related study, Elmroth and coworkers observed faster binding by other platinum(II) compounds to a 13-nt RNA hairpin in comparison with its DNA analogue. Although that study used different reaction conditions than employed here, most notably lower ionic strength, the reported rate constants are within an order of magnitude of those in **Table A.1, Appendix A**.[12] Combined, these observations support RNA as a kinetically competitive target for cisplatin.

The application of polyelectrolyte theory to the platination of RNA or DNA suggests a model involving entry of a charged platinum species into the condensed cation atmosphere of a nucleic acid, followed by irreversible monoadduct and diadduct formation.[12,58-60] The range of literature values for the rate of monoadduct formation on duplex DNA by $[Pt(NH_3)_2Cl(OH_2)]^+$ vary from ~0.1-1 $M^{-1}s^{-1}$.[61-63] From this study, the calculated second order rate constant for the platination of the DNA HP is 0.33(3) $M^{-1}s^{-1}$ and lies within this range, while the rates observed for the RNA constructs are somewhat faster at ~2 $M^{-1}s^{-1}$ (**Table A.1, Appendix A**). The observation that similar rates are obtained for monoadduct formation on two structurally distinct RNAs indicates that broader factors such as electrostatic potential and oligomer flexibility likely dictate enhanced reactivity when compared with DNA. Individual contributions of these factors are currently under investigation.

MALDI-MS allows identification of nucleic acids with bound $[Pt(NH_3)_2]^{2+}$ fragments[33] and was used to analyze bulk reaction mixtures and dPAGE isolated oligomers in this study. MALDI-MS analysis of platinated oligomers isolated from dPAGE shows an average of one additional $[Pt(NH_3)_2]^{2+}$ fragment in the product bands. This observation supports a model in which specific

sites within each oligomer react quickly with cisplatin and are responsible for the structural distortions leading to altered gel mobility. Previous observations of kinetically preferred sites for platinum adduct formation on DNA have been reported. Enhanced reactivity can be based on electronegativity and target site geometry, as influenced by the nucleotide identity as well as oligonucleotide length, and secondary and tertiary structure.[49.53.64-71] Particularly relevant to this study is the observation of cross-strand adduct formation by $[Pt(NH_3)_2(OH_2)_2]^{2+}$ in telomeric DNA model sequences.[48,53] An even greater variety of platinum adducts might be expected for RNA based on its structural diversity and ability to specifically chelate divalent metals.[18-20]

The biological lifetime of each nucleic acid is an important factor in translating the faster *in vitro* rates observed for RNA in this study into a cellular context. In normal human cells the most rapidly turned-over class of RNA is mRNA. Median mRNA lifetimes in human cell lines have been reported to be ~10 hr, with a wide range of decay rates that vary by ~500-fold.[72] Both tRNA and rRNAs have significantly slower turnover rates, and lifetimes predicted to be on the order of days for average adults.[73] The lifetimes and abundance of cellular RNAs suggest that platinum drug binding could occur on a timescale that may affect RNA processes within treated cells. The types of cellular RNAs that are sufficiently accessible for platinum adduct formation, and the range of cellular consequences that could result from cisplatin interactions with RNA, are topics that remain to be addressed.

Summary and Bridge to Chapter III:

Chapter II describes the how Pt(II) complexes derived from cisplatin coordinate to a structured RNA that is derived the active site of the spliceosome, an incredibly complex cellular machine. The results of this study motivated us to broaden our investigations of how the platination of RNA may be tied to the drug's activity. Along these lines, Chapter III describes how platinum adducts act to disrupt the activity of four different types of RNA processing enzymes.

CHAPTER III

ENZYMATIC PROCESSING OF PLATINATED RNAS

Introduction:

This chapter was coauthored by Prof. Dr. Victoria J. DeRose who guided experimentation, contributed many meaningful ideas and co-wrote the corresponding manuscript. This chapter includes work published in the *Journal of the American Chemical Society* (**2010**, *132*, 1946-1952, © 2010 American Chemical Society).

Cisplatin and RNA Processing:

Cisplatin, *cis*-diamminedichloroplatinum(II), is broadly employed in the treatment of many cancers and is frequently used as a model for the development of nucleic acid targeted anti-tumor complexes. Years of extensive study have provided evidence that cisplatin's activity stems from drug binding to neighboring purine nucleotides in sequences of genomic DNA, inducing structural distortions.[1-3] Cellular proteins that recognize these distortions start a cascade of events, ultimately resulting in apoptosis.[4-6] Despite RNA's chemical similarity to DNA and a growing appreciation of the cellular resources devoted to producing, maintaining, and regulating the transcriptome,[7-10] relatively little is known about how cisplatin affects biological processes involving RNA.

Previous reports have described the disruption by cisplatin of translation[11] and splicing[12] in cell extracts. These results are complemented by *in vitro* studies describing RNA oligonucleotide targeting by cisplatin[13-18] and by several Pt-drug conjugates.[19,20] In addition to these studies, our lab has recently reported that cisplatin is capable of crosslinking structurally complex RNAs.[21] Elmroth and co-workers[18] and our laboratory[21] have reported that *in vitro*, RNA binding is kinetically preferred over drug coordination to DNA. Taken together these initial findings raise important questions regarding which types of cellular RNAs may be targeted by cisplatin, and whether cellular RNA function is significantly impaired as a result.

In RNA life cycles, a number of enzymes carry out the chemical reactions required to produce, regulate, and recycle the transcriptome.[7,8,10,22] Because RNA-protein interactions are sensitive to RNA structure, we hypothesized that platinum binding to RNA would disrupt the function of enzymes that process RNA. In this chapter we determined how RNA processing by 5'→3' and 3'→5' exonucleases, a purine-specific endoribonuclease, and a reverse transcriptase are affected by cisplatin-RNA adducts *in vitro*. Each of these enzymes is inhibited at the site of a Pt(II)-RNA adduct, but with slightly different products that depend on the adduct and the enzyme. This enzymatic inhibition likely results from a combination of nucleobase modification and more general structural distortions caused by platinum binding. Additionally, we have examined the reaction of platinated RNAs with thiourea and report that cisplatin-RNA adducts are reversed by prolonged incubation, providing an experimental means to address future biological queries requiring platinum removal from RNA.

Inhibition of Exonuclease Activity by Platinum(II)-RNA Adducts:

Because RNA damage and mis-processing are increasingly implicated in disease mechanisms,[23-25] it is of interest to investigate the mechanisms by which platination of RNA may be capable of disrupting the dynamic function of the transcriptome. Exonucleases, specifically directional phosphodiesterases, have been previously shown to stop at metallated DNA sequences.[26] Exonucleolytic cleavage by both the 3'→5' phosphodiesterase from *Croatalus adamanteus* (VPD, Phosphodiesterase I) and the 5'→3' phosphodiesterase from bovine spleen (SPD, Phosphodiesterase II) is blocked by binding of Pt and Rh complexes to DNA nucleobases.[27-33] The RNA transcriptome requires the function of many exonucleases that act in RNA maturation and degradation processes and facilitate post-transcriptional control of gene expression.[22,34] Examples of important, directional cellular RNA exonucleases include Xrn1 (5'→3') and components of the exosome complex (3'→5').[35] mRNA turnover by these enzymes is highly dependent on RNA stability elements such as 5'- m^7-G caps, 3'-poly(A) tails,[35] and stable secondary structures.[36] RNA platination may also inhibit or alter exonuclease activity, affecting RNA processing pathways.

VPD and SPD exonucleases have been used previously to locate transplatin crosslinks in RNA duplexes,[37] and to identify the binding locations of platinum complexes in 4-mer GA_3 RNAs.[38] In these experiments, exonuclease digestion proceeds up to nucleotides involved in platinum binding, producing RNA fragments that retain bound metals. We systematically tested whether similar enzymatic inhibition resulted from cisplatin binding to single-stranded 13-mer RNAs containing isolated purine sequences that are known to be targeted by cisplatin. In these

RNA (5'→3')	VPD Digest [a]	SPD Digest [b]	U2 Digest [c]
$(U)_6$-GG-$(U)_5$	X	X	$(U)_6$G *and* $(U)_5$
$(U)_6$-AG-$(U)_5$	X	X	$(U)_6$A *and* $(U)_5$
$(U)_6$-GA-$(U)_5$	X	X	$(U)_6$G *and* $(U)_5$ *minor* A$(U)_5$
$(U)_6$-GU-$(U)_5$	X	X	$(U)_6$G *and* $(U)_6$
[d] $(U)_6$-GG-$(U)_5$ + 1 Pt	$(U)_6$-GG(Pt)	UGG-$(U)_5$ (Pt)	$(U)_6$-GG-$(U)_5$ (Pt) (No reaction)
$(U)_6$-AG-$(U)_5$ + 1 Pt	$(U)_6$-AG(Pt)	UAG-$(U)_5$ (Pt)	$(U)_6$-AG-$(U)_5$ (Pt) (No reaction)
$(U)_6$-GA-$(U)_5$ + 1 Pt	$(U)_6$-GA(Pt)	UGA-$(U)_5$ (Pt)	$(U)_6$-GA-$(U)_5$ (Pt) *and* $(U)_6$-GA(Pt) (Partial Reaction)
$(U)_6$-GU-$(U)_5$ + 1 Pt	$(U)_6$-G(Pt) *and* $(U)_6$-GU(Pt)	UG-$(U)_5$ (Pt) *and* G-$(U)_5$ (Pt)	$(U)_6$-GU-$(U)_5$ (Pt) (No reaction)

Table 3.1. Products from the enzymatic processing of 13-mer RNAs. [a] VPD: 3′→5′ Venom Phosphodiesterase. [b] SPD: 5′→3′ Spleen Phosphodiesterase. [c] U2: RNase U2, cleaves 3′ to A or G. [d] "Pt" indicates[$Pt(NH_3)_2$]. "X" indicates no observed products.

experiments, reaction of 5'-$(U)_6$-XY-$(U)_5$ (XY = GG, AG, GA, or GU) RNAs with an aquated form of cisplatin produced a dominant product containing a single [$Pt(NH_3)_2$] fragment when analyzed by MALDI-MS (**Figures 3.1a** and **3.1b,** as well as **B.1** and **B.3-B.6, Appendix B**).[21] Peaks from platinated RNAs display masses corresponding to the parent RNA plus 227 amu, depicting two less H's than would be expected from attachment of a $Pt(NH_3)_2$ fragment (229 amu). This is due to the proton transfers necessary to offset binding of Pt^{2+} and still produce singly charged molecular ions.[39] Platinated RNAs were subsequently digested using VPD and SPD exonucleases, after which MALDI-MS was used to characterize the products of each reaction. The results of these experiments are summarized in **Table 3.1**. Spectra corresponding to each entry are included as Supplementary Information, **Figures B.3-B.6** in **Appendix B**.

In all cases VPD (3'→5') digestion of platinated RNAs containing two neighboring internal purines extends up to, but not beyond the 3' purine (**Figure 3.1c and Table 3.1**). These results correspond well with previous experiments using DNA, where metallation is presumed to alter DNA structure and disrupt enzyme recognition, protecting an oligonucleotide from further digestion.[40,41] VPD digestion of the platinated RNA strand containing a single G reproducibly gives [UUUUUUG + $Pt(NH_3)_2$ +H]$^+$ as the major detected product, as expected for

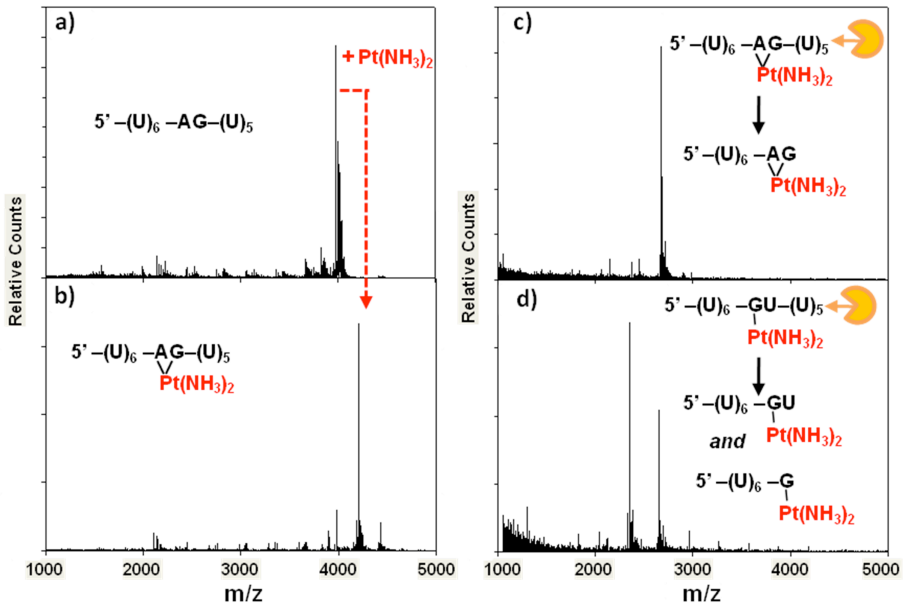

Figure 3.1. Platination and 3'→5' exonuclease digestion of RNAs. MALDI-MS spectra of (a) 5'-$(U)_6$-AG-$(U)_5$-3' RNA, (b) platinated 5'-$(U)_6$-AG-$(U)_5$-3' RNA, (c) platinated 5'-$(U)_6$-AG-$(U)_5$-3' RNA digested by VPD (3'→5') exonuclease, and (d) platinated 5'-$(U)_6$-GU-$(U)_5$-3' RNA digested by VPD (3'→5') exonuclease.

monofunctional adducts forming at the single G. Interestingly, a major secondary peak representing [UUUUUUGU + $Pt(NH_3)_2$ + H]$^+$ RNA fragment is also detected (**Figure 3.1d**). The differences between these products and those obtained from digestion of the platinated XY= GA, AG, and GG RNAs presumably reflects differential processing of mono- versus difunctional platinum adducts. A detailed examination of MALDI-MS spectra obtained from the platinated 5'-$(U)_6$-GU-$(U)_5$ RNA, however, does not show masses for an additional Cl, H_2O, or OH platinum ligand as expected to be present in a monofunctional adduct (**Figure B.1, Appendix B**). Although we suspect that this ligand may be lost during ionization processes,[42,43] it is also possible that the fourth Pt(II) coordination site is occupied by an RNA ligand, perhaps by a neighboring U nucleobase. In biologically relevant pH ranges, the potential N3 amine ligands in uridine (and thymidine) nucleobases are not typically considered to be targets for cisplatin because they are protonated at pH values below 10.[44] Platination of thymine and uracil have, however, both been observed.[45,46] In addition, characterization of a platinated d(TpG) DNA dinucleotide by NMR spectroscopy found evidence for solvent-dependent Pt(II) coordination to either the N3 of a neighboring pyrimidine base in aqueous solution,[47] or alternatively, interaction with non-bridging oxygens in the phosphodiester backbone in less polar solvents.[48] The multiple products resulting

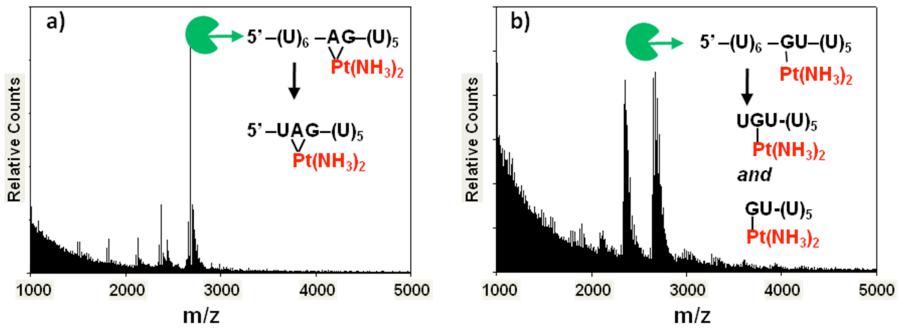

Figure 3.2. 5'→3' digestion of platinated RNAs. MALDI-MS spectra of (a) SPD (5'→3') digestion of platinated 5'-$(U)_6$-AG-$(U)_5$-3' RNA and (b) SPD (5'→3') digestion of platinated 5'-$(U)_6$-GU-$(U)_5$-3' RNA.

from nuclease digestion of the platinated 5'-$(U)_6$-GU-$(U)_5$ RNA may reflect a combination of these types of Pt(II) interactions. Digestion of the same singly platinated RNAs using SPD (5'→3') also shows that this exonuclease is inhibited at platinated RNA sequences. For RNAs containing two internal purines, SPD digestion stops at the 5'U that precedes each predicted platinum adduct (**Figure 3.2a and Figures B.3-B.6, Appendix B**). These results, and similar observations by Chottard and coworkers,[34] contrast with what is typically observed for cisplatin diadducts occurring with DNA, where SPD cleavage proceeds all the way up to a platinum binding site.[40,41] In addition, it is again found that the platinum adducts formed with the 5'-$(U)_6$-GU-$(U)_5$ RNA disrupt exonuclease activity differently than platinum adducts formed with the XY= GA, AG, and GG RNAs. SPD digestion of the platinated XY= GU RNA, produces $[GUUUUU + Pt + H]^+$ and $[UGUUUUUU + Pt + H]^+$ RNA fragments (**Figure 3.2b**). As with VPD digestion, the presence of multiple digestion products may reflect different types of platinum coordination occurring at this site. One model explaining the variances observed in how both VPD and SPD process different types of platinum adducts is that each type of adduct uniquely alters RNA structure. Platinum coordination to a single nucleobase is expected to cause less distortion in the phosphodiester backbone of an RNA than that resulting from platinum chelation. While cisplatin broadly disrupts exonuclease processing, these results show that the precise outcome of this inhibition relies on both the type of platinum adduct formed with an RNA and on how a given protein recognizes specific aspects of RNA structure.

Cellular 5'→3' and 3'→5' exonucleases often act concertedly to degrade RNAs and have synergistic responsibilities in RNA processing.[35] For this reason a single platinum adduct occurring on an RNA may eventually be approached by nucleases from each direction. Prolonged incubation of the platinated RNAs used in this study with both 3'→5' and 5'→3' exonucleases

results in low molecular weight products of only a few nucleotides in length (data not shown). In some cases, these products may represent the end of a drug-damaged RNA's cellular lifecycle.

Influence of Platinum(II)-RNA Adducts on RNA Processing by RNase U2:

In addition to exonucleases, a number of sequence- and structure-specific endoribonucleases (RNases) are used to trim and modify RNAs in a cell. RNases such as RNase P and Drosha (RNase III) are critical in maturation of the transcriptome.[49,50] New evidence showing that certain RNases are active in cellular stress response[51] suggests that if platination is capable of disrupting RNase function, cells may then become handicapped in their ability to respond to platinum damage.

RNases T1 and U2 specifically recognize purine ribonucleotides and catalyze cleavage of the 3' phosphodiester bond attached to a G or an A.[52,53] Monofunctional $[Pt(NH_3)_3Cl]^+$ coordination to the N7 atom of purine nucleobases has been shown to disrupt molecular recognition by RNase T1 and RNase U2.[54] Cleavage patterns produced by partial RNase T1 digestion have been used in several studies in order to infer platination sites and monitor broad structural changes in RNA

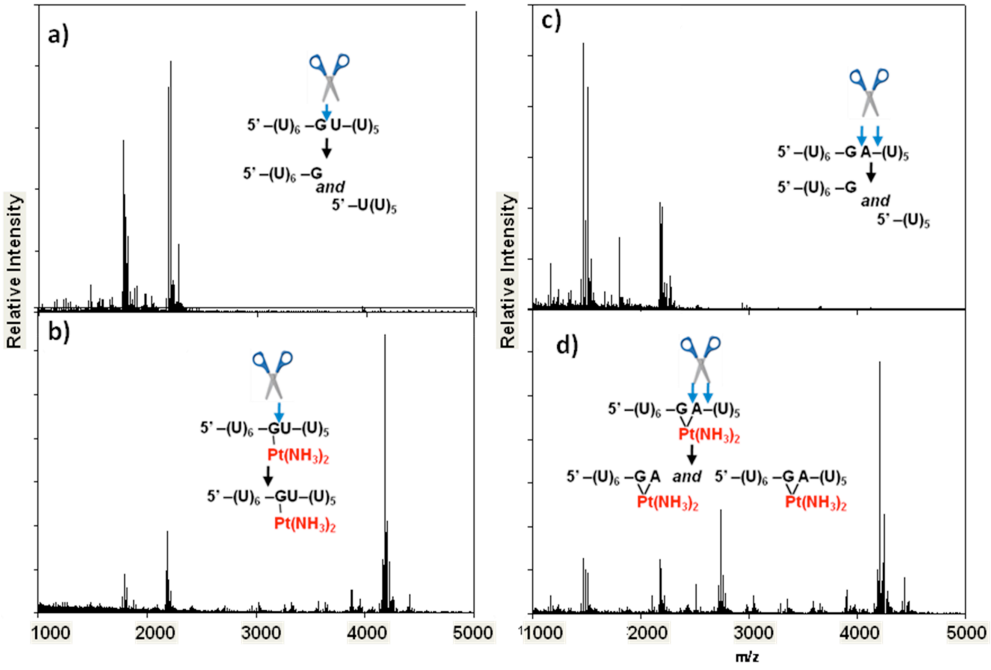

Figure 3.3. RNase U2 processing of platinated RNAs. MALDI-MS spectra obtained following (a) RNase U2 digestion of 5'-$(U)_6$-GU-$(U)_5$-3' RNA, (b) RNase U2 digestion of platinated 5'-$(U)_6$-GU-$(U)_5$-3' RNA, (c) RNase U2 digestion of 5'-$(U)_6$-GA-$(U)_5$-3' RNA, and (d) RNase U2 digestion of platinated 5'-$(U)_6$-GA-$(U)_5$-3' RNA.

resulting from platination.[16-18] Our findings using processive exonucleases led us to investigate whether endonucleolytic cleavage was similarly dependent on the type of platinum adduct formed or dependent upon additional factors such as RNA sequence. To test this, platinated 13-mer RNAs were reacted with RNase U2 (under conditions that cleave 3' both A and G), and digestion products were again characterized by MALDI-MS. For platinated sequences containing XY=GG, AG, and GU, RNase U2 cleavage is not observed, being blocked at the purine nucleotides predicted to be involved in platinum binding (**Figure 3.3a and b**). Surprisingly, however, digestion of the platinated 5'-$(U)_6$-GA-$(U)_5$-3' RNA shows a reaction product corresponding to [UUUUUUGA + $Pt(NH_3)_2$ + H],$^+$ depicting RNase cleavage 3' to an adenosine predicted to be involved in a cisplatin diadduct (**Figure 3.3c and d**). In DNA, closure of monofunctional 5'-d(AG*)-3' cisplatin adducts is preferred over closure of 5'-d(G*A)-3' adducts,[55] raising the possibility that cisplatin does not readily form a diadduct with the GA-containing RNA. However, data obtained from VPD (3'→5') digestion of the same platinated 5'-$(U)_6$-GA-$(U)_5$-3' RNA (**Figure B.2, Appendix B**) shows no digestion beyond the 3' adenosine, supporting its involvement in a cisplatin diadduct. These cumulative data suggest that the platinated G*A* RNA adduct is uniquely recognized and processed by RNase U2, whereas other purine-Pt(II) adducts are not. The basis for this selectivity may arise from the RNase's known A>G preference, allowing the endonuclease in some cases to partially recognize the 3' platinated A despite platinum modification. Together, the inhibition of both 5'→3' and 3'→5' exonucleases and an endoribonuclease show that cisplatin-RNA adducts disrupt a representative of each of the 3 major classes of intracellular RNA-degrading enzymes[22] and suggests that platination may disrupt RNA processing reactions in drug-treated cells.

Platinum(II)-RNA Adducts Disrupt cDNA Synthesis:

Accessing the information stored within an RNA transcript typically relies on successful recognition of an RNA sequence through the formation of Watson-Crick base pairs. In addition to processes such as si- and miRNA genetic regulation that rely on sequence complementarity *in trans*, cellular machines such as the ribosome and reverse transcriptases (RTs) move over long sequences of RNA where even relatively infrequent platination could potentially stall or otherwise disrupt function. Correspondingly, reverse transcription is commonly used to study both natural (e.g. hypermodified nucleobases such as wybutosine) and unnatural (e.g. 2'-OH acylation used in SHAPE chemistry) RNA modifications,[56,57] making it a technique amenable to monitor platination of RNA. Recently Rijal, and Chow have reported that cisplatin binding to exposed purines in the *E. coli* ribosome may be studied by RT-based primer extension of RNA

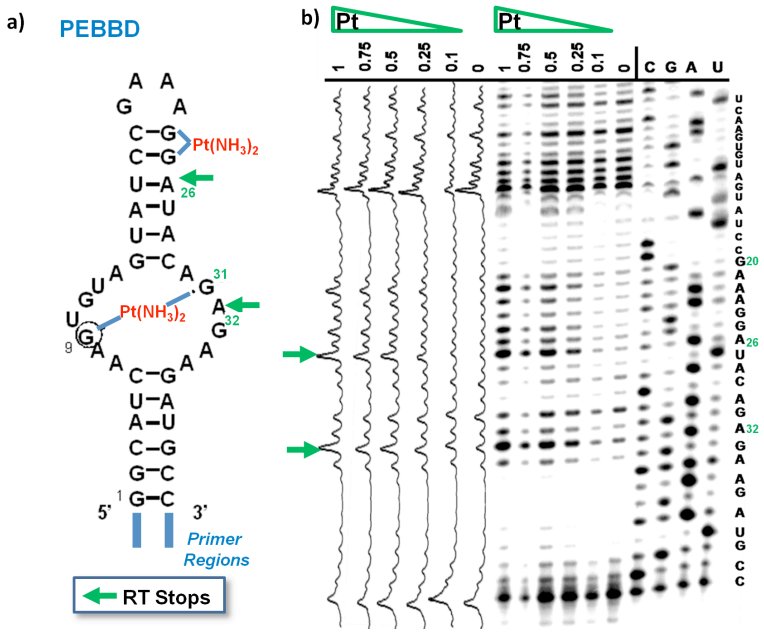

Figure 3.4. Reverse transcription of platinated PEBBD. a) Sequence of the BBD region of PEBBD. 5' and 3' sequences attached for *in vitro* PCR amplification of coding DNA, transcription, and reverse transcription are represented by blue lines. RT stops are represented by green arrows. b) Reverse transcription of platinated PEBBD analyzed by 15% sequencing dPAGE along with a plot of band intensities quantified using ImageQuant software.

isolated from drug-treated cells.[15] We extended this methodology to locate platinum adducts with an RNA termed PEBBD (Primer-Extended BBD) (**Figure 3.4a)**. We have recently reported that the internal loop contained in the PEBBD sequence forms intramolecular crosslinks when reacted with cisplatin.[21] To explore the ability of Pt(II) adducts to affect RT-based primer extension, PEBBD RNA was reacted with increasing amounts of an aquated form of cisplatin, annealed to a 5' end-labeled DNA primer and reverse transcribed using M-MuLV RT. Primer extension was monitored using sequencing dPAGE (**Figure 3.4b**). cDNA synthesis proceeds 5'→3' (toward the 5' end of the RNA), and shows several platinum-concentration dependent disruptions. The first major disruption of RT at A32 occurs immediately 3' to a G that we identified previously, using chemical footprinting, to be involved in platinum crosslinking across the internal loop of this RNA.[21] A second major interruption (A26) is observed immediately prior to a GG sequence adjacent to a capping GAAA tetraloop, indicating platination at this site. Additional RT stops in the GAAA tetraloop may indicate platinum binding to this region of PEBBD. Tetraloops of the general GNRA sequence are highly conserved RNA structural motifs and have been predicted to contain metal-binding sites.[58-60] It is interesting to postulate that RT inhibition in this region

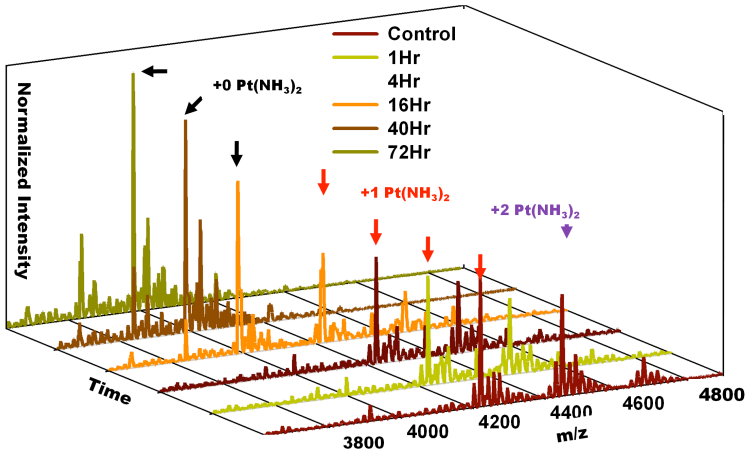

Figure 3.5 Reversal of platinum(II)-RNA adducts using thiourea. MALDI-MS spectra of the reaction of platinated 5'-$(U)_6$-GG-$(U)_5$-3' RNA with thiourea taken over the course of 72 h. Similar results are observed with a platinated 5'-$(U)_6$-GU-$(U)_5$-3' RNA (data not shown).

results from cisplatin targeting of this semi-"native" metal ion-binding site. Information from nucleotides on the 5' side of the internal loop is obscured by platinum-independent inhibition under these RT conditions, perhaps due to formation of stable secondary structures with remaining regions of the 5' primer sequence.[15] These data suggest that reverse transcription is broadly applicable to the identification of platinated sites in RNA, and further suggest that platination could disrupt similar enzymatic processing events requiring RNA recognition *in vivo*.

Reversal of Platinum(II)-RNA Adducts Using Thiourea:

The removal of cisplatin adducts from DNA through reaction with sulfur-containing small molecules has been studied pursuant to an understanding of how biomolecular thiol and thioketonethioketone nucleophiles might compete for cisplatin binding or remove drug adducts in the cell.[61] Additionally, platinum removal is a necessary step in several common experimental methods used to study cisplatin binding to DNA, and S-donors provide a milder alternative to the reaction conditions required for more commonly used cyanide salts.[26,62,63] We therefore studied the reaction of thiourea with platinated RNAs, using MALDI-MS to monitor the disappearance of platinated 5'-$(U)_6$-GU-$(U)_5$-3'and 5'-$(U)_6$-GG-$(U)_5$-3' RNAs. When a 200 µM solution of platinated RNA is reacted with an equal volume of a saturated thiourea solution at 37 ºC, products corresponding to platinated RNAs disappear while products representing un-modified RNAs increase in relative abundance (**Figure 3.5**). While MALDI-MS is not strictly a quantitative technique and therefore cannot be used to assess the kinetics of the platinum

removal, the spectra indicate the complete disappearance of platinated RNAs at 72 h under these conditions with no detectable degradation of the RNA. This reaction should be amenable to future studies seeking to remove cisplatin from pools of RNA isolated from drug-treated cells, and suggests that sulfur containing biomolecules have the potential to reverse cisplatin-RNA adducts.

Platination of RNA Generally Disrupts RNA Processing:

The results of these experiments demonstrate that single [$Pt(NH_3)_2$] adducts in an RNA oligonucleotide inhibit exonuclease, endonuclease, and reverse-transcription activities in a sequence-specific manner. Combined, these results show that platination of RNA disrupts the function of a number of enzymes that are analogous to those necessary for proper function of the transcriptome. Successful RNA maturation, splicing, regulation, translation, and degradation are all reliant upon the chemical fidelity of RNA transcripts. Platinum modification of individual nucleobases or more general alterations in RNA tertiary structure resulting from treatment with Pt(II) compounds may disrupt these critical processes *in vivo*. In the complex environment of a cell, additional factors may influence the processing of platinated RNAs, such as recently discovered RNA surveillance mechanisms responsible for handling RNA damaged by oxidative stress.[25,62] Taken together, these results drive interest in new studies that seek to deconvolute the effects of RNA platination from other cell-wide responses.

Summary and Bridge to Chapter IV:

Chapter III describes how Pt(II) coordination to an RNA interferes with enzyme recognition and coupled functions, leading us to suggest that such disruption could take place in drug-treated cells. Having learned that thiourea could reverse Pt(II) adducts formed on RNA we became interested in the reaction of Pt(II) compounds with RNAs that contained synthetically installed S substitutions at specific positions along the phosphodiester backbone. Chapter IV describes our success in engineering a new RNA-RNA crosslinking method based on Pt(II) targeting of such substitutions.

CHAPTER IV

SITE-SPECIFIC PLATINUM(II) CROSSLINKING IN A RIBOZYME ACTIVE SITE

Introduction:

This chapter was coauthored by Prof. Dr. Victoria J. DeRose, who originally suggested that we pursue this interesting line of research. She guided experimentation, contributed many meaningful ideas and co-wrote the corresponding manuscript which is now under consideration for publication in *The Journal of the American Chemical Society*.

Engineering an RNA Crosslinking Strategy:

Complex RNA structures are involved in an expanding list of important biological processes.[1,2] The incorporation of site-specific crosslinking probes has proven to be a powerful means by which to study the often intricately folded architectures of these RNAs.[3] Extending reports utilizing the nucleic acid coordination properties of Pt(II) complexes[4] to probe DNA and RNA conformation,[5-7] solvent exposure of nucleotides within the ribosome,[8] and biomolecular contacts made in ribonucleprotein (RNP) complexes,[9-11] we have engineered a new site-specific RNA-RNA crosslinking strategy based on Pt(II) targeting of phosphorothioate substitutions. In this strategy Pt(II) complexes are kinetically recruited[12-15] and anchored to phosphorothioate substitutions embedded within an RNA. A second Pt(II) coordination site can then form crosslinks[16-19] to other nearby nucleotides (**Scheme 4.1**). Here we describe the surprising selectivity of Pt(II) crosslinks formed within the catalytic core of the Hammerhead ribozyme (HHrz).

"Hooking" the Hammerhead Ribozyme

The HHrz forms a 3-helix junction RNA motif with a complex core architecture that catalyzes a site-specific phosphorotransesterification reaction.[20.21] HHrz catalysis has been proposed to involve coordination of a divalent metal to the pro-(*R*) non-bridging oxygen of the phosphodiester

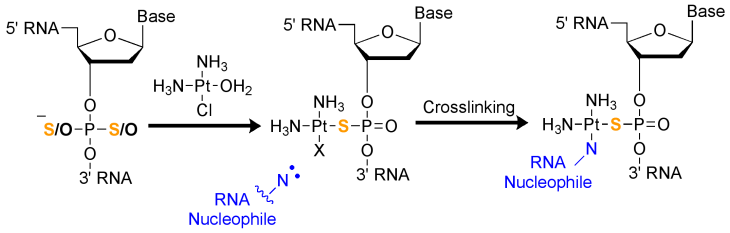

Scheme 4.1. Platinum(II)-phosphorothioate RNA crosslinking.

bond at the C17-C1.1 linkage that is cleaved during ribozyme-mediated catalysis (**Figure 4.1**).[20-22] We were optimistic that a Pt(II) probe might mimic such a metal and covalently capture RNA nucleophiles capable of acting as ligands for a metal bound to this site. Crosslinking studies were carried out using a two-stranded HHrz construct comprised of an "enzyme" strand (HHrzES) and a non-cleavable, phosphorothioate-substituted "substrate" strand. Platination of phosphorothioate substitutions installed adjacent to ribonucleotides resulted in surprisingly high levels of RNA cleavage at these locations (data not shown). Studies involving a model RNA construct were used to demonstrate that Pt(II) coordination to a phosphorothioate sulfur atom is capable of inducing site-specific RNA cleavage (**Figure C.3, Appendix C**) over the time course of these experiments, prompting the concomitant use of deoxyribonucleotides with phosphorothioate substitutions (**Scheme 4.1**).

Crosslinking experiments were performed using the annealed HHrz reacted with three equivalents of cis-$[Pt(NH_3)_2(OH_2)Cl]^+$ under ionic conditions that support tertiary folding of the ribozyme (1 mM Mg^{2+}, 100 mM Na^+).[23] This resulted in the formation of interstrand crosslinks, indicated by the formation of high molecular-weight products observed in dPAGE experiments (**Figure 4.1**). Importantly, crosslinking was not observed between the HHrzES and an unmodified substrate strand, SS(dC17), demonstrating the requirement for an embedded phosphorothioate to form intermolecular crosslinks. The C1.1 crosslinking site was further confirmed to be formed at the installed phosphorothioate through mild alkali hydrolysis mapping[2,7] of the crosslinks formed using the 5' end-labeled SS(dC17, C1.1ps) RNA (**Figure C.1, Appendix C**). In order to identify the nucleotide(s) trapped by the Pt(II) probe, crosslinks generated using the 5' end-labeled HHrzES were similarly mapped. In this experiment a loss of hydrolysis products 3' to U7 indicates G8 as the major site of Pt(II)-induced crosslinking (**Figure 4.2b**). Presumably in the crosslinked HHrz, $[Pt(NH_3)_2]$ is chelated between the C1.1 phosphorothioate substitution and the N7 atom of G8.[24] Interestingly, increasingly strong hydrolysis treatment results in a second fall off in cleavage intensity following A9, indicating that in some cases, Pt(II)-crosslinking may also take place to the N7 atom of G10.1.

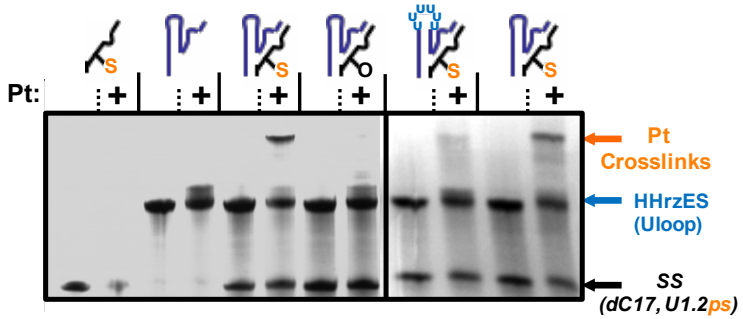

Figure 4.1. Pt(II)-induced crosslinking of the HHrzES-SS(dC17,C1.1ps) ribozyme. From left to right: (i) individual ribozyme components, (ii) the HHrzES-SS(dC17,C1.1ps) construct, (iii) a control HHrzES-SS(dC17) construct lacking a phosphorothioate linkage, and (iv) a docking deficient HHrz(Uloop)-SS(dC17, C1.1ps) construct. Conditions: 40 µM RNA in 1mM $Mg(NO_3)_2$, 100 mM $NaNO_3$, 10 mM Na_2PO_4, pH 7.0, 16 h, 37°C, analyzed by 20% dPAGE and stained with methylene blue.

Crosslinking in a Target-Rich Coordination Environment

In order to better conceptualize structural features influencing the formation of Pt(II)-phosphorothioate crosslinks, we used a HHrz crystal structure recently reported by Scott and coworkers[25] to build in a $[Pt(NH_3)_2(OH_2)]$ fragment bound to either the Rp (**Figure 4.3**) or Sp (**Figure C.2, Appendix C**) stereoisomer of a C1.1 phosphorothioate. Holding the RNA structure static, molecular mechanics calculations were used to minimize conformational strain and steric clash between Pt(II) probe and the RNA. Interestingly, the models obtained show the N7 atoms of several nucleobases located ~6.2-9 Å away directed toward the interior of the ribozyme's active site and the Pt(II) probe. In this seemingly target-rich coordination environment, the specificity of crosslinking to the G8 position is somewhat remarkable. Crosslinking is expected to occur through an associative mechanism[26] and may favor the N7 atom of G8 due to factors such as local structural dynamics and geometric alignment. In order to further investigate the influence of such factors we characterized HHrzES-SS(dC17, C1.1ps) crosslinking kinetics and tested the crosslinking efficiency of related RNA constructs.

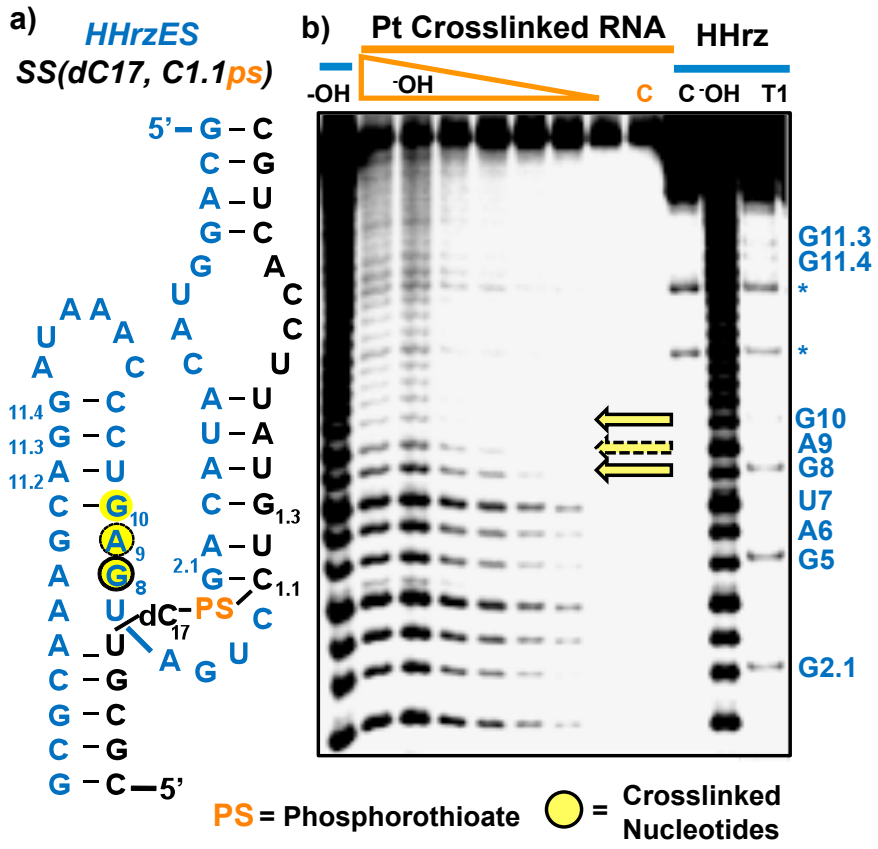

Figure 4.2. Location of Pt(II) crosslinks formed in the HHrzES-SS(dC17, C1.1ps) ribozyme. a) Secondary structure of the HHrzES-SS(dC17, C1.1ps) ribozyme construct used in this work.[21] b) Cleavage products produced by the alkali hydrolysis of Pt-crosslinked HHrzES-SS(dC17, C1.1ps) formed using 5' end-labeled HHrzES. Control lanes: **C:** 5' end-labeled HHrzES **T1:** G-specific sequence ladder generated by partial nuclease digestion with RNase T1 **-OH:** Reference alkali hydrolysis ladder. Platinum crosslinked lanes: **C:** dPAGE isolated, Pt-crosslinked HHrz-SS(dC17, C1.1ps) **–OH lanes:** dPAGE isolated, Pt-crosslinked HHrz-SS(dC17, C1.1ps) treated using alkali hydrolysis conditions for increasing amounts of time. Yellow arrows designate platinum crosslinking sites.

Rapid Crosslinking in a Ribozyme Active Site

Kinetics experiments were carried out using the 5' end-labeled SS(dC17, C1.1ps) to monitor crosslink formation over times ranging from 1 to 8 h (**Figure 4.3**). Averaged over three experiments, crosslinking is observed to take place at a rate of 0.23 ± 0.02 min^{-1} ($t_{1/2}$ ~ 10 min) with a calculated second order rate constant of 31 M^{-1} s^{-1}. This rate constant is approximately 15-fold higher than the ~2 M^{-1} s^{-1} rate constants observed for platination of unmodified hairpin-like

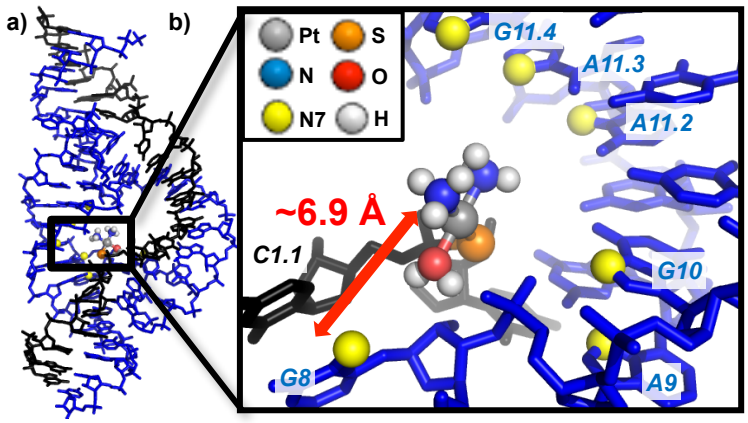

Figure 4.3. Crosslinking in the active site of the HHrz. (a) Crystal structure of the HHrz[25] (pdb: 2OEU) (b) Model of $Pt(NH_3)_2(OH_2)$ bound to the *R* stereoisomer of a C1.1 phosphorothioate built as described in Appendix C. The distance from Pt(II) to G8, the major site of Pt^{II} crosslinking, is indicated. Distances to other purine N7 sites are given in Figure S4.2, Appendix C.

RNAs under identical conditions.[7] An approximately 3-fold kinetic preference for Pt(II) coordination to phosphorothioate substitutions over equivalent GpG sequences has been reported in single stranded DNAs.[14] Taken together, these data suggest Pt(II) coordination as the rate-limiting step involved in HHrz crosslinking. In the HHrz, enhanced electrostatics are expected to further increase the rate of Pt(II)-complex formation. Extension of this model implies that Pt(II) crosslinking takes place rapidly following initial metal coordination and provides an upper limit for the lifetime of a RNA bound Pt(II) species of approximately 4 min. Dynamic rearrangements of RNA structure can occur on the micro- to millisecond timeframe[27] making it difficult to obtain precise information regarding the folded state of the HHrz that gives rise to the observed crosslinks from these data alone. In order to experimentally address the tertiary organization necessary to crosslink the ribozyme we also characterized Pt(II) crosslinking using a docking-deficient HHrz mutant. In the HHrz(Uloop) construct, replacement of the 5'-CAAAUA-3' terminal loop with a series of U removes contacts required for accurate folding of the ribozyme and presumably organization of the molecule's catalytic core.[20,23a] Platination of the HHrz(Uloop)-SS(dC17, C1.1ps) ribozyme results in a significantly less crosslink formation (**Figure 4.1**). This finding demonstrates that Pt(II) crosslinking in the core of the HHrz is dependent on accurate tertiary folding.

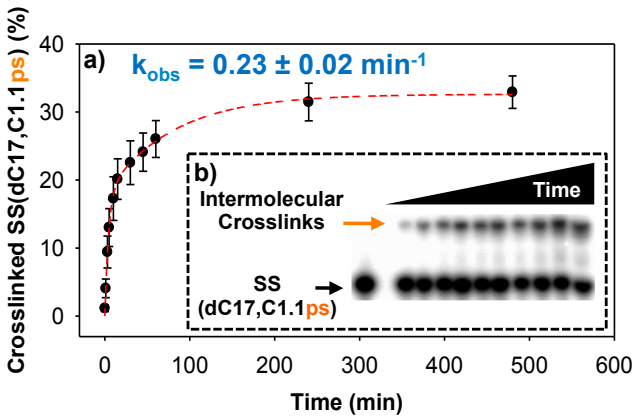

Figure 4.4. Rapid crosslinking of the HHrzES-SS(dC17, C1.1ps) ribozyme. a) Kinetic trace obtained for Pt(II)-crosslinking of the HHrzES-SS(dC17, C1.1ps) ribozyme using the conditions listed in Figure 1. b) Typical autoradiograph image obtained during kinetic studies.

Structure-Dependent Crosslinking

We then sought to examine the range of structural contexts in which Pt-(II) phosphorothioate crosslinking could occur. Somewhat surprisingly, platination of an HHrz construct containing a phosphorothioate substitution at the C1.1-U1.2 linkage directly adjacent to the original C17,C1.1ps site did not result in intermolecular crosslinking (**Figure C.4, Appendix C**). In these experiments [$Pt(NH_3)_2$] coordination to the SS(dC17, U1.2ps) substrate strand was confirmed using MALDI-MS, suggesting that the lack of crosslinking at this site was not due to a loss of Pt(II) coordination to the target phosphorothioate (data not shown). Molecular modeling of the HHrz-SS(dC17, U1.2ps) construct indicates significantly larger distances to possible Pt(II)-coordinating nucleobases (**Figure C.2, Appendix C**) as well as the potential for a Pt(II) probe to form intramolecular adducts with the neighboring G1.3 nucleotide.[24] Such coordination would act to preclude formation of intermolecular crosslinking in general and would limit the sequence contexts in which this crosslinking strategy could be employed. Control studies attempting to crosslink both SS(dC17, U2.1ps) and SS(dC17, U1.1ps) RNAs to a fully base-paired complement (**Figure C.5, Appendix C**) were unsuccessful.

A Promising New Crosslinking Strategy

In summary we have presented a new RNA-RNA crosslinking strategy based on the targeting of a kinetically inert Pt(II) complex to a specific thio-substituted position within a structured RNA. Once anchored to this position the Pt(II) probe selectively crosslinks to nearby nucleotides. In this example we embedded a phosphorothioate substitution at the scissile phosphate of the

HHRz. Biochemical evidence indicates metal ion coordination to the C1.1 phosphodiester during the HHRz reaction,[20-22] but current crystallographic models identify a Mn^{2+} atom coordinated to the G10.1 site[25] (**Figure 4.2**). Under the conditions used in our experiments, G10.1 is the weaker of crosslinked species observed. The major crosslinking position, G8, is phylogenetically conserved, however mutational analyses of this position do not indicate direct participation by the G8 nucleobase in HHRz catalysis.[20] The ability to use stereopure populations of phosphorothioate substituted RNAs[30] along with isomeric Pt(II) complexes holds the potential to allow future investigations to be conducted at a more precise level. This technique may also be useful in identifying interacting structural domains in large RNA and RNP complexes, in particular because metal ions frequently mediate tertiary contacts in these RNAs. Preliminary studies demonstrating that Pt(II)-phosphorothioate crosslinks are reversible using thiourea[11, 31] (**Figure C.6, Appendix C**) suggest that it may also be possible to adapt this crosslinking strategy to function in high-throughput contexts and add to the expanding repertoire of techniques being used to probe the structure of the transciptome.[32]

Summary and Bridge to Chapter V

Chapter IV describes the targeting of a Pt(II) complex to a phosphorothioate substitution embedded within the catalytic core of the Hammerhead ribozyme. Once Pt(II) is anchored to the phosphorothioate substitution, Pt(II) crosslinks form rapidly to nearby nucleotides with a surprising degree of structural selectivity. In the course of these experiments it was found that Pt(II) induced cleavage when coordinated to a phosphorothioate-substituted ribonucleotide containing a 2'-OH nucleophile. To investigate this metal-dependent activity we carried out the studies described in Chapter V which describes our efforts to understand fundamental details of Pt(II) coordination to phosphorothioate substitutions, namely, how Pt(II) is able to cleave, desulfurize, and isomerize phosphorothioate substituted RNAs.

CHAPTER V

PLATINUM(II)-ACTIVATED CLEAVAGE, DESULFURIZATION AND ISOMERIZATION OF PHOSPHOROTHIOATE SUBSTITUTED RNAS

Introduction:

This chapter contains contributions from Emma Downs, Josiah Vincek, Alex Kendall, and Dr. Victoria DeRose. Emma Downs performed NMR and MALDI-MS experiments characterizing Pt(II) coordination to the 5'-UpsU-3' dinucleotide described in the text. Josiah Vincek obtained the majority of the MALDI-MS data as well as the kinetic traces presented in this study. Alex Kendall performed DFT calculations on Pt(II)-coordinated O,O'-diethylthiophosphate species, helped edit this chapter and continues to study this reaction. Dr. Victoria DeRose provided very helpful comments on the ideas presented in this chapter and edited it as part of its inclusion in this dissertation. I wrote this chapter, developed the mechanistic hypothesis presented within it, as well as assisted in and helped guide each line of experimentation.

Platinum(II) Coordination to Phosphorothioates:

Nature relies on RNA to accurately transfer, regulate and transform genetic information.[1-3] RNA's remarkable ability to catalyze many of the reactions involved in these processes using a limited set of nucleobase functionalities continues to raise fundamental questions regarding biocatalytic strategies.[4] In many instances, complex tertiary folds position RNA nucleobases along with divalent metal ions with angstrom-level precision in order to activate specific phosphoryl transfer reactions.[5-7] One powerful approach in characterizing the roles that metal ions play in the mechanisms of these reactions has been to install site-specific phosphorothioate (PS) substitutions.[8,9] Substituting one of the non-bridging oxygens in the RNA phosphodiester backbone for a "softer", more nucleophilic S atom can disrupt coordination to physiological metals such as Mg^{2+} and Ca^{2+} and facilitate interactions with softer metals such as Cd^{2+}, producing diagnostic shifts in the metal ion requirements for RNA catalysis. These "thio effects"[10] form the basis of classical metal ion "rescue" experiments.

Despite the broad application of PS substitutions as mechanistic probes, relatively few studies have experimentally addressed soft metal ion coordination to the substitutions outside of the context of an RNA or protein active site. In previous work, Lönnberg and coworkers have described the metal-dependent reactivity of a PS linkage embedded within a 5'-UpsU-3' construct (where "ps" is used to denote a 3'-5' PS linkage between two nucleotides).[11] In this study it is observed that hard metal ions (Mg^{2+}, Gd^{3+}) activate cleavage of the 5'-UpsU-3' construct to a significantly lesser extent than they enhance cleavage of a non-substituted 5'-UpU-3' analog containing a standard phosphodiester bond. The same hard metal ions are not observed to promote isomerization or desulfurization reactions. Contrasting this, thiophilic metal ions (Zn^{2+}, Cd^{2+}) are observed to increase the rate of 5'-UpsU-3' cleavage well beyond the extent to which they promote cleavage of 5'-UpU-3'. In addition, Zn^{2+} promotes desulfurization as well as isomerization of the PS bond in 5'-UpsU-3', producing both 3'-5' and 2'-5' phosphodiesters. Interestingly, the extent to which each metal ion promotes cleavage of 5'-UpsU-3' correlates well with the stability of corresponding M^{2+}-adenosine 5'-*O*-thiomonophosphate complexes described by Sigel and coworkers.[12,13] These findings lead Lönnberg and coworkers to propose a mechanistic model in which hard metal ions coordinate primarily to the non-bridging oxygen of an installed PS, while softer metal ions prefer coordination to the S atom.[11] Soft metal ion coordination is proposed to stabilize the dianionic thiophosphorane transition state common to each type of phosphoryl transfer reaction observed in this study. This stabilization is proposed to extend the lifetime of this species such that it may be considered a "borderline" intermediate rather than a transition state. Pseudorotation[17] around this intermediate is proposed to give rise to the diverse (i.e cleaved, desulfurized, and isomerized) products observed in this study. The authors additionally suggest that a M^{2+}-bound hydroxo ligand would conveniently fulfill the role of a general base in this reaction although they did not address this possibility experimentally. Such analysis would prove challenging as the metal ions studied in the report are kinetically labile, coordinating to the PS linkage only transiently.

Here we report how Pt(II), a similarly soft metal ion, is able to activate cleavage of PS-substituted RNAs in the absence of an RNA active site. In PS-containing oligonucleotide and small-molecule models, Pt(II)-catalyzed reactions also result in substantial amounts of desulfurization and isomerization, generating a mixture of 3'-5' and 2'-5' phosphodiesters in place of the original PS. Cumulatively, our data suggest a mechanism in which Pt(II) coordination to the PS sulfur atom withdraws electron density from the central phosphorous, activating it to nucleophilic attack from an adjacent and deprotonated 2'-OH (**Scheme 5.1**). Based on analogy to previous studies,[11,15-17] we suggest that pseudorotation around a pentacoordinate phosphorane

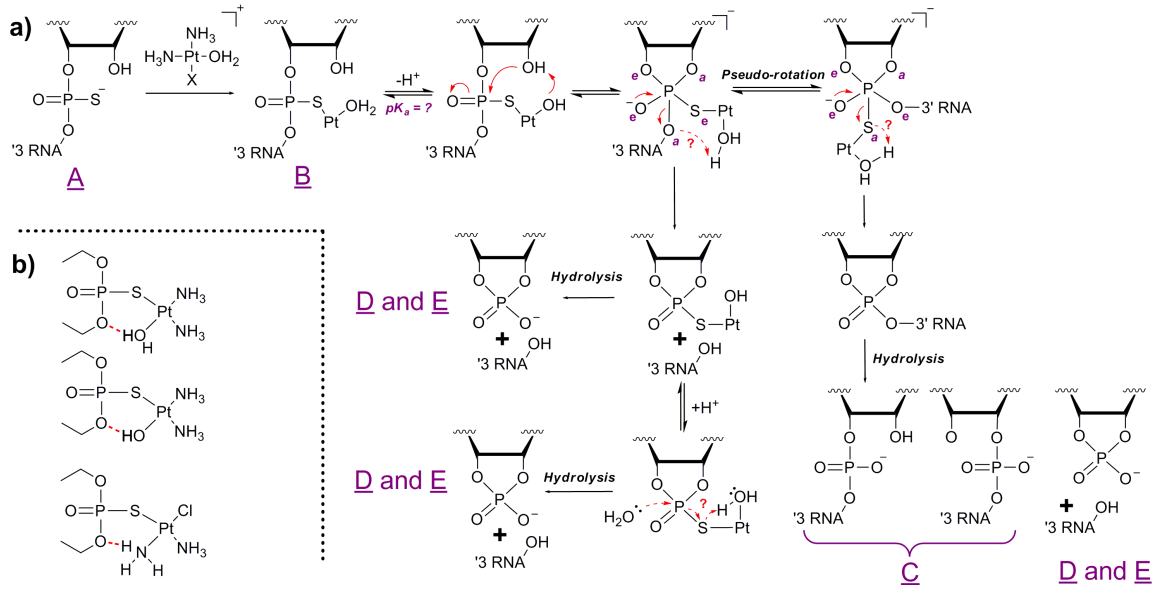

Scheme 5.1. The reaction of Pt(II) complexes with phosphorothioate substitutions. a) Proposed reaction mechanism for $[Pt(NH_3)_2XY]^{n+}$ (X,Y = OH_2, ^-OH, ^-Cl) induced cleavage, desulfurization and isomerization of phosphorothioate substituted RNAs. The NH_3 ligands of Pt are omitted for clarity. Axially and equatorial positions in the pentacoordinate phosphorane are indicated by "*a*" and "*e*" respectively. b) Hydrogen-bonding interactions predicted by molecular modeling of Pt(II) species coordinated to O,O'-diethylthiophosphate.

intermediate is responsible for the variety of cleaved, desulfurized and isomerized RNA products that result from this reaction.

We initially became interested in Pt(II) coordination to PS substitutions during an effort to engineer a new RNA-RNA crosslinking strategy based on *cis*-$[Pt(NH_3)_2(OH_2)Cl]^+$ coordination to PS-substituted RNAs.[18] In the course of these studies it was observed that when a PS substitution is installed 3' to a ribonucleotide with a native 2'-OH, facile cleavage of this bond takes place following treatment with square planar Pt(II) complexes (data not shown). The rate of this cleavage reaction in model oligonucleotides far exceeds that observed with similarly "soft" metal ion such as Cd^{2+}, typically used in metal ion rescue experiments (equivalent conditions, **Table D.1**, **Appendix D**). In order to characterize this reaction we have pursued a series of MALDI-MS, ^{31}P NMR, and pH-dependent kinetic studies. Here we present these results which collectively suggest that a Pt(II)-coordinated hydroxo ligand is responsible for deprotonation of the ribose 2'-OH that initiates this reaction (**Scheme 5.1**). Interestingly, the PS-coordinated Pt(II)-aqua species that result may also serve as general acids in several mechanistic pathways. Preliminary DFT studies portray electrophilic activation of the PS phosphorous atom and suggest a role for

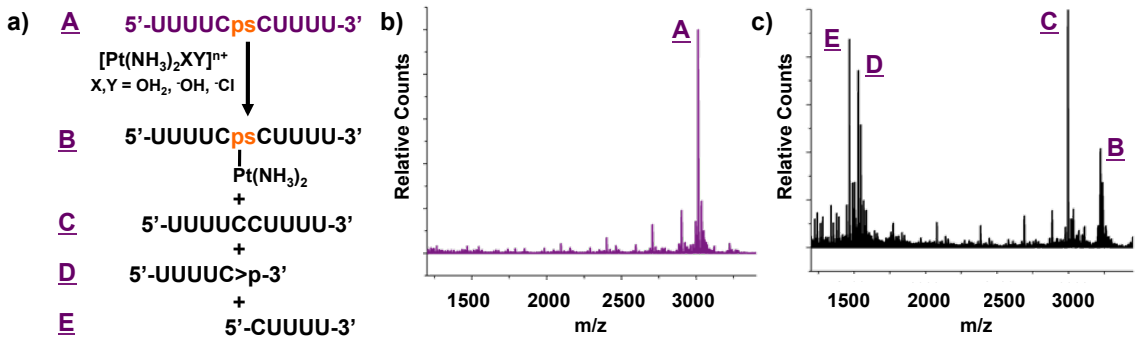

Figure 5.1. Platinum(II)-promoted cleavage and desulfurization of PS-substituted RNAs. a) The sequence of the 10-mer RNA construct used in this work and the RNA products that result from reaction with Pt(II) complexes. The location of the PS substitution is highlighted in orange. Purple letters preceding each species correspond to labeling in the spectra and are used throughout the subsequent text and figures. b) MALDI-MS spectrum of unreacted 10-mer RNA. c) MALDI-MS spectrum of the products of the reaction after 4 hours. Conditions: 40μM RNA, 120μM Pt(II), 1mM $Mg(NO_3)_2$, 100mM $NaNO_3$, 10mM MES, pH 6.5, 37°C, 4 h. Reactions purified by C_{18} ZipTips and analyzed by positive ion mode MALDI-MS (see Materials and Methods, Appendix D).

secondary H-bonding interactions by Pt(II)-coordinated ligands. Combined, these initial studies reflect the importance of several dynamic equilibria in the reaction of Pt(II) complexes with PS-substituted RNAs. Additional experiments are proposed that would help characterize these equilibria and support our developing hypotheses. Increasing knowledge of metal ion-phosphodiester/phosphorothioate chemistry may facilitate understanding how metal ions influence the reaction chemistry of these important types of chemical bonds both *in vitro* and *in vivo*.

Reaction of Phosphorothioate-Substituted RNAs with Platinum(II) Complexes:

In our initial studies, reaction of Pt(II) complexes with PS-substituted oligos whose sequences contained mixtures of A, C, G, and U nucleotides resulted in a surprising level of RNA cleavage at the location of the embedded PS (data not shown). Because Pt(II) complexes readily coordinate to A's and G's,[19,20] potentially complicating efforts to characterize the cleavage reaction, further experiments employed a construct in which a single PS substitution was embedded within a 10-mer RNA containing only C and U nucleotides not expected to coordinate to Pt(II) under the conditions used in this study (A, **Figure 5.1a**).

Solutions, of "aquated" Pt(II) species were prepared by reaction of *cis*-$Pt(NH_3)_2Cl_2$ with 0.95 equiv. of $AgNO_3$. Due to competing equilibria[21] a pH-dependent mixture of *cis*-$[Pt(NH_3)_2XY]^{n+}$ (X,Y = OH_2, ^-OH, ^-Cl) species are expected to result from this reaction. Based on preliminary ^{195}Pt NMR studies, $[Pt(NH_3)_2Cl(OH_2)]^+$ is the predominate species formed at pH 6.5 (Hostetter, DeRose *unpublished*). This mixture of Pt(II) complexes was then reacted at a 3:1 Pt(II):RNA ratio with the PS-substituted 10-mer RNA (A) under ionic conditions used in previous studies with RNA (1mM $Mg(NO_3)_2$, 1mM $NaNO_3$, 10mM MES, pH 6.5).[18] Nitrate salts were used in these experiments to prevent the formation of Pt(II)-Cl species. Reaction products were subsequently characterized by MALDI-MS. In the resulting spectra three to five major species are observed depending on the extent of the reaction. These are: A) unreacted starting material (m/z= 3012); B) $Pt(NH_3)$- and $Pt(NH_3)_2$-bound 10mer RNA (m/z= 3223 and m/z= 3240 respectively); C) desulfurized 10-mer RNA (m/z= 2996); D) 5'-UUUUC>p-3' (m/z= 1529, where ">p" indicates a 2'-3' cyclic phosphate); and E) 5'-CUUUU-3' RNA (m/z= 1467) (**Scheme 5.1**, **Figure 5.1b** and **c**). D and E represent products resulting from cleavage at the site of the PS linkage.

The presence of a cyclic phosphate on the fragment of RNA corresponding to the 5' half of 10-mer used in these experiments (D) suggested that Pt(II) coordination to the PS substitution could activate intramolecular attack of the 2'-OH adjacent to the installed substitution, resulting in both cleaved products D and E. The additional presence of desulfurized, full-length products (C) parallels previous observations by Lönnberg and coworkers in similar experiments, who hypothesized that pseudorotation of a metal-coordinated phosphorane intermediate gives rise to desulfurized and isomerized products.[11] The observation of Pt(II)-coordinated intermediates in our studies suggested the opportunity to build on the hypotheses presented by these authors.

Verification of 3'-5' to 2'-5' Isomerization During Desulfurization:

An important caveat to early MALDI-MS studies was that this technique did not provide direct evidence that isomerization from a 3'-5' to 2'-5' linkage accompanied desulfurization. The 16 amu mass difference observed between the parent RNA (A) and desulfurized products (C) simply depicts exchange of a S atom for an O atom (16 amu net mass difference). In order to establish that isomerization was simultaneously occurring, ^{31}P NMR experiments were pursued. In these experiments a 5'-UpsU-3' construct (identical to the one employed by Lönnberg and coworkers[11]) was treated with 1.5 equiv. of activated Pt(II) complexes and followed over times ranging from 1 to 3 days (**Figure 5.2a**). Initially, two peaks corresponding to PS-substituted *R* and *S* stereoisomers appear at ~56 ppm (the *R* steroisomer expected to be further downfield based on previous observations,[22,23] **Figure 5.2b**). At 24 hrs following platination additional peaks

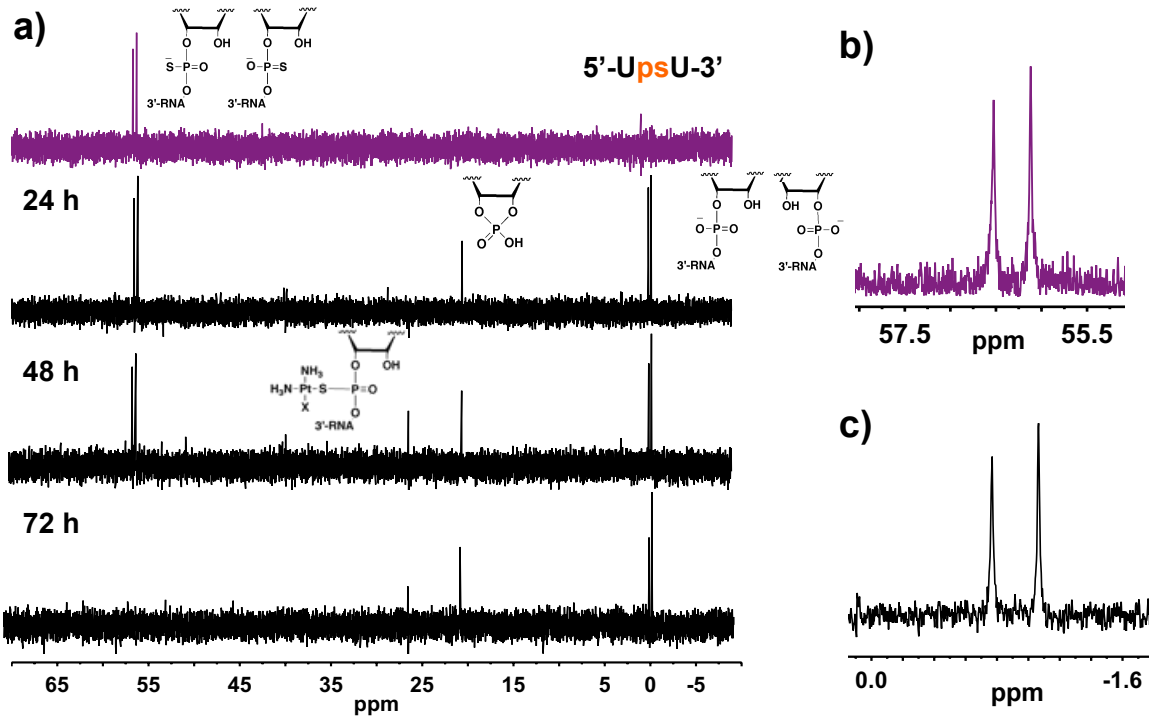

Figure 5.2 ^{31}P NMR spectra obtained following the reaction of 5'-UpsU-3' with activated Pt(II) complexes. Conditions: 1mM 5'-UpsU-3', 1.5 mM Pt(II), 100 mM $NaNO_3$, 1mM $Mg(NO_3)_2$, 10 mM HEPES, pH 7.5, 25°C. a) 31P NMR spectra over the course of the reaction with the chemical species corresponding to each peak indicated. b) Enlargement of the spectral region corresponding to the phosphothioate diastereomers. c) Enlargement of the spectral region corresponding to 2'-5' and 3'-5' phosphodiesters.

appear corresponding to both 3'-5' and 2'-5' phosphodiesters (~0 ppm, **Figure 5.2c**) and a cyclic phosphate (~19.8 ppm). At longer time points an additional peak appears that is tentatively assigned to a Pt(II)-coordinated PS (~25.8 ppm) based on previous observations of upfield shifts following Cd^{2+} coordination to a PS substitution.[22] The appearance of a peak corresponding to reaction intermediates following the initial appearance of reaction products suggests the possibility of multiple reaction pathways, one of which results in the slow accumulation of Pt(II)-coordinated intermediates. The lower intensity of this peak at the 72 hr time point suggests that these intermediates are gradually converted to reaction products. The appearance of peaks corresponding to both 3'-5' and 2'-5' phosphodiesters leads us to conclude that the desulfurized products observed in MALDI-MS studies are in fact an approximately equal mixture of 3'-5' and 2'-5' phosphodiester isomers.

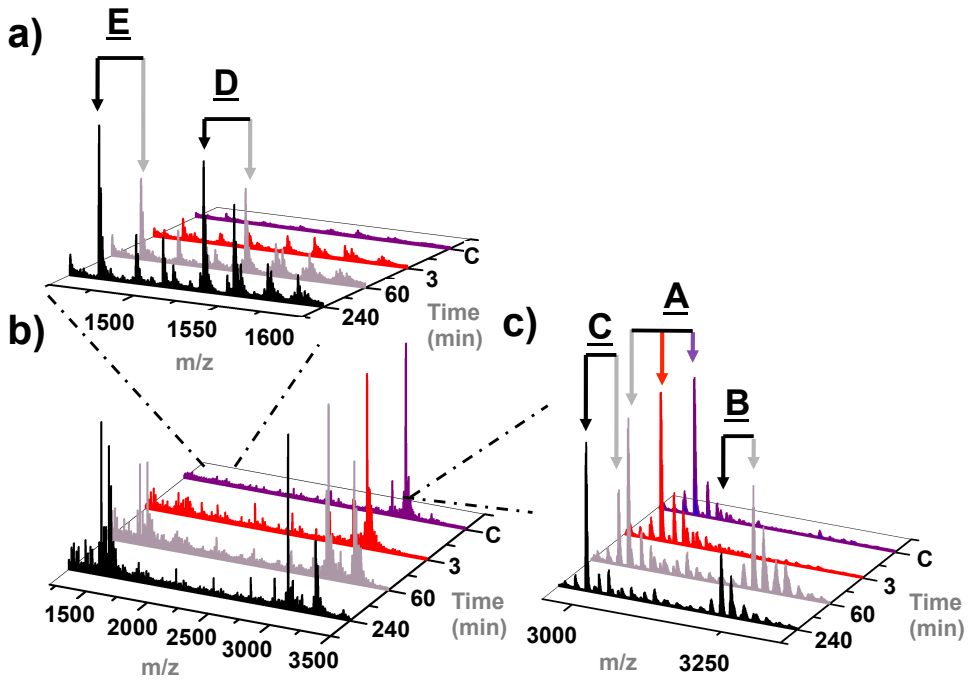

Figure 5.3. Time course MALDI-MS spectra of Pt(II)-promoted cleavage, isomerization and desulfurization of PS-substituted RNA at pH 6.5. Product labels correspond to Figure 5.1. a) Enlargement of the spectral region between 1450 and 1600 amu. b) Full MALDI-MS spectra. c) Enlargment of the spectral region between 2950 and 3350 amu. Conditions identical to Figure 5.1, times as noted in the figure.

Accumulation of Platinum(II)-Coordinated Intermediates:

The observation of Pt(II)-coordinated intermediates (B) in both preliminary MALDI-MS studies and in NMR studies inspired us to further examine the build-up of these species throughout the course of platination of 5'-UUUUCpsCUUUU-3' (A). As shown in **Figure 5.3** MALDI-MS was used to characterize the accumulation of Pt(II)-coordinated intermediates at times ranging from 3 min to 4 h. While MALDI-MS is not strictly quantitative, the intensities of two peaks within a narrow spectral window can be used to assess the relative abundance of each species in a given sample[24] and here provide insight into the relative amounts of each product in the inset spectra. In these types of experiments, little to no Pt(II)-coordinated intermediates (B) are observed at early time points, while at 1 h these intermediates as well as reaction products (C, D, E) are clearly apparent. After 4 hours at pH 6.5, peaks corresponding to the parent PS-substituted RNA are no longer observed and Pt(II)-coordinated intermediates are less abundant than at the 1 h time point, depicting conversion of both species to reaction products.

An important question that arose during these studies concerned the identity of the Pt(II) species coordinated to the PS (see **Scheme 5.1**). The mass difference between the parent PS-substituted RNA (A) (m/z= 3012) and peaks corresponding to the two Pt(II)-coordinated intermediates observed (e.g. $Pt(NH_3)$-PS RNA (m/z = 3223) and $Pt(NH_3)_2$-PS RNA (m/z = 3240)), do not depict other ligands expected to be present based on mono-functional coordination of a $[Pt(NH_3)_2X]$ (X= OH_2, OH, Cl) species to the PS. We have previously noted the absence of exchangeable Pt(II) ligands (e.g. OH, OH_2, Cl) in MALDI-MS studies of Pt(II) coordination to RNA[25] (and others to DNA[26,27]), however loss of an additional NH_3 ligand was a new feature in these types of experiments. We hypothesized that loss of this ligand could result from the *trans*-labilizing effect of the PS sulfur atom.[28] Strong experimental[29] and theoretical[30] evidence exists demonstrating loss of an Pt(II) NH_3 ligand when *trans* to a thiol or thioether, suggesting that the NH_3 ligand *trans* to the PS substitution may be similarly labilized.

pH-Dependent Accumulation of Reaction Intermediates:

Initial MALDI-MS studies showed that this technique allowed detection of Pt(II)-coordinated RNA intermediates (B). Extending this, we hoped that by studying the accumulation of Pt(II)-coordinated intermediates at various pH's we would be able to comment on the relative stability of protonated versus deprotonated forms of these species. The pKa values of aqua ligands coordinated to $[Pt(NH_3)_2XY]^{n+}$ (X,Y = OH_2, -OH, Cl) species range from ~3.8 to 7.8 (depending on the identity of both exchangeable ligands).[16,31] The pKa values of aqua ligands bound to a PS-coordinated Pt(II) species are expected to lie within a somewhat similar range. The protonation state of both these species is expected to influence Pt(II)-phosphorothioate reactivity by determining the rate at which Pt(II) species coordinate to the anionic PS-substituted RNA as well as the rate at which they subsequently react (**Scheme 5.1**). We therefore conducted a series of MALDI-MS experiments, comparing the build-up of Pt(II)-coordinated intermediates at various pH's after equivalent reaction times. As shown in **Figure 5.4,** at 4 h all PS-RNA reactants (A) have been consumed, except for in the reaction carried out at pH 8.0. Pt(II)-coordinated intermediates (B) are observed to accumulate to a large extent in reactions performed at pH 3.5. Surprisingly, this reaction also appears to predominantly form desulfurized products C and less cleaved products D and E. At pH 5.5 and pH 6.5 intermediate levels of Pt(II)-coordinated species (B) are observed along with significant amounts of cleaved and desulfurized products (C, D, and E) (**Figure 5.4**). The same intermediates are observed to a significantly lesser extent at pH 8.0 and are accompanied by relatively low levels of reaction products.

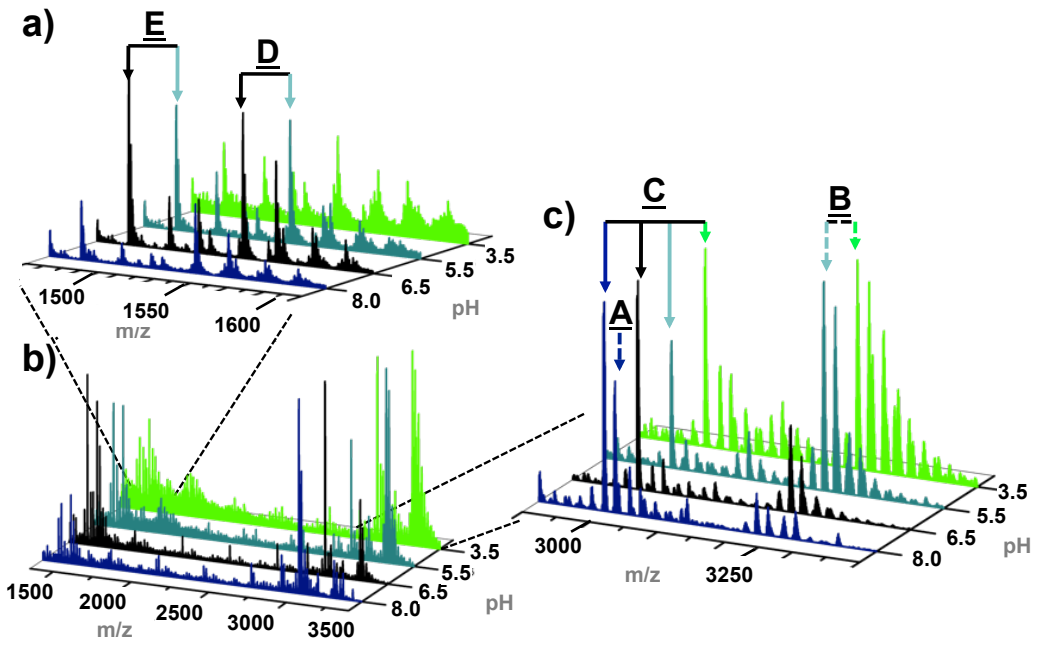

Figure 5.4. The reaction of PS-substituted RNA with Pt(II) complexes after 4 h at different pH values. Product labels correspond to Figure 5.1. a) Enlargement of the spectral region between 1450 and 1600 amu. b) Full MALDI-MS spectra. c) Enlargement of the spectral region between 2900 and 3500 amu. Conditions as in Figure 5.1 with pH varied as indicated in the figure (see Materials and Methods, Appendix D).

The profiles of these pH-dependent reactions likely depict the influence of several competing equilibria in this reaction. First among these is the equilibrium occurring between protonated and unprotonated forms of $[Pt(NH_3)_2XY]^{n+}$ (X,Y = OH_2, -OH, Cl) compounds prior to reaction with the PS-substituted RNA (A). At low pH values this equilibrium is expected to favor cationic Pt(II) aqua species[21] that are expected to associate faster with the anionic PS-substituted RNA than neutral Pt(II) hydroxo and chloride complexes present at higher pH.[32-34] The presence of unreacted starting material (A) at 4 h at pH 8.0 fits well with this hypothesis. Secondly, the accumulation of Pt(II)-coordinated RNA intermediates (B) at low pH (**Figure 5.4c**) suggests that these intermediates are stabilized by protonation. The observation that these Pt(II)-coordinated intermediates convert more to readily to products as pH increases from 3.5 to 6.5 further suggests that deprotonation of a PS-coordinated Pt(II) species may be important in determining the reaction's progress. One model explaining these data is that at low pH values Pt(II)-aqua complexes rapidly coordinate to the PS-substituted RNA, but must be subsequently deprotonated in order to form cleaved and desulfurized products (**Scheme 5.1**). This model supports the

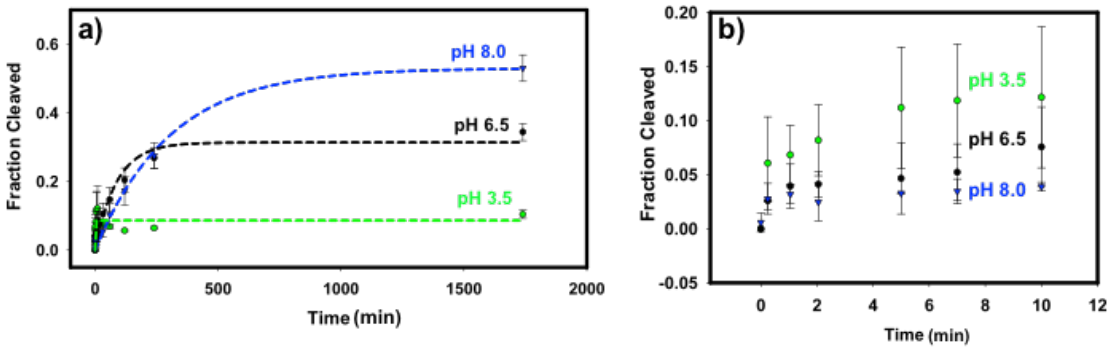

Figure 5.5. Kinetic characterization of Pt(II)-induced cleavage of PS-substituted RNA. a) Kinetic traces obtained from experiments performed at indicated pH values depicting the reaction's progress over 27 h. b) Kinetic data from time points ranging from 0 to 10 min. Data colored by pH: pH 8.0- blue, pH 6.5- black, pH 3.5- green. Data are the average of at least two experiments. Conditions as in Figure 1 with varying pH and buffer identity (see Material and Methods, Appendix D).

proposition that a Pt(II)-bound hydroxo ligand acts as the general base in this reaction. Interestingly, this model can be extended to propose that Pt(II)-aqua species subsequently act as general acids (**Scheme 5.1**). Such a role for metal bound aqua ligands has been proposed previously for Zn^{2+} reactions.[35] An alternative explanation of these data involves increasing cleavage activity by solvent-mediated deprotonation of the 2'-OH adjacent to the PS linkage at higher pH values. Although not completely discounted by the data in **Figure 5.4**, this possibility seems less likely based on the pH dependence observed in these experiments. Pt(II)-coordinated intermediates appear to efficiently react to form products at pH values of 5.5 and 6.5, well below the pKa of ~15 expected for a solvent-exposed ribose 2'-OH.[36]

pH-Dependent Kinetic Studies of Platinum(II) Promoted Cleavage:

Because MALDI-MS does not provide a strictly quantitative readout of reaction kinetics we simultaneously pursued kinetic studies using 5' end-labeled RNA to monitor Pt(II)-induced cleavage of 5'-UUUUCpsCUUUU-3' at time points ranging from 30 sec to 27 h and at pH values of 3.5, 6.5, and 8.0. As shown in **Figure 5.5**, the rates of these reactions appear to increase with decreasing pH value, while total product yields show an inverse dependence on pH. Thus, at ~4 hrs the relative amounts of cleaved products are highest in the reaction carried out at pH 6.5, roughly matching the data obtained when the same reaction is analyzed by MALDI-MS (**Figure 5.4**). Similarly, these data depict a fast but low-yielding reaction at pH 3.5 as well as a slower (but

eventually higher yielding) reaction at pH 8.0. The slower reaction rates observed at high pH suggest that Pt(II) coordination to the PS is rate-limiting under these conditions. This is expected, as coordination of the neutral $[Pt(NH_3)_2ClOH]$ species present at pH 8.0 to an anionic PS-substituted RNA should be slow relative to coordination of the cationic $[Pt(NH_3)_2)Cl(OH_2)]^+$ species present at pH 6.5 and below. The observation that reactions at pH 8.0 consistently produce more cleaved products than reactions performed at pH 6.5 or 3.5 correlates well with the hypothesis that once bound to the PS, Pt(II) hydroxo species are significantly more reactive. These observations remain qualitative, as preliminary attempts to fit kinetic data to single (or even second) order rate equations have not produced acceptable fits when both early and extended timepoints are considered simultaneously. This apparent complexity further suggests the importance of multiple equilbria in these reactions. One limitation of these experiments is that denaturing polyacrylamide gel electrophoresis (dPAGE) separation used to characterize these reactions is unable to provide the same resolution as MALDI-MS. Consequently, we are only able to measure the amount of RNA cleavage taking place in these experiments, but not the conversion of starting material to platinated intermediates (B) or desulfurized products (C).

Activation of the Phosphorothioate Following Platinum(II) Coordination:

In addition to supplying a platform for general acid-base chemistry, Pt(II) coordination to a PS substitution is expected to withdraw electron density from the central P atom in the PS substitution, activating it towards nucleophilic attack. In order to provide a semi-quantitative analysis of this type of activation as well gain insight into the unique nature of a metal-coordinated PS bond[37,38] we carried out a series of preliminary computational studies aimed at determining the influence of the Pt(II) coordination on the buildup of positive charge at the P center. As a minimal model for a PS substitution we employed the molecule O,O'-diethylthiophosphate. DFT calculations were carried out using a LAVCP extended B3LYP 6-31G* basis set in order to accommodate the P, S and Pt atoms.[39] The results of these experiments are shown in **Figure 5.6**.

These data depict several features relevant to discussion of Pt(II)-induced cleavage, desulfurization and isomerization of PS substitutions. First, based on its calculated atomic electrostatic charge, the thiophosphate P atom is predicted to be significantly less electropositive than an equivalent diethylphosphate analog. This feature is interesting when considered in the context in which PS substitutions are normally employed, where differences in metal ion affinity are typically considered to be the largest factor underlying the "thio effect".[10] Second, coordination of Pt(II) species to the PS is predicted to increase the electropositive nature of the P

Phosphorothioate Complex	Charge	Atomic Electrostatic Charge			Minimized Geometry	Electrostatic Potential
		Pt	S	P		
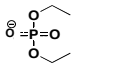	-1	N/A	N/A	1.37	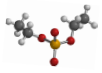	
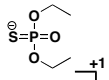	-1	N/A	-0.64	1.09	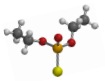	
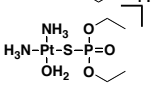	+1	0.93	-0.56	1.41	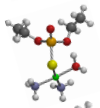	
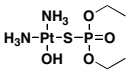	0	0.97	-0.64	1.36	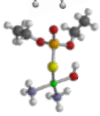	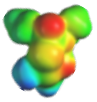
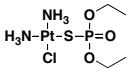	0	0.90	-0.56	1.44	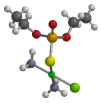	

Figure 5.6 Molecular modeling of Pt(II) coordination to O,O'-diethylthiophosphate. Structures, calculated electrostatic charge values, molecular structures and electrostatic potential maps computed using the BL3YP functional with a 6-31*G LAVCP-extended basis set.

center, restoring it to roughly the same level of electrostatic charge predicted for the diethylphosphate analog. Third, the structures predicted for these complexes depict the potential for hydrogen bonds to form between Pt(II) ligands and esteric oxygens (**Scheme 5.1b**). This feature suggests that a Pt(II)-aqua species could be placed within proper proximity to act as a general acid in the pathways proposed in **Scheme 5.1**. This finding further suggests that exchange-inert Pt(II) ligands may not be "innocent bystanders" in these reactions.[40] Aqua and hydroxo ligands in particular may form hydrogen bonds which could stabilize conformations of PS-coordinated Pt(II)-species and potentially influence pseudorotation (**Scheme 5.1b**). Finally, the identity of the "X" ligand in these complexes seems to have a minimal effect on activation of the P center. This finding contrasts an alternative hypothesis in which the electron withdrawing capacity of these ligands could be expected to influence PS reactivity.

Proposed Mechanism Describing Platinum(II) Phosphorothioate Reactivity:

Cumulatively, current data suggest the mechanism proposed in **Scheme 5.1** for reactions of Pt(II) species with PS-substituted RNA oligonucleotides. In this mechanism a cationic $[Pt(NH_3)_2(OH_2)X]^+$ (X = OH_2, Cl^-, ^-OH) complex coordinates to a PS thio ligand. A Pt(II)-coordinated hydroxo ligand is then responsible for deprotonating the adjacent 2'-OH. This hypothesis is supported by the accumulation of Pt(II)-coordinated intermediates at low pH.

Following deprotonation, an anionic phosphorane intermediate is formed, stabilized by Pt(II) coordination to the S atom. Pseudorotation around this intermediate can place either the 3' nucleotide or the Pt(II)-coordinated S atom in an apical position, poised to depart. The anionic oxygen of the thiophosphorane is not expected to be apically positioned based on previous work showing a lack of isomerization and desulfurization observed in hydroxide-catalyzed cleavage of PS substitutions.[12] Departure of either axial substituent may be facilitated by a metal-bound aqua ligand acting as a general acid by protonating the leaving group.[35] This would be an interesting example of how a single metal ion could provide both general acid and general base roles in phosphoryl transfer catalysis. Departure of the 3' nucleotide from the thiophosphorane intermediate results in Pt(II)-coordinated cyclic thiophosphates which seem to undergo rapid hydrolysis based on our inability to detect these species in our experiments. Interestingly, a Pt(II) aqua ligand could be envisioned to facilitate the hydrolysis of these complexes as well by potentially donating a proton to the departing thiol (**Scheme 5.1**). In the alternative thiophosphorane conformation, an axial Pt(II) thiol species departs. This would result in a sterically encumbered and unstable phosphotriester expected to undergo rapid hydrolysis to a mixture of 3'-5' and 2'-5' phosphodiester isomers as well as cleaved RNA products. Pt(II) thiol species result in all of these potential mechanisms. Interestingly we detect a number of low-nuclearity Pt(II) clusters of the general form $[Pt(NH_3)S]_nNa$ by MALDI-MS following these reactions (**Figure D.1**). The mechanism described here fits well with the experimental evidence gathered to date, although several important aspects of this reaction remain to be explored. Primary among these are determining the pKa of the aqua ligand bound to Pt(II) while it is coordinated to the PS, and direct measurements of Pt(II)-PS association rates.

Phosphoryl transfer reactions are critical in biology.[41,42] Metal ions often play essential roles in these types of reactions, especially in RNA.[4-7,43] Our understanding of these roles has been greatly extended by the use of site-specific PS substitutions.[7-9] Building on this, coordination of a Pt(II) species to the sulfur atom of a PS has been shown to be capable of activating site-specific RNA cleavage, desulfurization, and isomerization. The reaction leading to these products is proposed to occur through the mechanism described in **Scheme 5.1**. Developing a thorough understanding of the equilibria in this system may lead to the development of new experimental models for phosphoryl transfer catalysis[44,45] as well as provide insight into the myriad of ways in which Nature uses metal ions to perform similar chemistry in the core of complex cellular machines.

Future Work- Determining the pKa of Aqua Ligand Bound to a Platinated Phosphorothioate:

The O,O'-diethylthiophosphate molecule employed in DFT studies may provide a useful experimental model for determining the pK_a an of aqua ligand bound to a PS-coordinated Pt(II) center. Spectroscopic handles exist in this system include ^{1}H and ^{31}P NMR features. UV-active charge-transfer bands are also expected between Pt(II) and S and may also provide information regarding the protonation state of a Pt(II) coordinated aqua/hydroxo ligand. Monitoring changes in these spectral features as a function of pH should provide the means to ascertain the acidity of the aqua ligand bound to Pt(II).

Future Work- Synthesis of Platinum Triammine Complexes:

An interesting and important control to many of the preceding experiments will involve synthesis of $[Pt(NH_3)_3Cl]^+$.[47] A third exchange-inert NH_3 ligand is expected to preclude formation of reactive, PS-coordinated Pt(II) aqua species (**Scheme 5.1**) and shut down pathways that depend on intramolecular proton transfer. It also seems possible, given the absence of a second coordinated NH_3 in preliminary MALDI-MS studies (see previous sections), that the NH_3 ligand *trans* to the PS S atom may be labilized. Synthesis of Pt(II) complexes with chelating triamine ligands will presumably prevent loss of this ligand and allow us to fully explore this mechanism.

Summary and Bridge to Chapter VI:

Chapter V describes the reaction of Pt(II) complexes with phosphorothioate-substituted RNAs. Surprisingly, in addition to cleaved RNA products, this reaction produces a mixture of 3'-5' and 2'-5' phosphodiesters in place of the original phosphorothioate substitution. As outlined in **Scheme 5.1**, this reaction is believed to proceed through a stabilized pentacoordinate phosphorane intermediate. Continued studies aimed at determining the role of Pt(II)-coordinated ligands in the proposed mechanism may help further define the chemical basis for the "thio effect". Chapter VI again touches on these studies as it summarizes the insights gained regarding Pt(II) coordination to RNA and the future of this type of research.

CHAPTER VI

CONCLUDING REMARKS AND FUTURE DIRECIONS

Introduction:

This chapter includes topics generated by the mixing of ideas in the collaborative research environment fostered in the DeRose lab. Dr. Vickie DeRose is wonderfully curious and many of the ideas discussed in this chapter are her original ideas. Individuals in our lab have already begun work on several of these projects. Specifically, ongoing studies trying to understand the effects of Pt(II) drug treatment on RNA biology in yeast are actively being pursued by both Alethia Hostetter and Maire Osborn. Many of the ideas discussed in the 'technological applications' section of this chapter are independent ideas I have entertained during the last year during my search for a new place to pursue scientific research.

Concluding Remarks:

This dissertation describes how Pt(II) complexes coordinate to RNA. Chapter I outlines how the coordination chemistry of relatively simple square-planar Pt(II) compounds enables their use as frontline antitumor drugs. While for many years DNA has been the accepted molecular target of Pt(II) antitumor complexes, a small but growing line of evidence points towards the possibility that RNA targeting may also contribute to the *in vivo* activity of these drugs. Chapter II describes the ability of Pt(II) complexes to rapidly form intramolecular crosslinks in a structured RNA. RNA's ability to fold into incredibly complex biomolecular architectures, harboring features such as pre-formed metal ion coordination sites, raises important questions regarding how Pt(II) complexes may bind to these diverse and intricate structures. Chapter III describes how Pt(II) coordination to RNA influences the activities of RNA processing enzymes similar to those used by the cell to tailor RNA so that it may act in a myriad of biological roles. Pt(II) coordination generally disrupts the function of these enzymes raising new questions regarding how RNA damage inflicted by Pt(II) coordination is manifested in the mechanisms of Pt(II) antitumor drugs. This chapter also describes the reversal of Pt(II)-RNA adducts by thiourea, demonstrating the

relative affinity of Pt(II) for sulfur. In Chapter IV this thiophilicity is capitalized upon in the engineering of a new RNA-RNA crosslinking strategy based on the selective targeting of Pt(II) complexes to phosphorothioate substitutions installed at specific locations within RNAs. A phosphorothioate substitution installed in the catalytic core of the Hammerhead ribozyme recruits Pt(II) complexes to this site, anchoring them to this position where they can subsequently form crosslinks to nearby nucleotides in the active site of this catalytic RNA. Similarly, Pt(II) coordination to phosphorothioate substitutions embedded between ribonucleotides is able to activate a series of phosphoryl transfer reactions that result in both RNA cleavage as well as the isomerization of the phosphorothioate bond to produce a mixture of 3'-5' and 2'-5' phosphodiesters. Chapter V describes this reactivity, which seems to be based on the unique stabilization of a phosphorane intermediate. Cumulatively, these studies survey many aspects of Pt(II)-RNA chemistry and lay the groundwork for continued research aimed at determining the consequences of platinating cellular RNAs as well the creation of new nucleic acids technologies based on Pt(II) coordination to RNA.

Elucidating the Effects of Platinum(II) Coordination to RNA *In Vivo*:

Because Pt(II) antitumor drugs coordinate to many targets including proteins, DNA and RNA, elucidating the specific effects of Pt(II) coordination to RNA *in vivo* is a daunting task. **Figure 6.1** outlines a variety of important questions regarding the *in vivo* targeting of RNA and several experimental strategies that may be used to address them. These questions range from determining binding locations of Pt(II) antitumor drugs in specific RNA targets, to understanding broader effects such as the influence of Pt(II)-RNA damage in inducing apoptosis.

Specifically, the ability of Pt(II)-RNA adducts to disrupt reverse transcription (as described in Chapter III), has enabled us to begin to ask questions regarding specific Pt(II) binding locations *in vivo*. Ongoing research has employed primer extension analysis to characterize Pt(II) drug binding to ribosomes in *S. cereviseae*. Already these studies are producing exciting results, showing platination of both solvent-exposed nucleotides and nucleotides located in more buried regions including the peptidyl transferase center (Osborn and DeRose, *unpublished*).

Another line of research has begun to ask how translation is affected by Pt(II) coordination to mRNA targets. In these studies, RNA sequences expected to be targeted by Pt(II) antitumor drugs have been embedded within the untranslated regions of mRNAs encoded for on plasmid vectors. When such a structure is placed between regions of an mRNA that encode specific fluorescent

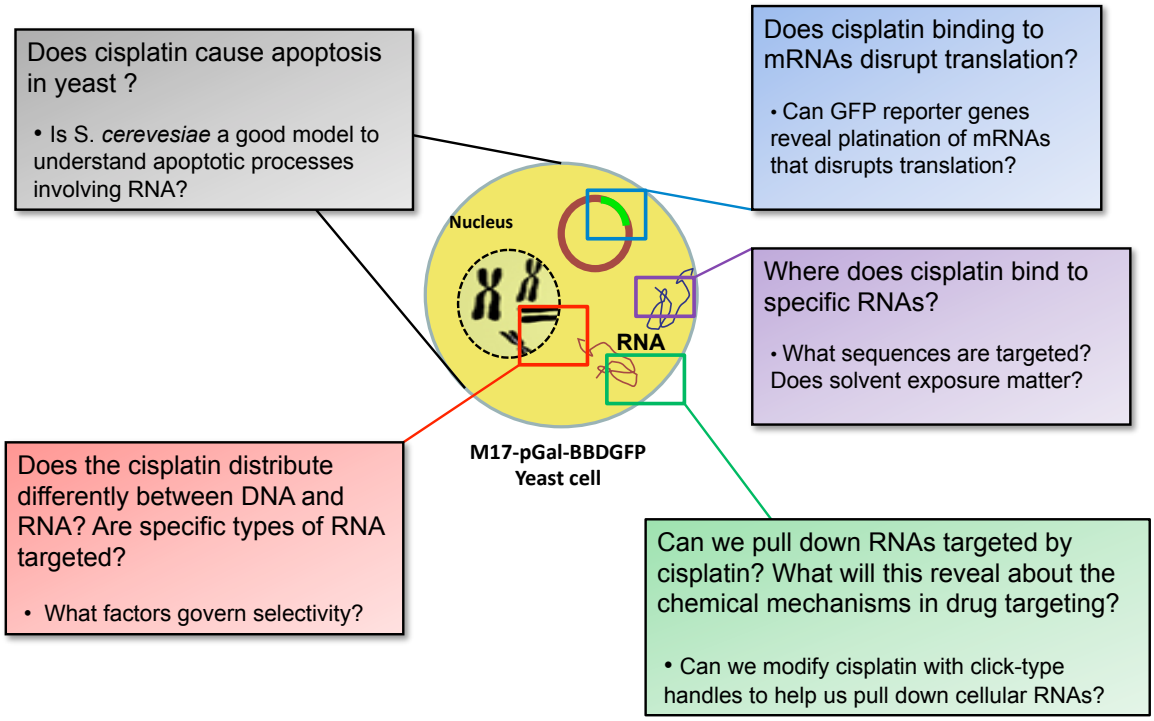

Figure 6.1. Ongoing research questions regarding the effects of platinating RNA in the cell.

reporters, we hope to monitor differential expression levels as a means of assessing the effects of Pt(II) antitumor drug binding to mRNA on translation.

The use of thiourea to reverse Pt(II)-RNA adducts (as described in Chapter III), is one component of developing a means to survey the different types RNAs targeted by Pt(II) drugs using "pull-down" type experiments. In such a strategy Pt(II) ligands could be engineered to allow selective recovery of Pt(II)-bound RNAs. Reversal of Pt(II)-RNA adducts, potentially using thiourea, followed by amplification of these sequences would allow us to address the sequence contexts and perhaps structural motifs targeted by Pt(II) complexes.

Next, the selective isolation of different types of RNA from Pt(II)-treated cells may provide new insights into how factors such as cellular localization affect the types of RNAs targeted by Pt(II) antitumor drugs. Alethia Hostetter is currently using inductively coupled plasma mass spectrometry (ICP-MS) to quantify Pt(II) drug binding in these types of experiments. Preliminary results show substantial platination of both mRNA and rRNA (Hostetter and DeRose, *unpublished*).

Finally, in studies also being pursued by Alethia Hostetter, we have become interested in the ability of cisplatin to initiate apoptosis in yeast. Using selective staining techniques in

combination with high resolution fluorescence microscopy, we are gaining new insights into the *in vivo* biological effects of Pt(II) antitumor drugs.

Combined, the aforementioned studies are an essential component of forming a comprehensive description of the molecular mechanisms of Pt(II) antitumor drugs.

Technological Applications of Platinum(II) Coordination to RNA:

In unmodified RNA and DNA sequences, Pt(II) typically coordinates to the N7 atom of both G and A nucleotides. Because these nucleotides comprise approximately half of the genome, technological applications of Pt(II) coordination must either capitalize on this broad specificity or artificially enhance it to achieve homogenous populations of platinated oligonucleotides. Both of these strategies are being pursued in the development of a number of new technologies including our own efforts to engineer new RNA crosslinking strategies.

In one high profile example of coordinating Pt(II) to both DNAs and RNAs, the biotechnology start-up firm Halcyon Molecular has promised to deliver a "$100 genome" based on the selective labeling of nucleic acid sequences using Pt(II).[1] Using recently developed methods to stretch single strands of genomic DNA over silicon slides[2] the company aims to selectively label G and T nucleotides using Pt(II) and Hg(II) respectively. Using dark field scanning transmission electron microscopy[3] to detect base-specific heavy-atom labeling, the company has promised to provide accurate, full-length reads in under 10 minutes and transform biomedicine into an 'information science'. Extending this technology to RNA may involve significant hurdles, however these efforts emphasize the utility of Pt(II) in nucleic acids technologies.

One of the major outstanding challenges in RNA science lies in determining the structures of the RNAs that comprise the transcriptome. While X-ray crystallography has proven to be an invaluable tool, this technique is limited in its ability to keep pace with an ever-expanding list of important biological RNAs. Along these lines, several research groups are developing strategies to map RNA structure in solution using chemistries amenable to high-throughput analysis. The "MOHCA bombs" developed by Das and coworkers[4] as well as SHAPE chemistry pioneered by the Weeks group[5] lead these efforts. Similarly, we hope to adapt the crosslinking strategy described in Chapter IV to function in higher throughput contexts. The ability to statistically incorporate phosphorothioate substitutions into RNA sequences by transcription using α-thio-NTP's[6] would provide a starting point for this development. Following crosslinking of these RNAs by Pt(II) complexes a combination of strategies including exonuclease digestion, Pt(II) removal by thiourea, and/or cleavage of embedded phosphorothioate substitutions by iodine reagents[7] could provide the means to identify crosslinked positions. Overlaying these results on

the predicted secondary structure of a given RNA could provide important information regarding the folded structure of the RNA in solution and add to the expanding list of techniques being used to rapidly probe RNA structure.

Finally, although not a strict 'technological' application, the opportunity to use the reactivity observed between Pt(II) complexes and phosphorothioate substitutions described in Chapter V may hold potential to provide a new model system for studying phosphoryl transfer reactions both in structurally simple situations and in the complex active sites of ribozymes. The ability of Pt(II) coordination to act as a platform for general acid-base chemistry may help reveal the role metal ions play in facilitating catalysis in these systems.

APPENDIX A

SUPPORTING INFORMATION FOR CHAPTER II: RAPID CROSSLINKING OF AN RNA INTERNAL LOOP BY THE ANTICANCER DRUG CISPLATIN

Materials and Methods:

Nucleic Acid Substrates: All RNAs, except BBD, were purchased from Dharmacon, Inc. DNA was purchased from Integrated DNA Technologies. BBD was transcribed in vitro from a plasmid template using T7 RNA polymerase. All nucleic acid substrates were purified by 20% dPAGE, eluted, then desalted and concentrated using Millipore YM-3 Centricon tubes. Subsequent buffer exchange and desalting was often accomplished using GE Healthcare G-25 microspin columns.

5′ End-Labeling: Prior to radiolabeling, the 5′ end of BBD was dephosphorylated using Antarctic phosphatase (New England Biolabs). 5′-OH Oligonucleotides were end-labeled with T4 poly-nucleotide kinase (USB) using γ32P-ATP (Perkin-Elmer). End-labeled oligonucleotides were purified by 20% dPAGE followed by overnight elution from excised gel bands. The resulting eluent was ethanol-precipitated and desalted or buffer-exchanged as described above.

Cisplatin Aquation: Cisplatin (Sigma-Aldrich) was stored as a 1 mM solution in 10 mM NaCl in the dark at 4 °C. Immediately before use, cisplatin was aquated with 0.95 equiv of 12 mM AgNO3 (stored in the dark). The aquation reaction was incubated at 50 °C for 1 h, at which time AgCl was precipitated by centrifugation. The supernatant solution was removed and diluted accordingly. On the basis of ^{195}Pt NMR (data not shown), the main platinum species varied by pH: $[Pt(NH_3)_2Cl(OH_2)]+$ for pH 6.8 and $[Pt(NH_3)ClOH]$ for pH 7.8.

Platination of BBD (Figure 2.2b): A trace amount of 5′ end-labeled BBD with 0.2 μM unlabeled BBD was annealed by heating to 90 °C for 90 s followed by cooling to room temperature, then reacted with 0–40 μM cisplatin in deionized water for 1.5 h at 37 °C. The bulk reaction mixtures were mixed with formamide loading buffer and immediately applied to 18% dPAGE. Results were imaged using a Molecular Dynamics phosphor screen and scanned on a Molecular Dynamics Storm 860.

Comparative Platination of SBBD and BBD (Figure 2.2c): Twenty micromolar (0.2 nmol) of BBD RNA, each individual SBBD strand, or the SBBD hybrid was annealed and rested on ice for

30 min. RNAs were then incubated in the presence of absence of 200 μM cisplatin (added as a 1 mM solution with 8 mM NaCl) in 5 mm triethanolamine (TEA) pH 6.8 for 12–16 h at 37 °C. Reaction mixtures were analyzed on 20% dPAGE and visualized by staining with methylene blue.

Isolation of 5′ End-Labeled, Cross-Linked RNAs: BBD: 5′ End-labeled BBD in the presence of 0.1 μM unlabeled BBD was annealed and reacted with aquated cisplatin in 100 mM $NaNO_3$, 1 mM $Mg(NO_3)_2$, and 5 mM 3-(N-morpholino)propanesulfonic acid (MOPS) (pH 6.8) at 37 °C for 23 h. Reaction products were isolated via excision from 18% dPAGE. RNA was eluted overnight into deionized water and desalted using in-house prepared G-25 sephadex spin columns (BioRad). SBBD: One 5′ end-labeled strand was annealed in 10 μM of the unlabeled complement RNA in 12.5 mM NH_4NO_3 and reacted with 100 μM aquated cisplatin for 23 h. The cross-linked product was excised from 20% PAGE and eluted overnight into deionized water. Following speedvac concentration, SBBD cross-links were desalted using G-25 sephadex spin columns (GE Healthcare).

Hydrolysis Mapping of Cross-Linked RNAs: Trace 5′ end-labeled, cross-linked RNAs were dried to completion in the presence of 0.2 pmol unlabeled RNA corresponding to the 5′ end-labeled strand. Samples were then resuspended in 50 mM Na_2CO_3/$NaHCO_3$ (pH 9.5) and 1 mM EDTA and reacted at 90 °C for times ranging from 5 to 25 min. The reaction was quenched by the addition of 8 M urea, 10 mM sodium citrate (pH 3.5), and 0.005% (w/v) xylene cyanol loading buffer and held on dry ice until electrophoresis. The results were analyzed on 15 or 20% dPAGE (BBD and SBBD, respectively) then visualized via phosphorimaging.

Reference lanes of 5′ end-labeled un-cross-linked RNAs were generated from hydrolysis as above and by partial nuclease digestion by RNase T1 (Ambion) or U2 (Pierce/Thermo Scientific). Briefly, 5′ end-labeled RNA with 0.2 μM of the corresponding unlabeled RNA in 8 M urea, 10 mM sodium citrate (pH 3.5), and 0.005% (w/v) xylene cyanol was reacted for at 50 °C for 12–15 min with 1U T1 RNase or 0.2U U2 RNase. Samples were then held on dry ice until electrophoresis.

Kinetic Analysis: Prior to kinetic analysis, 0.1 μM oligonucleotide with trace 5′ end-labeled material was annealed in buffered solution by heating to 90 °C for 90 s followed by gradual cooling to room temperature or, for the case of the SBBD hybrid, resting on ice for 30 min. Buffers included either 100 mM $NaNO_3$, 1 mM $Mg(NO_3)_2$, and 5 mM triethanolamine (TEA) (pH 7.8) or 100 mM $NaNO_3$, 1 mM $Mg(NO_3)_2$, and 5 mM (MOPS) (pH 6.8) depending on desired pH. Freshly aquated cisplatin was added to final concentrations of 13, 25, or 50 μM, and the reactions were incubated at 37 °C for times ranging from 1 min to 35 h. Aliquots were removed and

stopped by ethanol precipitation or dilution with formamide and freezing. These aliquots were applied to 18–19% dPAGE and visualized by autoradiography. Each kinetic experiment was repeated at least three times. Molecular dynamics ImageQuant software version 5.0 was used to quantify the reaction mixtures from each kinetics experiment. Rate constants were generated from data analysis using SigmaPlot version 8.0.

MALDI-MS: Isolation of platinated oligonucleotides for MALDI-MS analysis: 30 μM of an oligonucleotide was annealed in 100 mM $NaNO_3$, 1 mM $Mg(NO_3)_2$, and 5 mM MOPS (pH 6.8) and reacted with either 90 μM aquated cisplatin for LSBBD or 150 μM for RNA HP and DNA HP. Samples were incubated at 37 °C for 5 h, at which time they were applied to 19% dPAGE. Products were stained with methylene blue and excised. Oligonucleotides were recovered via electroelution using a Schleicher and Schuell Elutrap electro-separation system, concentrated, and desalted. Bulk time-course reactions for MALDI-MS analysis: 0.6 nmol of an oligonucleotide was reacted under identical conditions to those used in kinetics experiments (see above). Reactions were incubated for 1 or 23 h and stopped by ethanol precipitation, dried, and desalted using G-25 sephadex spin columns.

Oligonucleotide samples (~50–100 pmol) were additionally desalted on C18 ZipTips (Millipore) following the manufacturer's protocol for RNA. RNA was eluted in a matrix solution containing 41 mg/mL 3-hydroxypiccolinic acid and 4.5 mg/mL diammonium citrate then applied to the sample plate. MALDI-MS analysis was performed on a Waters QTof Premier mass spectrometer in positive-ion mode using V-mode optics.

SBBD Thermal Denaturation: Thermal denaturation of SBBD, in a "kinetics" buffer of 100 mM $NaNO_3$, 1 mM $Mg(NO_3)_2$, and 5 mM TEA (pH 7.8), was monitored on a Varian Cary 300 Bio UV–visible spectrophotometer with multicell holder and temperature controller. These data were fit with the accompanying software, giving a Tm of 59 °C and a calculated Kd at 37 °C of $6.8 \times 10{-}9$ M. On the basis of this Kd, approximately 60% of the SBBD hybrid would be formed during the kinetic analyses, which used a concentration of 0.1 μM for each SBBD strand.

Figure A.1:

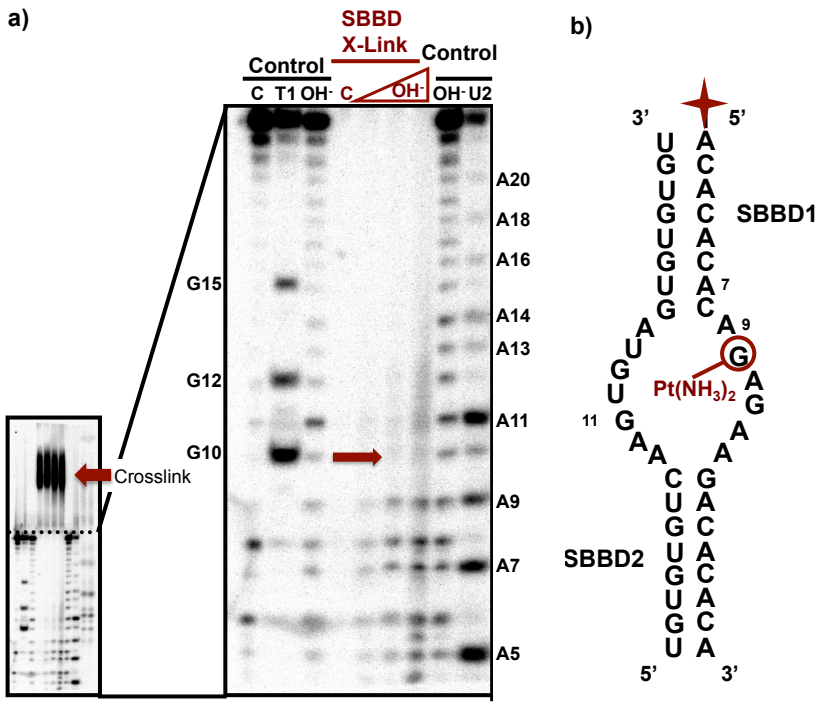

Figure A.1. Location of platinum crosslinks formed with SBBD1. (a) The predicted secondary structure of hybridized SBBD1 and SBBD2 RNAs with the location of the major cisplatin induced crosslink on the SBBD1 strand highlighted. (b) 20% dPAGE analysis of the products of partial alkali hydrolysis of the SBBD crosslink with 5'-end-labeled SBBD1. Lanes: Control- **C:** 5' end-labeled SBBD1. **T1:** G specific sequence ladder generated by partial nuclease digestion of SBBD1 RNA by T1 RNase. **U2:** A specific sequence ladder generated by partial nuclease digestion of SBBD1 RNA by U2 RNAse. **OH^-:** Reference alkali hydrolysis ladder for SBBD1. SBBD Crosslink Samples- **C:** dPAGE-isolated SBBD crosslink. **OH^- Lanes:** dPAGE-isolated SBBD crosslink treated under alkali hydrolysis for increasing amounts of time.

Figure A.2:

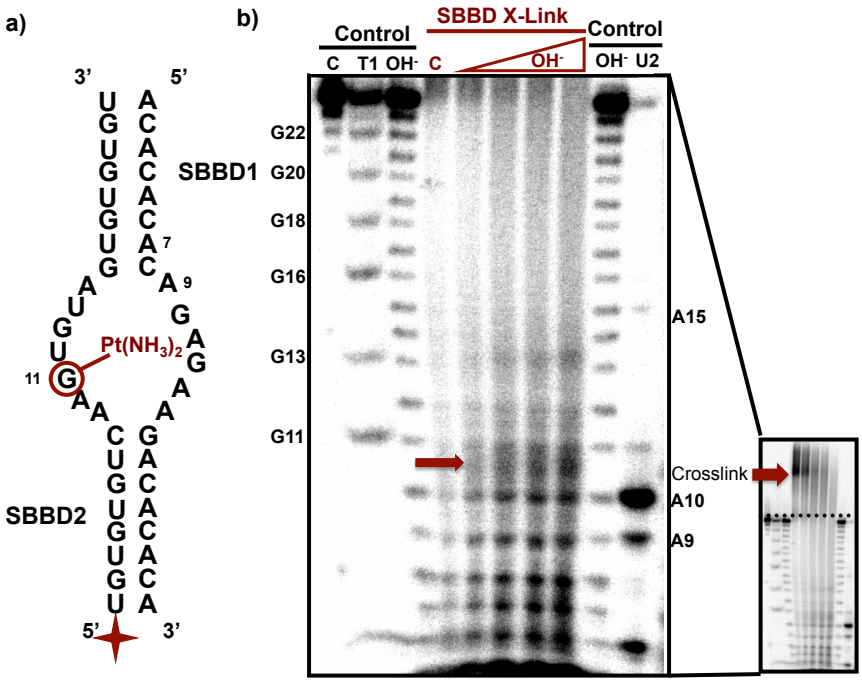

Figure A.2. Location of platinum crosslinks formed with SBBD2. (a) 20% denaturing PAGE analysis of the products of partial alkali hydrolysis of the SBBD crosslink with 5'-end-labeled SBBD2. Lanes: Control- **C:** 5' end-labeled SBBD2. **T1:** G-specific sequence ladder generated by partial nuclease digestion of SBBD2 RNA by T1 RNase. **U2:** A-specific sequence ladder generated by partial nuclease digestion of SBBD2 RNA by U2 RNAse. **OH^-:** reference alkali hydrolysis ladder for SBBD2. SBBD Crosslink Samples- **C:** dPAGE-isolated SBBD2 crosslink **OH^- Lanes:** dPAGE-isolated SBBD crosslink treated under alkali hydrolysis for increasing amounts of time. (b) The predicted secondary structure of hybridized SBBD1 and SBBD2 RNAs with the location of the major $[Pt(NH_3)_2]^{2+}$ on the SBBD2 strand highlighted.

Figure A.3:

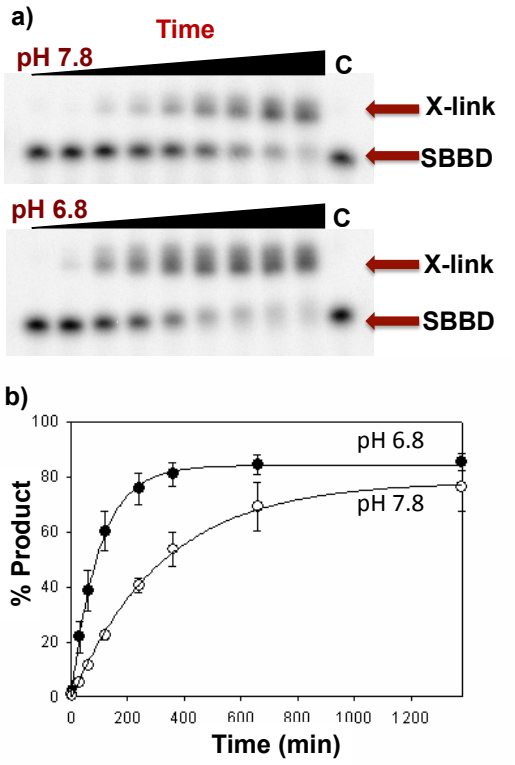

Figure A.3. Kinetic analysis of SBBD crosslinking. (a) dPAGE radiograms depicting products of cisplatin binding to SBBD in pH 6.8 and 7.8 over time. (b) Comparison of the reaction rates of SBBD in pH 6.8 (filled circles) and 7.8 (open circles). Conditions: (a) Reactions were performed with 0.1 µM SBBD duplex with either 50 µM cisplatin in 5 mM TEA (pH 7.8) or 25 µM cisplatin in 5 mM MOPS (pH 6.8). Both reactions were in 100 mM $NaNO_3$, 1 mM $Mg(NO_3)_2$, and at 37 °C. Reactions analyzed by 20% dPAGE.

Figure A.4:

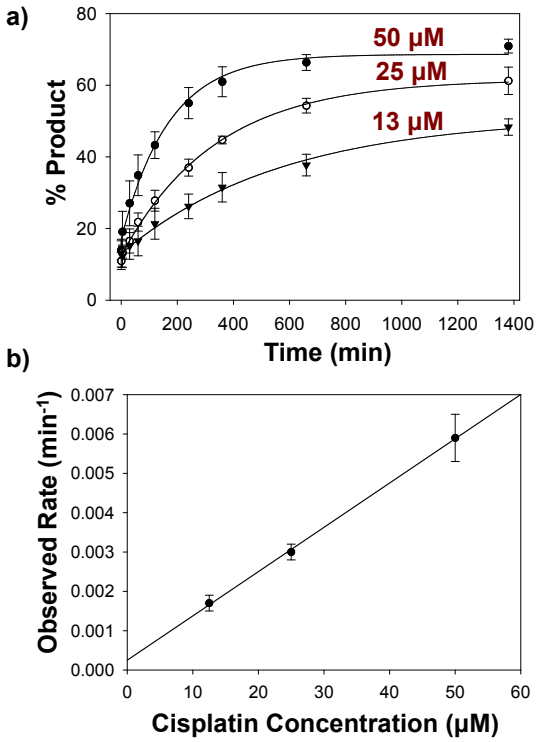

Figure A.4. Platinum(II) concentration-dependent crosslinking of BBD RNA. (a) BBD kinetics with 50 µM (filled circles), 25 µM (open circles), and 12.5 µM (triangles) cisplatin. (b) Observed rate constant (k_{obs}) versus cisplatin concentration. Conditions: Reactions were performed in 100 mM $NaNO_3$, 1 mM $Mg(NO_3)_2$, and 5 mM TEA (pH 7.8) at 37 °C.

Table A.1:

Construct[a]	µM CP	pH	k_{obs} (10^{-4} min^{-1})	k_{rxn2} (M^{-1} s^{-1})[b]
BBD	50	7.8	59(6)	2.0(2)
BBD	25	7.8	30(2)	2.0(1)
BBD	12.5	7.8	17(2)	2.3(2)
BBD	25	6.8	128(11)	8.5(7)
RNA HP	50	7.8	50(1)	1.7(3)
DNA HP	50	7.8	10(1)	0.33(3)
SSBBD	50	7.8	31(2)	1.1(1)
SSBBD	25	6.8	102(3)	6.8(2)

Table A.1. Platination rates of RNA and DNA constructs. **a)** All experiments used 0.1 µM oligonucleotide (or 0.1 mM SBBD duplex) and were performed at 37 °C with 100 mM $NaNO_3$ and 1 mM $Mg(NO_3)_2$. Trials at pH 7.8, and 6.8 were done in 5 mM TEA and MOPS respectively. **b)** Because all kinetics were performed under pseudo-first order conditions, second order rate constants were obtained by dividing k_{obs} by the concentration of cisplatin used.

APPENDIX B

SUPPORTING INFORMATION FOR CHAPTER III: ENZYMATIC PROCESSING OF PLATINATED RNAS

Materials and Methods:

Nucleic Acid Substrates: 13-mer RNAs were ordered from Dharmacon, Inc., deprotected following the manufacturer's protocol and were reacted without further purification. DNA was purchased from Integrated DNA Technologies. PEBBD was transcribed from a dsDNA template containing primers necessary for PCR amplification and for transcription by T7 RNA polymerase. Following transcription PEBBD RNA was purified using 15-20% dPAGE, eluted then desalted and concentrated using Millipore YM-3 Centricon tubes. Subsequent buffer exchange and desalting was often accomplished with G-25 Sephadex size exclusion resin (GE Healthcare) on laboratory prepared microcentrifuge columns (BioRad). Oligonucleotide concentrations were determined using a Varian Cary 300 Bio UV-visible spectrophotometer.

Cisplatin Aquation: Cisplatin (Sigma-Aldrich) was stored as a 1mM solution in 10mM NaCl and stored in the dark at 4 °C. Immediately before use, cisplatin was aquated by reaction with 0.95 equiv. of 12mM $AgNO_3$ (stored in the dark). The aquation reaction was incubated at 50°C for 1 h, at which time AgCl was precipitated by centrifugation. The supernatant solution was removed and diluted accordingly. The predominant platinum species formed varies by pH with $[Pt(NH_3)_2Cl(OH_2)]^+$ expected to be the main Pt-complex present at pH 7.0 (by ^{195}Pt NMR, data not shown).

Platination of 13-mer RNAs: 80μM RNA (typically 8 nmol) was reacted with 240 μM aquated cisplatin in the presence of 1mM $Mg(NO_3)_2$, 100 mM $NaNO_3$, in 10 mM Na_2PO_4 buffer (pH 7.0) for 16 hr, 37 °C. Reactions were stopped by application to G-25 Sephadex spin-columns to remove unbound platinum, then eluted and dried to completion by SpeedVac, and resuspended in deionized water. At this time aliquots were removed and subjected to MALDI-MS in order to establish proper platination. MALDI-MS showed these reaction conditions to produce predominantly mono-platinated RNAs that were then used in nuclease-processing studies without further purification.

No significant amount of intermolecular crosslinked products were observed, even between platinated 5'-$(U)_6$-GU-$(U)_5$-3' RNA strands, and attempts to force such crosslinking were unsuccessful (data not shown). Presumably, even under the moderately strong ionic conditions employed (120 mM Na^+, 1mM Mg^{2+}) electrostatic repulsion between two negatively charged and non-complementary RNA oligonucleotides prevents platinum crosslinking.

3'→5' Venom Phosphodiesterase (VPD) Digestion of Platinated RNAs: Venom phosphodiesterase from *Crotalus adamanteus* (Phosphodiesterase I, VPD) was obtained as a lyophilized solid (Sigma-Aldrich). ~5 mg of the white solid (≥0.01 unit/mg) was dissolved in 500 uL of a 50% glycerol solution containing 10 mM $Zn(OAc)_2$ and used as an enzyme stock of ~1 x 10^{-4} U/ul. Digestion reactions were carried out by addition of ~1 x 10^{-4} U of VPD stock to 400 pmol of platinated RNA (100 μM in H_2O). Reactions were incubated 2 h at 50 °C at which time protein was removed by phenol-chloroform extraction and two washes with 24:1 chloroform:isoamylalcohol. The aqueous layer was retained and dried to completion by SpeedVac. RNA was further purified by C_{18} ZipTips (Millipore) before MALDI-MS (*vida infra*).

5'→3' Spleen Phosphodiesterase (SPD) Digestion of Platinated RNAs: Calf spleen phosphodiesterase (Phosphodiesterase II, SPD) was obtained as a 0.1 U/uL 50% glycerol solution (EMD Chemicals) and used as received. Digestion reactions were carried out by addition of 0.1U SPD to 400pmol of platinated RNA (~100 μM in H_2O). Reactions were incubated 4hr at 50 °C at which time protein was removed by phenol-chloroform extraction and two washes with 24:1 chloroform:isoamylalcohol. The aqueous layer was retained and dried to completion by SpeedVac. RNA was further purified by C_{18} ZipTips before MALDI-MS (*vida infra*).

RNase U2 Digestion of Platinated RNAs: RNase U2 was obtained as a 1 U/uL, 50% glycerol solution (ThermoScientific) and used as received. Digestion reactions were carried out by addition of 1U RNase U2 to 400 pmol platinated or un-platinated RNA (~100 μM in H_2O). Reactions were incubated 1 h at 50 °C and were then purified by C_{18} ZipTips prior to MALDI-MS analysis (*vida infra*).

MALDI-MS: Dried RNA samples were resuspended in deionized water and purified using C_{18} ZipTips using a procedure modified from the manufacturer's protocol for RNA[58]: ZipTips were washed by aspiration three times with 1:1 MeCN:H_2O, and equilibrated by washing three times with 0.1% trifluoroacetic acid (TFA). RNAs were bound to the tip by repeated aspiration of the analyte solution. Bound RNA was washed three times by aspiration with 0.1% TFA, three times with deionized water, and then eluted from the column using two washes of 1:1 MeCN:H_2O. The eluent was dried to completion by SpeedVac and resuspended in a matrix consisting of 375 mM 2',4',6'-trihydroxyacetophenone (THAP, Sigma-Aldrich), 30 mM diammonium citrate in 3:1

EtOH:H_2O, with added NH_4^+ loaded Dowex cation exchange beads (Aldrich) and applied to the sample plate. MALDI-MS analysis was performed on a Waters QToF Premier mass spectrometer in positive-ion mode using V-mode optics.

5' End-Labeling: The DNA primer used for reverse transcription of PEBBD was radiolabeled with T4 poly-nucleotide kinase (Fermentas) using γ^{32}P-ATP (Perkin-Elmer). The end-labeled primer was purified by 20% dPAGE, imaged by phosphor screen and excised. Excised gel bands were eluted overnight in deionized water. The resultant eluent was ethanol precipitated and further desalted using G-25 Sephadex spin-columns.

Platination of PEBBD: 20 μM (200 pmol) PEBBD RNA was annealed and platinated with 0 to 1 equiv activated cisplatin in 1 mM $Mg(NO_3)_2$, 10 mM $NaNO_3$, 5 mM 3-morpholinopropanesulfonic acid (MOPS), pH 6.8 for 12 h at 37 °C. Reactions were passed through G-25 Sephadex spin-columns to remove unbound platinum, and the eluent was dried to completion by SpeedVac. Reactions were resuspended in deionized water prior to reverse transcription.

Reverse Transcription of Platinated PEBBD: Platinated PEBBD samples were reverse transcribed using M-MuLV reverse transcriptase (Fermentas) using a procedure based on the manufacturer's protocol. Briefly, 100pmol of the appropriate 5'-end-labeled DNA primer was annealed to platinated PEBBD in the manufacturer's supplied reaction buffer and then incubated at 42 °C for 1 h after addition of the enzyme. The reactions were diluted with formamide loading buffer containing 0.005% (w/v) xylene cyanol and bromophenol blue and analyzed using 15% dPAGE. ImageQuant version 5.0 software(Molecular Dynamics) was used to quantify band intensities. Microsoft Excel 2004 was used to normalize and graph Image Quant generated intensity values.

Sequence referencing lanes were generated with a Sequenase Version 2.0 DNA Sequencing kit (USB Corporation) following the manufacturer's protocol, using an appropriate DNA template and the same 5' end-labeled primer used with PEBBD.

Platinum Removal by Thiourea: 400 pmol of the platinated 5'-$(U)_6$-GU-$(U)_5$-3' or 5'-$(U)_6$-GG-$(U)_5$-3' RNA (200 μM in H_2O, 2 uL) was reacted with an equal volume (2 uL) of a saturated thiourea solution. Reactions were incubated at 37 °C for varying amounts of time, purified using C_{18} ZipTips and analyzed by MALDI-MS.

PEBBD RNA Sequence and Primers:

PEBBD:

5'- GGAAGACAAGAAUAACGCUCAAGCAUCAAGUGUAGUAUCCGAAAGGAUACAG AGAAGAUGC*UUCGACACGAUGCUCACAACAGAC* -3'

RT PRIMER:

5'- *GTCTGTTGTGAGCATCGTGTCGAA*-3'

Standard Transcription Conditions:

An DNA template encoding a consensus T7 promoter sequence immediately before the PEBBD sequence as well primers appropriate for PCR amplification were obtained from Integrated DNA Technologies. Following amplification and Taq fill-in, DNA templates were annealed and transcribed using T7 RNA polymerase expressed in our laboratory. A typical transcription reaction contained ~1ug/uL DNA template, 0.01U/uL inorganic pyrophosphotase, ~0.1 ug/uL T7 RNA polymerase and 100 mM NTP's in a solution of 12 mM $MgCl_2$, 2 mM spermidine, 40 mM dithiothreitol, 80 mM HEPES, pH 7.5. Transcription reactions were typically incubated overnight, DNAse (Fermentas) treated following the manufacturers protocol, and phenol chloroform extracted. Samples were diluted with formamide loading buffer and applied to 20% dPAGE gels, excised by UV shadowing and eluted in deionized water.

Figure B.1:

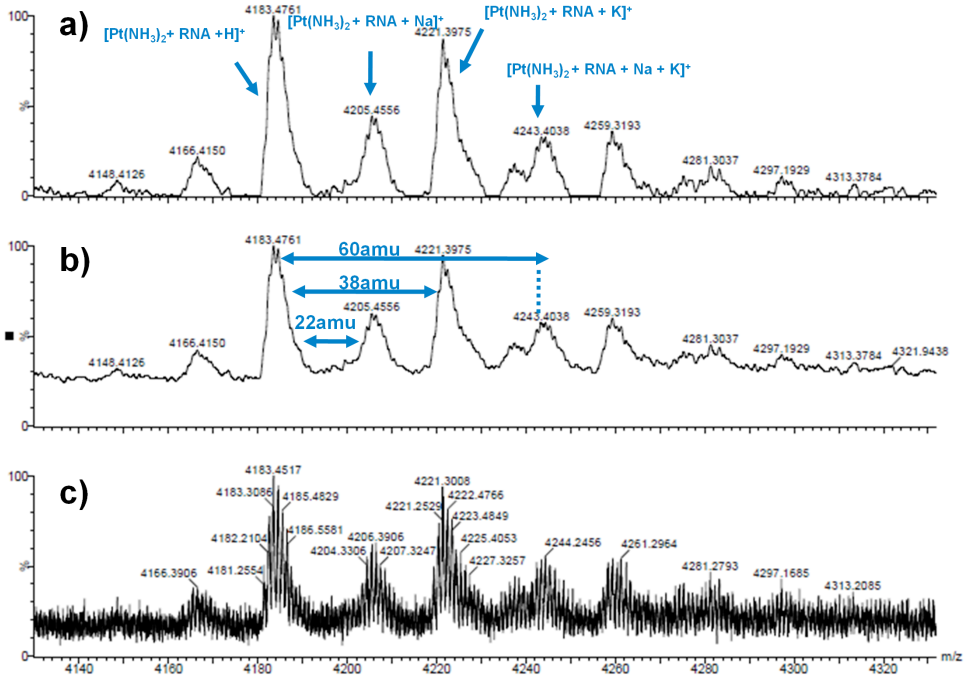

Figure B.1. MALDI-MS spectra of platinated 5'-$(U)_6$-GU-$(U)_5$-3' RNA. a) Smoothed, background subtracted MALDI-MS spectrum of platinated 5'-$(U)_6$-GU-$(U)_5$-3' RNA. Peaks assigned as indicated. b) Smoothed MALDI-MS spectrum of platinated 5'-$(U)_6$-GU-$(U)_5$-3' RNA. Rounded mass differences between different peaks indicated in blue. c) Unprocessed MALDI-MS spectrum of platinated 5'-$(U)_6$-GU-$(U)_5$-3'. The calculated average mass of the un-platinated RNA is 3957 amu. Addition of a [$Pt(NH_3)_2$-2H] fragment adds 227 amu (RNA + $Pt(NH_3)_2$ = 4184 amu). Peaks corresponding to additional Cl (35 amu) or aqua (18 amu) ligands are not observed.

Figure B.2:

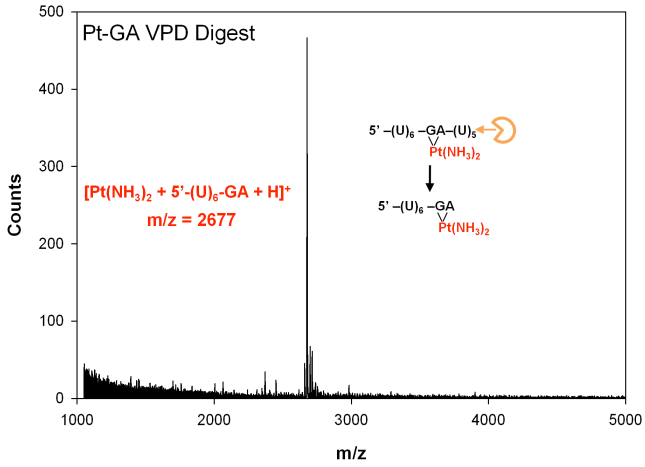

Figure B.2. VPD (3'→5') digestion of platinated 5'-$(U)_6$-GA-$(U)_5$-3' RNA. MALDI-MS spectrum of the products of VPD digestion of platinated 5'-$(U)_6$-GA-$(U)_5$-3' RNA. The major peak represents digestion up to the internal A (calculated m/z = 2677, measured m/z = 2677). Digestion of an RNA containing a monofunctional $[Pt(NH_3)_2X]$ adduct at G would be expected to give products corresponding to $[Pt(NH_3)_2$ + 5'-$(U)_6$-G + $H]^+$ (calculated m/z = 2347). The absence of such products is taken to indicate cisplatin diadducts forming at the GA pair.

Figure B.3:

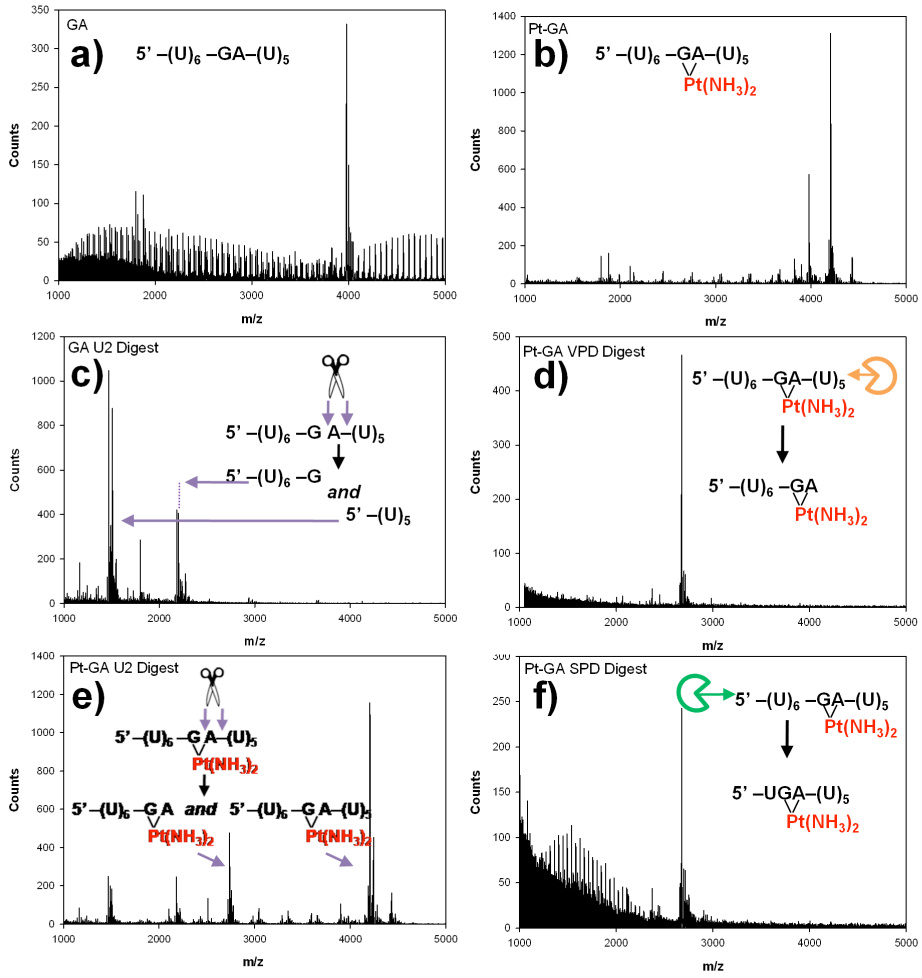

Figure B.3. MALDI-MS spectra of reactions involving 5'-$(U)_6$-GA-$(U)_5$-3' RNA. MALDI-MS spectra of: a) the unmodified RNA; b) the platinated RNA; c) RNase U2 digestion products of the unmodified RNA; d) VPD digestion products of the platinated RNA; e) RNase U2 digestion products of the platinated RNA; f) SPD digestion products of the platinated RNA.

Figure B.4:

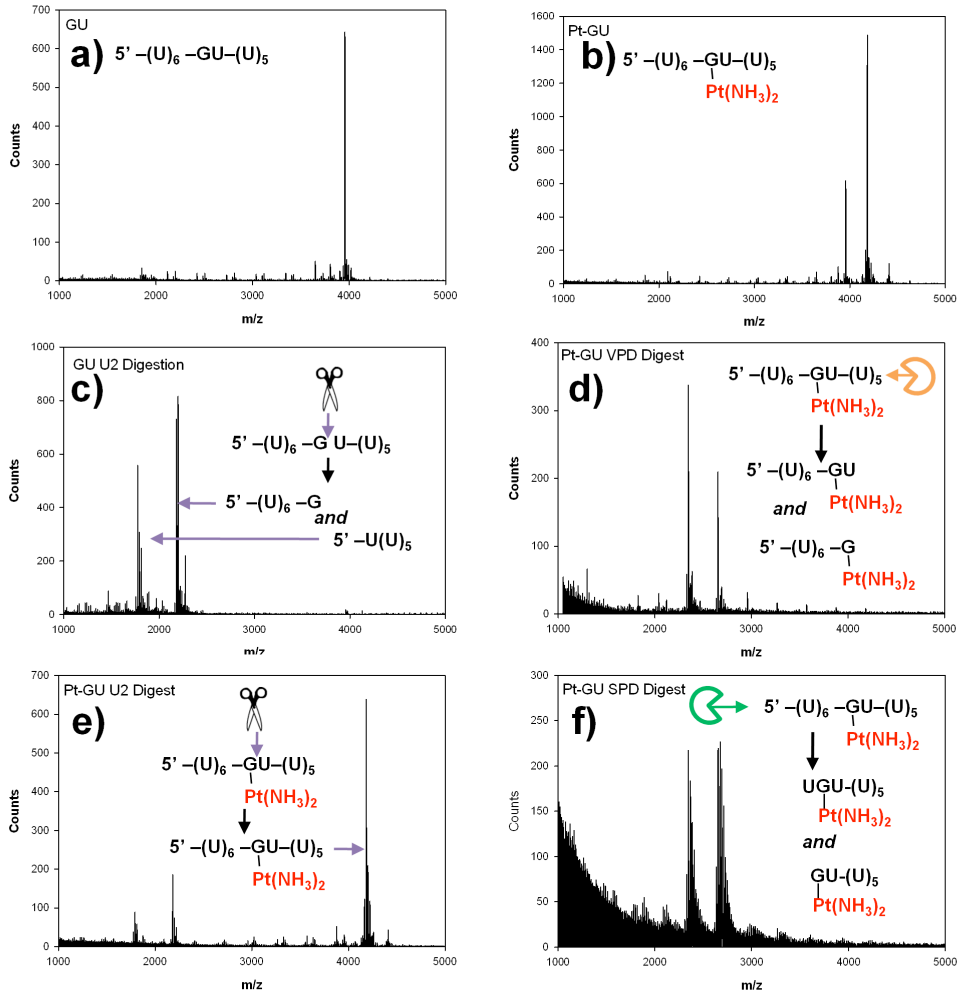

Figure B.4. MALDI-MS spectra of reactions involving 5'-$(U)_6$-GU-$(U)_5$-3' RNA. MALDI-MS spectra of: a) the unmodified RNA; b) the platinated RNA; c) RNase U2 digestion products of the unmodified RNA; d) VPD digestion products of the platinated RNA; e) RNase U2 digestion products of the platinated RNA; f) SPD digestion products of the platinated RNA.

Figure B.5:

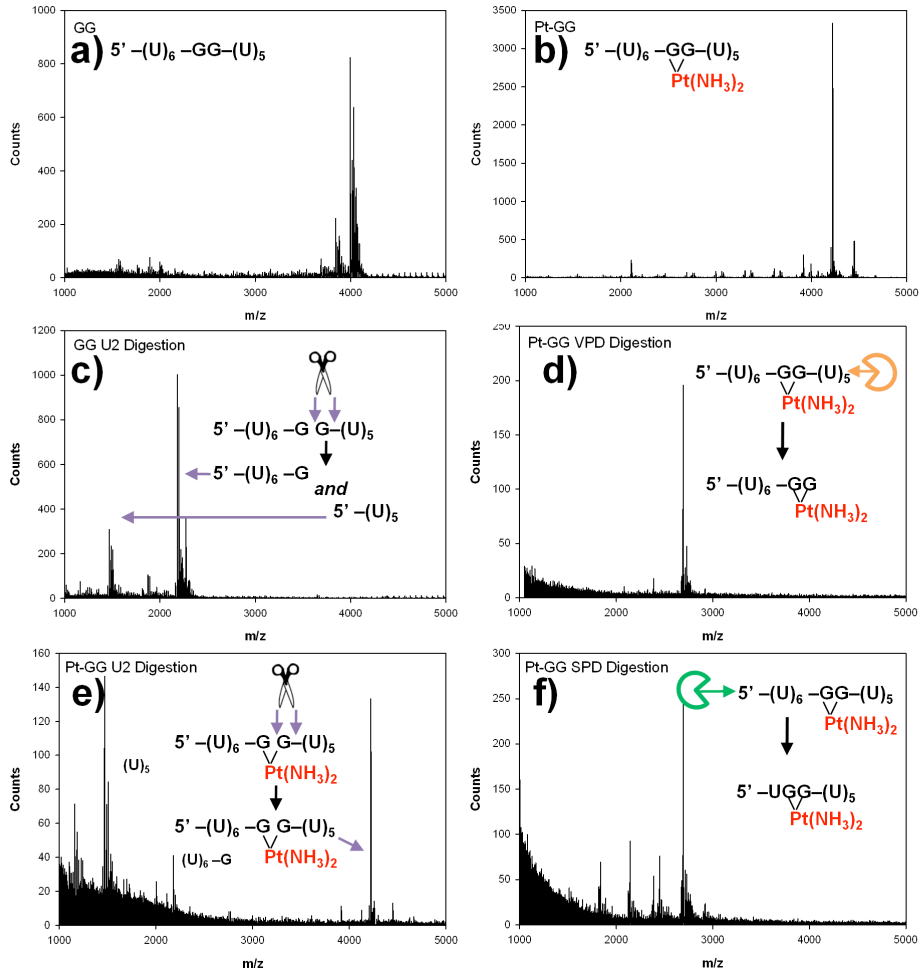

Figure B.5 MALDI-MS spectra of reactions involving 5'-$(U)_6$-GG-$(U)_5$-3' RNA. MALDI-MS spectra of: a) the unmodified RNA; b) the platinated RNA; c) RNase U2 digestion products of the unmodified RNA; d) VPD digestion products of the platinated RNA; e) RNase U2 digestion products of the platinated RNA; f) SPD digestion products of the platinated RNA. $(U)_6$-G and $(U)_5$ peaks in (e) result from cleavage of un-platinated RNAs (RNA products were not separated following platination reactions). The high relative intensity of these products reflects the low number of ions detected, overall, in this experiment and an observed bias for lower molecular weights during data collection over broad m/z ranges.

Figure B.6:

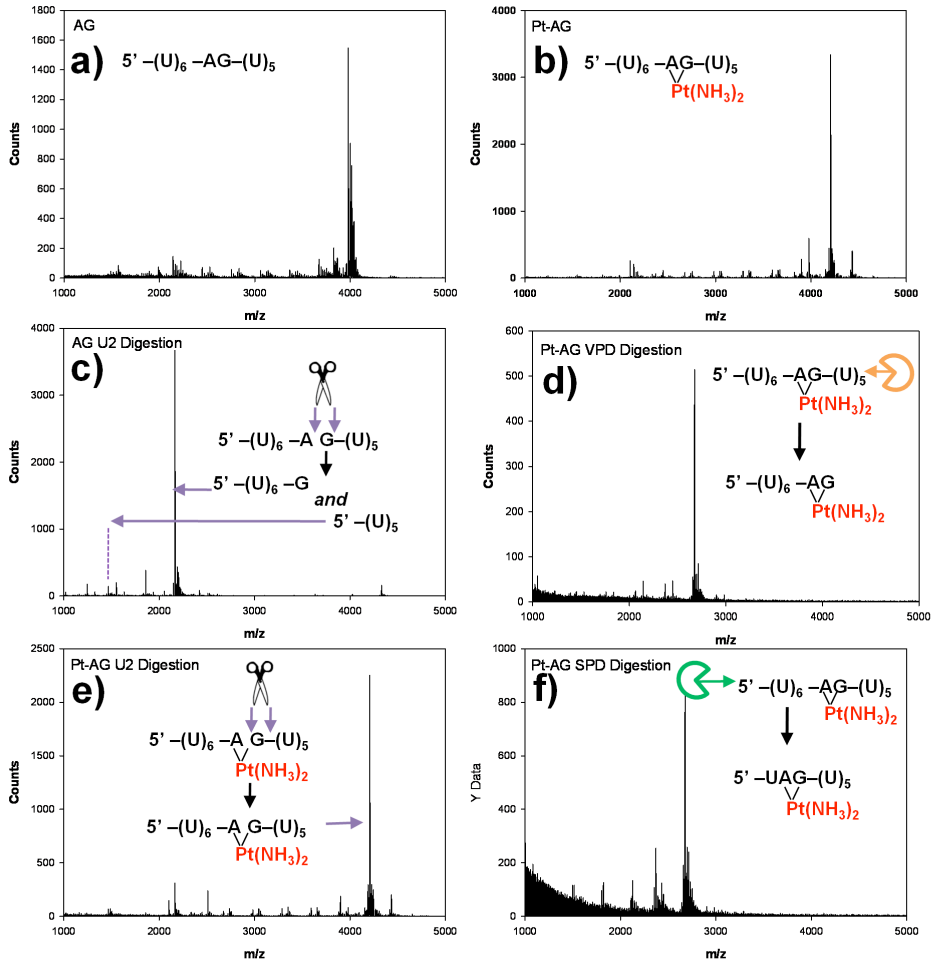

Figure B.6. MALDI-MS spectra of reactions involving 5'-$(U)_6$-AG-$(U)_5$-3' RNA. MALDI-MS spectra of: a) the unmodified RNA; b) the platinated RNA; c) RNase U2 digestion products of the unmodified RNA; d) VPD digestion products of the platinated RNA; e) RNase U2 digestion products of the platinated RNA; f) SPD digestion products of the platinated RNA. The 5'-$(U)_5$ products in (c) may be obscured by the formation of multiple alkali earth metal adducts, which can result in a spread of low-intensity peaks.

APPENDIX C

SUPPORTING INFORMATION FOR CHAPTER IV: SITE-SPECIFIC PLATINUM(II) CROSSLINKING IN A RIBOZYME ACTIVE SITE

Materials and Methods

Nucleic Acid Substrates: RNA oligonucleotides were ordered from Dharmacon Inc., deprotected following the manufacturer's protocol, dried by SpeedVac and resuspended in deionized water. Oligonucleotide concentrations were determined using a Varian Cary 300 Bio UV-visible spectrophotometer, measuring absorbance at 260 nm. MALDI-MS was routinely used to verify RNA quality before subsequent reaction.

***Cis*-$[Pt(NH_3)_2Cl(OH_2)]^+$:** *Cis*-$Pt(NH_3)_2Cl_2$, (Sigma-Aldrich) was prepared as a 1 mM aqueous solution in 10 mM NaCl and stored in the dark at 4 °C. Immediately before use *cis*-$Pt(NH_3)_2Cl_2$ was aquated by reaction with 0.95 volume equiv. of 12 mM $AgNO_3$ (stored in the dark). The aquation reaction was incubated at 50 °C for 1 h, at which time precipitated AgCl was removed by centrifugation. The resulting supernatant solution, 512 μM *cis*-$[Pt(NH_3)_2Cl(OH_2)]^+$, was removed and diluted accordingly. The predominant platinum species formed varies by pH with *cis*-$[Pt(NH_3)_2Cl(OH_2)]^+$ expected to be the main Pt-complex present at pH 7.0 (by ^{195}Pt NMR, data not shown).

Platination of HHrz constructs: A solution containing 400 pmol (giving a final concentration of 40 μM) of each RNA strand used in an experiment was annealed by incubation at 90 °C for 90 sec followed by slow cooling, and reacted with 120 μM *cis*-$[Pt(NH_3)_2Cl(OH_2)]^+$ (3:1 Pt:RNA ratio) in 1 mM $Mg(NO_3)_2$, 100 mM $NaNO_3$, 10 mM Na_2PO_4, pH 7.0. Reactions were incubated for 16 h at 37 °C. Following this, reactions were diluted with formamide and analyzed using 20% dPAGE (19:1 mono- to bis- acrylamide, 7M urea), and visualized by staining with methylene blue.

5' End-Labeling: RNAs were radiolabeled with T4 polynucleotide kinase (New England Biolabs) using $\gamma^{32}P$-ATP (Perkin-Elmer). End-labeled RNAs that were not further reacted with Pt(II) were purified using 20% dPAGE, excised from the gel and recovered as described below for Pt(II)-crosslinked products (*vida infra*).

Pt(II)-Crosslinking of 5' End-Labeled RNA for Use in Mapping Studies: In order to increase the yield of radioactive crosslinked products, 5' end-labeled RNAs were reacted with *cis*-$[Pt(NH_3)_2)(OH_2)Cl]^+$ prior to gel purification. To do so, end-labeling reactions were diluted and protein was removed by phenol-chloroform extraction followed by two washes with 24:1 chloroform:isoamyl alcohol. The RNA-containing aqueous phase was then desalted using G-25 Sephadex size exclusion resin (GE Healthcare) on laboratory-prepared microcentifuge columns (BioRad) and dried to completion by SpeedVac. This 5' end-labeled RNA was resuspended and used in platination reactions described above, with non-labeled RNA added as needed. Crosslinking reactions were diluted with formamide and analyzed by 20% dPAGE. Results were imaged using Molecular Dynamics phosphor screens scanned using a Storm 860 Scanner, and visualized using ImageQuant version 5.1 software (Molecular Dynamics). RNA bands were excised and eluted in 2 ml of 100 mM acetic acid, adjusted to pH 3.8 with TEMED. The acidity of this solution helps to prevent RNA degradation as well as potentially prevents hydrolysis reactions occurring at the Pt-phosphorothioate crosslink. After overnight elution, the RNA-containing eluent was removed and condensed using successive phase separations with *n*-butanol.[1] In this extraction procedure, a portion of the gel-eluted urea partitions into the organic phase and it is possible to obtain a very small RNA pellet, indicative of significantly desalted products. We believe that removing urea prior to the mild heating and condensation involved in SpeedVac drying may help preserve platinum crosslinks by preventing ligand substitution reactions at the crosslinked site. Dried and desalted RNAs were resuspended in deionized water.

Hydrolysis Mapping of Pt(II)-Crosslinked RNAs: End-labeled, crosslinked RNAs in deionized water (typically 2 μL) were reacted with an equal volume of 50 mM Na_2CO_3/$NaHCO_3$ (pH 9.5), 1 mM EDTA and incubated at 90 °C for times ranging from 5 to 25 min. Reactions were quenched by the addition of 8 M urea, 10 mM sodium citrate (pH 3.5), 0.005% (w/v) xylene cyanol loading buffer and were held on dry ice until electrophoresis. Results were analyzed on 20% dPAGE gels and visualized via phosphorimaging. Reference lanes of 5′ end-labeled un-crosslinked RNAs were generated by alkali hydrolysis as described above as well as by partial nuclease digestion using RNase T1 (Ambion). Briefly, 5′ end-labeled RNA along with 0.2 μM unlabeled RNA was digested with 1U T1 RNase in 8 M urea, 10 mM sodium citrate (pH 3.5), and 0.005% (w/v) xylene cyanol at 50 °C for 12-15 min. These samples were similarly held on dry ice until electrophoresis.

Pt(II)-Crosslinking Kinetics: Trace 5' end-labeled SS(dC17, C1.1ps) was added to standard platination reactions using the HHrzES-SS(dC17, C1.1ps) construct. Aliquots were removed at 1, 3, 5, 10, 15, 30, 45, 60, 240, and 480 min, quenched by mixture with formamide loading buffer

and held on dry ice until electrophoresis. Products were separated using 20% dPAGE and quantified using ImageQuant software. The kinetic traces obtained were fit using SigmaPlot version 11.0 (Systat Software, Inc.). A double exponential, 4 parameter equation of the form $y = a(1-e^{-bx}) + c(1-e^{-dx})$ provided the best fit to the data ($R^2 = 0.999$). In this equation two reactive populations of the HHrzES-SS(dC17, C1.1ps) are portrayed: 18% of the total HHrz reacts with the reported $k_{obs} = 0.22\ min^{-1}$ ($0.0038\ s^{-1}$), 15% reacts with $k_{obs} = 0.01\ min^{-1}$ ($1.6 \times 10^{-4}\ s^{-1}$). These rates are divided by the concentration of Pt(II) used in the reactions to give calculated second order rate constants of $31\ M^{-1}\ s^{-1}$ and $1.3\ M^{-1}\ s^{-1}$ respectively.

Molecular Modeling: The crystal structure of the Mn^{2+}-containing HHrz (pdb:2OEU) was imported into Spartan '08 (Wavefunction, Inc.) Version 1.2.0. Sulfur substitutions were made at individual non-bridging oxygens of the phosphodiester bonds between C17-C1.1 as well as between C1.1-U1.2 to produce *R* and *S* stereoisomers of each phosphorothioate. Bond lengths and angles of the Pt-S-P unit were fixed based on previously reported NMR studies[2] and a crystal structure of a phosphorothioate-bound Pt-terpyridine complex.[3] For each stereoisomer, a square-planar $[Pt(NH_3)_2(OH_2)]$ fragment was attached to the phosphorothioate sulfur ligand. All heavy atoms in the structure, except for the G10.1/A9-coordinated Mn^{2+} which was removed, were then held static except for the phosphorothioate S and attached $[Pt(NH_3)_2(OH_2)]$ fragment. It is recognized that this procedure neglects the inherent flexibility of the RNA biopolymer, and suggests further studies in order to understand how structural dynamics may contribute to the formation of Pt crosslinks. Several constraints were then placed on Pt coordination geometry and bond lengths: 90° bond angles were enforced between platinum substituents, the Pt-S-P bond angle was fixed at 98° based on the Pt-terpyridine structure,[3] and fixed bond lengths were derived from related reports.[3,4] Structures were then minimized using built-in molecular mechanics (MMFF) algorithms. The obtained structures were exported as ".pdb" files into Pymol Molecular Graphics System version 1.2r3pre which was used to measure distances and generate figure graphics.

Cleavage at Phosphorothioate Substitutions by *cis*-$[Pt(NH_3)_2Cl(OH_2)]^+$: In order to test the ability of *cis*-$[Pt(NH_3)_2Cl(OH_2)]^+$ to cleave at phosphorothioate substitutions, the RNA sequence 5'-UUUUCpsCUUUU-3' was obtained (Dharmacon Inc.). A 40 μM solution (final concentration) of this RNA was reacted with 120 μM *cis*-$[Pt(NH_3)_2Cl(OH_2)]^+$ in 1 mM $Mg(NO_3)_2$, 100 mM $NaNO_3$, 10 mM Na_2PO_4, pH 7.0. Reactions were incubated for 16 h at 37 °C and desalted prior to MALDI-MS using C_{18} ZipTips (Millipore). In this procedure ZipTips were washed by aspiration three times with 1:1 MeCN:H_2O, and equilibrated by washing three times with 0.1% trifluoroacetic acid (TFA). RNAs were bound to the tip by repeated aspiration of the

analyte solution. Bound RNA was washed three times by aspiration with 0.1% TFA, three times with deionized water, and then eluted from the column using two washes of 1:1 MeCN:H_2O. This eluent was dried to completion by SpeedVac.

MALDI-MS: Dried RNA samples were resuspended in a matrix consisting of 375 mM 2',4',6'-trihydroxyacetophenone (THAP, Sigma-Aldrich), 30 mM diammonium citrate in 3:1 EtOH:H_2O, with added NH_4^+ loaded Dowex cation exchange beads (Aldrich) and applied to the sample plate. MALDI-MS analysis was performed on a Waters QToF Premier mass spectrometer in positive-ion mode using V-mode optics.

Reversal of Pt-Phosphorothioate Crosslinks by Thiourea. Trace amounts of 5' end-labeled, crosslinked RNAs in deionized water were reacted with an equal volume of a saturated thiourea solution and incubated at 37 ^oC for times ranging from 1 to 28 h. Short reactions, including the "0" time point, were held on dry ice while others completed. Results were analyzed using 20% dPAGE and visualized by phosphorimaging.

Figure C.1:

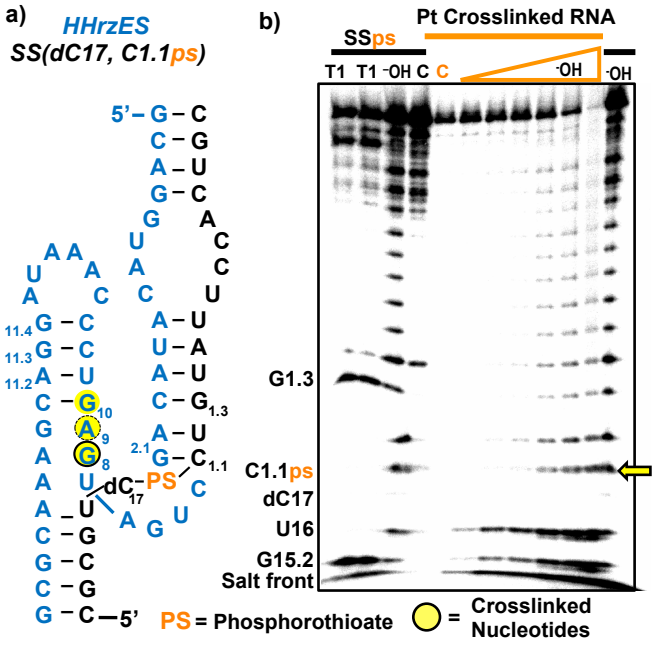

Figure C.1. Location of Pt(II) crosslinks formed in the HHrzES-SS(dC17, C1.1ps) ribozyme. **a)** Secondary structure of the HHrzES-SS(dC17, C1.1ps) construct. **b)** 20% dPAGE gel displaying the loss of hydrolysis products 3' to nucleotide U16, indicating crosslinking 3' to this location. Hydrolysis products are not expected at dC17 regardless of crosslinking. The absence of hydrolysis products 3' to dC17 however, indicates crosslinking to the C1.1 phosphorothioate.

Figure C.2:

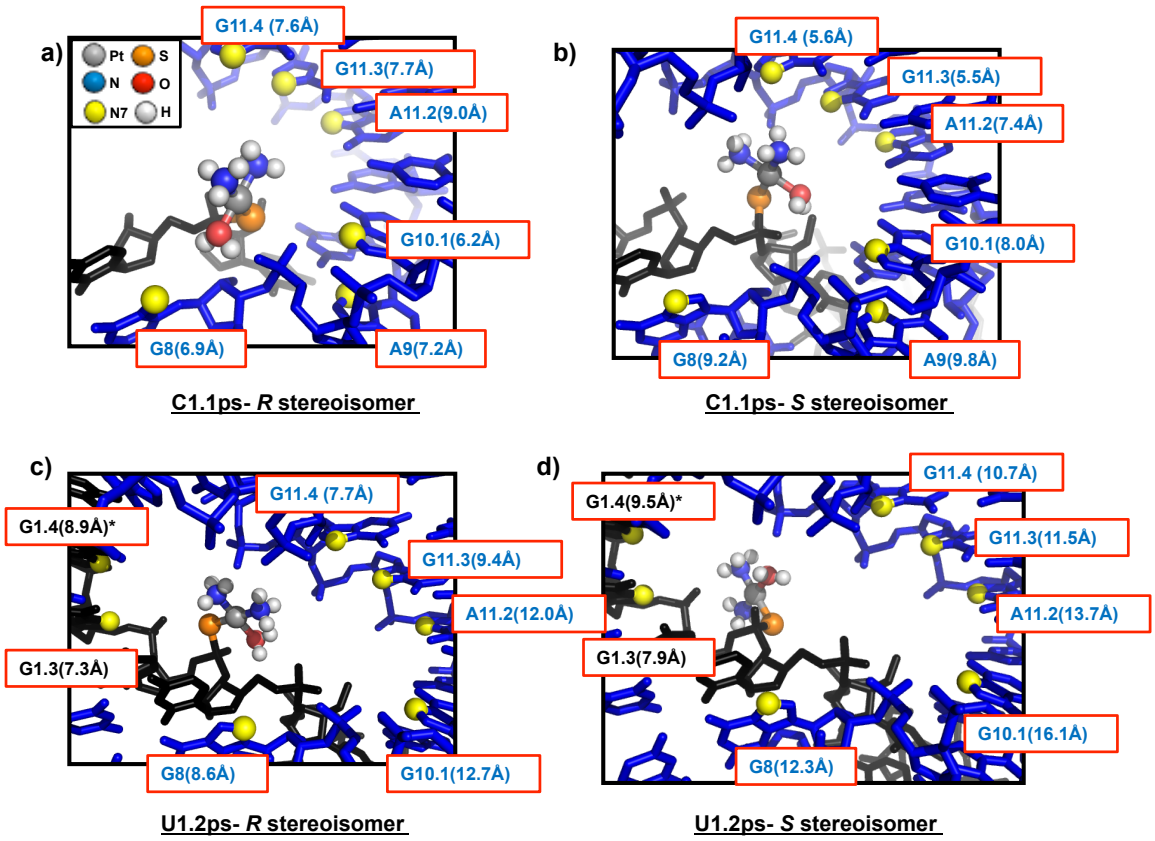

Figure C.2. Spartan '08 generated molecular models of a $[Pt(NH_3)_2(OH_2)]$ fragment bound to phosphorothioate substitutions in the HHrz. $[Pt(NH_3)_2(OH_2)]$ bound to **a)** the *R* stereoisomer of the C1.1 phosphorothioate; **b)** the *S* stereoisomer of the C1.1 phosphorothioate; **c)** the *R* stereoisomer of the U1.2 phosphorothioate; **d)** the *S* stereoisomer of the U1.2 phosphorothioate. Distances between Pt(II) atom and nearby purine N7 positions are indicated. The "*" representation at G1.4 indicates a G nucleotide at this position in the 2OEU structure used for this model that was not present in the HHrz construct used in the work.

Figure C.3:

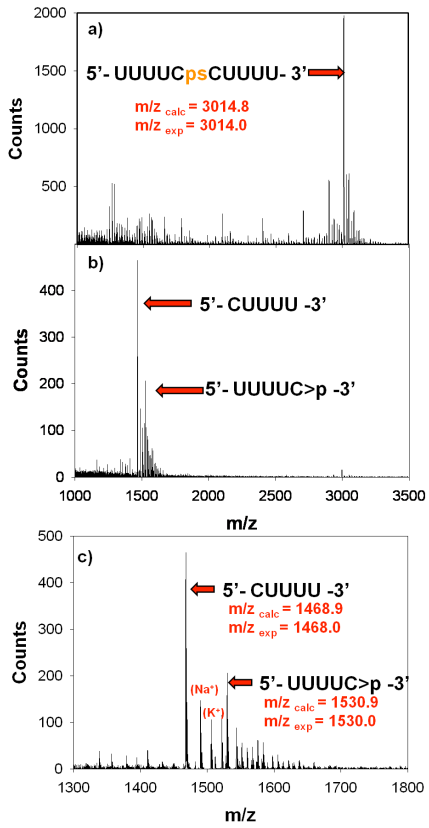

Figure C.3. MALDI-MS spectra depicting Pt(II)-induced cleavage of 5'-UUUUCpsCUUUU-3'. **a)** Control 5'-UUUUCpsCUUUU-3' RNA. **b)** Spectrum obtained following incubation of 5'-UUUUCpsCUUUU-3' with *cis*-$[Pt(NH_3)_2Cl(OH_2)]^+$ as described in Materials and Methods. **c)** Expanded view of the spectrum shown in (b) showing products from cleavage at the C*C phosphorothioate following treatment with *cis*-$[Pt(NH_3)_2)(OH_2)Cl]^{+\cdot}$ Notably, the 5'-cleavage fragment has a 2',3' cyclic phosphate indicating intramolecular nucleophilic attack at the platinated site. The platinum is not observed to be bound to either RNA fragment. Secondary peaks result from commonly observed (and difficult to fully eliminate) alkali earth metal adducts of each species.

Figure C.4:

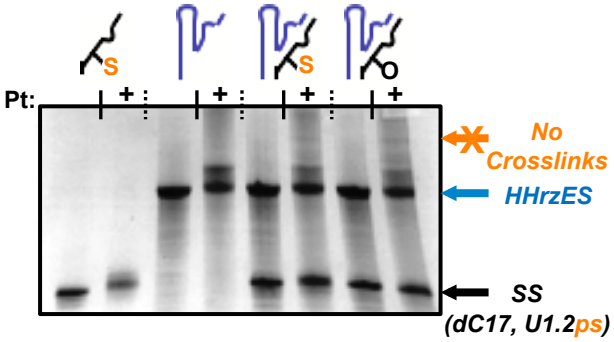

Figure C.4. 20% dPAGE gel depicting the lack of intermolecular crosslinking between HHrzES and SS(dC7, U1.2ps) RNAs following platination. Unlike the case for C1.1ps, the platinated U1.2ps does not form intermolecular crosslinks with the HHRz enzyme strand. Lanes shown are as in Figure 1 of the paper: SS(dC17, U1.2ps) alone, ES alone, ES:SS(dC17, U1.2ps), and ES:SS (no phosphorothioate), incubated in presence and absence of $[Pt(NH_3)_2Cl(OH_2)]^+$.

Figure C.5:

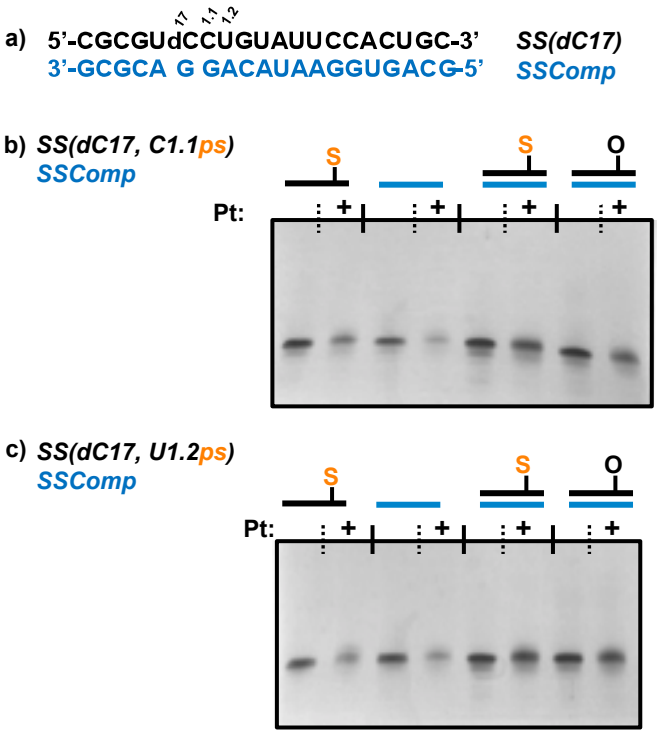

Figure C.5. Attempted crosslinking of phosphorothioate-substituted RNAs to a base-paired complement. **a)** Sequences of the SS and SSComp RNAs; **b)** 20% dPAGE gel depicting the lack of intermolecular crosslinking between SS(dC17, C1.1ps) and SS(Comp) RNAs following platination; **c)** 20% dPAGE gel depicting the lack of intermolecular crosslinking between SS(dC17, U1.2ps) and SSComp RNAs following platination. Platination conditions are identical to those used for HHrz ES:SS experiments.

Figure C.6:

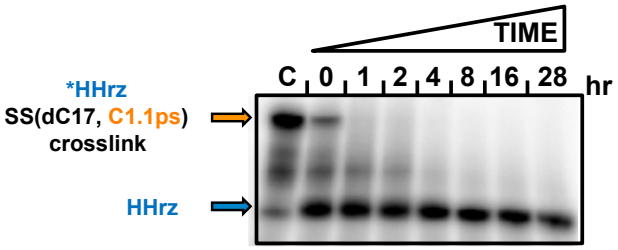

Figure C.6. Reversal of Pt(II)-phosphorothioate crosslinks using thiourea. 20% dPAGE gel depicting the reversal of Pt(II)-phosphorothioate crosslinks in the HHrz ES:SS(dC17, C1.1ps) complex by thiourea. Release of the 5'-end labeled HHrz enzyme strand is observed.

APPENDIX D

SUPPORTING INFORMATION FOR CHAPTER V: PLATINUM(II) ACTIVATED CLEAVAGE, DESULFURIZATION AND ISOMERIZATION OF PHOSPHOROTHIOATE SUBSTITUTED RNAS

Materials and Methods:

Nucleic Acid Substrates: All RNA oligonucleotides used in this work were purchased from Dharmacon Inc. and deprotected following the manufacturer's protocol. Oligonucleotide concentrations were determined using a Varian Cary 300 Bio UV-visible spectrophotometer, monitoring absorption at 260 nm.

Cis-Pt(NH_3)$_2$$Cl_2$ Aquation: *Cis*-Pt(NH_3)$_2$$Cl_2$, (Sigma-Aldrich) was prepared as a 1 mM aqueous solution in 10 mM NaCl and stored in the dark at 4 °C. Immediately before use *cis*-Pt(NH_3)$_2$$Cl_2$ was aquated by reaction with 0.95 volume equiv. of 12 mM $AgNO_3$ (stored in the dark). The aquation reaction was incubated at 50 °C for 1 h, at which time precipitated AgCl was removed by centrifugation. The resulting supernatant solution, a 512 μM mixture of *cis*-Pt(II) species, was removed and diluted accordingly. The predominant platinum species formed varies by pH with *cis*-[Pt(NH_3)$_2$Cl(OH_2)]$^+$ expected to be the main Pt-complex present at pH 7.0 (by ^{195}Pt NMR, data not shown).

Standard Platination Conditions: Typically, 40 μM RNA was reacted with 120 μM aquated *cis*-Pt(II) species in a background of 1 mM Mg(NO_3)$_2$, 100 mM Na(NO_3), 10 mM MES (2-(*N*-morpholino)ethanesulfonic acid) pH 6.5 at 37° C for the times indicated in the text. Reactions were typically carried out on a 10 μL scale. Reactions were then stopped by freezing on dry ice at -78° C and held there until purified by C_{18} ZipTips and analyzed by MALDI-MS.

MALDI-MS: RNA samples were purified using C_{18} ZipTips using a procedure modified from the manufacturer's protocol for RNA. ZipTips were washed by aspiration three times with 1:1 MeCN/H_2O solution, and equilibrated by washing three times with 0.1% trifluoroacetic acid (TFA). RNAs were bound to the tip by repeated aspiration of the analyte solution. Bound RNA was washed three times by aspiration with 0.1% TFA, three times with deionized water, and then eluted from the column using two washes of 1:1 MeCN/H_2O. The eluent was dried to completion

by SpeedVac and resuspended in a matrix consisting of 375 mM 2′,4′,6′ trihydroxyacetophenone (THAP, Sigma-Aldrich), 30 mM diammonium citrate in 3:1 EtOH/H2O, with added NH_4+ loaded Dowex cation exchange beads (Aldrich) and applied to the sample plate. MALDI-MS analysis was performed on a Waters QToF Premier mass spectrometer in positive-ion mode using V-mode optics.

pH Dependent MALDI-MS: Reactions were carried out using the standard platination conditions as described above with the identity and pH of the buffer varied as follows: pH 3.5- 10mM sodium acetate, pH 5.5- 10mM MES, pH 6.5 10mM MES, pH 8.0- 10 mM TRIS (tris(hydroxymethyl)aminomethane). The pH of buffered solutions was adjusted using HNO_3 and NaOH.

5' End-Labeling: The 10-mer PS-containing RNA, 5'-UUUUCpsUUUU-3' was radiolabeled with T4 poly nucleotide kinase (Fermentas) using γ^{32}P-ATP (Perkin-Elmer). End-labeled RNA was purified by 20% dPAGE, imaged by phosphor screen and excised. Excised gel bands were eluted overnight in deionized water. The resulting eluent was concentrated and desalted using G-25 Sephadex spin-columns.

pH Dependent Cleavage Kinetics: Trace 5' end-labeled RNA was added to the standard platination reactions described above, with pH varied as described. Typically, the volume of these reactions was scaled three fold (from 10 μL to 30 μL). Typically, 2 μL aliquots from each reaction were removed at appropriate time points and held on dry ice until electrophoresis. Immediately prior to electrophoresis, samples were mixed with formamide loading buffer (containing 0.005% (w/v) xylene cyanol and bromophenol blue). Reactions were analyzed using 20% dPAGE (7M urea), imaged by phosphorimaging. ImageQuant version 5.0 software (Molecular Dynamics) was used to quantify band intensities. SigmaPlot version 11.0 (Systat Software, Inc.) was used to generate kinetic traces.

NMR Spectroscopy. 1mM 5'-UpsU-3' RNA was combined with 1.5 mM aquated *cis*-Pt(II) species in 100 mM $NaNO_3$, 1 mM $Mg(NO_3)_2$, 10 mM HEPES, at pH 7.5 and 25°C (10% D_2O in water). When not being analyzed by NMR, the reaction was stored, protected from light, at room temperature. All RNA samples were placed in Shegemi D_2O matched quartz tubes (Shegemi Inc., Allison Park, PA). ^{1}H-decoupled ^{31}P NMR spectra were recorded at 202 Mhz on a Varian Unity spectrometer**.**

DFT Calculations: DFT calculations were performed using Spartan '08 (Wavefunction, Inc.) Version 1.2.0. Equilibrium geometries were optimized using the B3LYP functional with the LAVCP extended 6-31*G basis set. Atomic electrostatic potentials were calculated using the same level of theory. Electrostatic potential maps were generated using built-in software features.

Figure D.1:

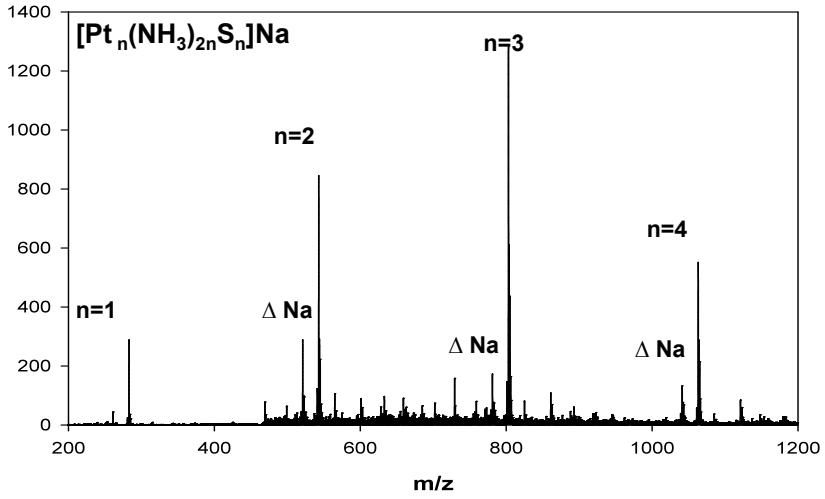

Figure D.1. MALDI-MS spectra depicting low nuclearity Pt complexes observed to result from the reaction of *cis*-Pt(II) species with PS-substituted RNAs.

Table D.1:

Metal Complex	Aqueous Metal Ion	Cleavage	Desulfurization
cis-$Pt(NH_3)_2Cl_2$	Pt(II)	+	+
trans-$Pt(NH_3)_2Cl_2$	Pt(II)	+	+
$PtCl_4$	Pt(II)	+	+
$AgNO_3$	Ag(I)	-	+
$Zn(CH_3CO_2)_2$	Zn(II)	-	-
$CoSO_4$	Co(II)	-	-
$NiSO_4$	Ni(II)	-	-
$Mn(CH_3CO_2)_2$	Mn(II)	-	-
$Co(NO_3)$	Co(II)	-	-
CaCl	Ca(II)	-	-
LiCl	Li(I)	-	-
$CuSO_4$	Cu(II)	-	-
$TbCl_3$	Tb(III)	-	-
$Fe(NH_4)_2(SO_4)_2$	Fe(II)	-	-
$Cu(CH_3CN)_4$	Cu(I)	-	-
CsCl	Cs(I)	-	-
$Cd(NO_3)_2$	Cd(II)	-	-

Table D.1. Summary of the results obtained following the reaction of various metal ions with 5'-UUUUCpsCUUUU-3'. Conditions: 40 μM RNA reacted with 120 μM metal in a background of 1 mM $Mg(NO_3)_2$, 100 mM $Na(NO_3)$, 10 mM MES, pH 6.5, 37° C for 16 hr.

REFERENCES

Chapter I:

(1) Hoeschele, J.D. *Dalton Trans.* **2009**, 10648-10650.

(2) Rosenberg, B.; Van Camp, L.; Krigas, T. *Nature* **1965**, *205*, 698-699.

(3) Rosenberg, B.; Van Camp, L.; Grimley, E. B.; Thomson, A. J. *J. Biol. Chem.* 1967, *242*, 1347-1352.

(4) Orvig, C.; Abrams, M. J. *Chem. Rev.* **1999**, *99*, 2201–2203.

(5) Wheate, N.J.; Walker, S.; Craig, G.E.; Oun, R. *Dalton Trans.* **2010**, *39*, 8113-8127.

(6) Wong, E.; Giandomenico, C.M. *Chem. Rev.*, **1999**, *99*, 2451-2466.

(7) Kelland, L. *Nat. Rev. Cancer* **2007**, *7*, 573-584.

(8) Weinberg, R.A.; Hanahan, D. *Cell* **2000**, *100*, 57-70.

(9) Hall, M.D.; Okabe, M.; Shen, D.-W.; Liang, X.J.; Gottesman, M.M. *Ann. Rev. Tox.* **2008**, *48*, 495-535.

(10) Jamieson, E.R,; Lippard, S.J. *Chem. Rev.* **1999**, *99*, 2467-2498.

(11) Hambley, T.W.; *Dalton Trans.* **2001**, 2711-2718.

(12) Wang, D.; Lippard, S.J. *Nat. Rev. Drug Discovery* **2005**, *4*, 307-320.

(13) Basu, A.; Krishnamurthy, S. *J. Nucleic Acids* **2010**, doi:10.4061/2010/201367

(14) Jung. Y.W.; Lippard, S.J. *Chem. Rev.* **2007**, *207*, 1387-1407.

(15) Fuertes, M.A.; Castilla, J.; Alonso, C.; Perez, J.M. *Curr. Med. Chem.* **2003**, *10*, 257-266.

(16) Reedjik, J. *Proc. Natl. Acad. Sci.* **2003**, *100*, 3611-3616.

(17) Crabtree, R. H. *The Organometallic Chemistry of the Transition Metals*, 3rd ed.; John Wiley and Sons: New York, 2001.

(18) Spessard, G. O.; Miessler, G.L. *Organometallic Chemistry*, Prentice Hall: Upper Saddle Creek, New Jersey, 1997.

(19) Ishida, S.; Lee, J.; Thiele, D.J.; Herskowitz, I. *Proc. Natl. Acad. Sci. U.S.A.* **2002**, *99*, 14298-14302.

(20) Hindmarsh, K.; House, D.A.; Turnbull, M.M. *Inorg. Chim. Acta* **1997**, *257*, 11-18.

(21) Ahmad S.; Isab A. A.; Ali S. *Trans. Met. Chem.* **2006**, *31*, 1003–1016.

(22) Chen, H.H.W.; Kuo, M.T. *Metal-Based Drugs* **2010**, doi:10.1155/2010/430939

(23) Boal, A.K.; Rosenzweig, A.C. *J. Am. Chem. Soc.* **2009**, *131*, 14196-14197.

(24) Hannon, M.J. *Pure Appl. Chem.* **2007**, *79*, 2243-2261.

(25) Wong, E.; Giandomenico, C.M. *Chem. Rev.* **1999**, *99*, 2451-2466.

(26) United States Food and Drug Administration: www.accessdata.fda.gov/scripts/cder/drugsatfda

(27) Knox, R.J.; Friedlos, F.; Lydall, D.A.; Roberts J.J. *Cancer Res.* **1986**, *46*, 1972-1979.

(28) Stordal, B.; Pavlakis, N.; Davey, R. *Cancer Treatment Rev.* **2007**, *33*, 347-357.

(29) Raymond, E.; Faivre, S.; Chaney, S.; Woynarowski, J.; Cvitkovic, E. *Mol. Cancer Ther.* **2002**, *1*, 227– 235.

(30) Feazell, R.P.;Nakayama-Ratchford, N.; Dai, H.; Lippard, S.J. *J. Am. Chem. Soc.* **2007**, *129*, 8438-8439.

(31) Dhar, S.; Daniel, W.L.; Giljohan, D.A.; Mirkin, C.A.; Lippard, S.J. *J. Am. Chem. Soc.* **2009**, *131*, 14652-14653.

(32) Fuertes, M.A.; Castilla, J.; Alonso, C.; Perez, J.M. *Curr. Med. Chem.* **2003**, *10*, 257-266.

(33) Wang, D.; Lippard, S.J. *Nat. Rev. Drug Disc.* **2004**, *3*, 535-535.

(34) DeRose, V. J. B., S; Kim,N-K; Vogt, M., DNA and RNA as Ligands. In *Comprehensive Coordination Chemistry II*, Elsevier: St. Louis, **2003**; pp 787-813.

(35) Neidle, S. *Nucleic Acid Structure and Function*, Oxford University Press: Oxford, 2002; p 182.

(36) Blackburn, G. M., Gait, M.J. *Nucleic Acids in Chemistry and Biology*, 2nd ed.; Oxford University Press: Oxford, 1996.

(37) Lippert, B. *Prog. Inorg. Chem.* **1989**, *37*, 1-97.

(38) Burstyn, J.N.; Heiger-Bernays, W.J.; Cohen, S.M.; Lippard, S.J. *Nuc. Acids Res.* **2000**, *28*, 4237-4243.

(39) Mantri, Y.; Lippard, S.J.; Baik, M.-H. Baik *J. Am. Chem. Soc.* **2007**, *129*, 5023-5030.

(40) Bailor, M.H.; Sun, X.; Al-Hashimi, H.M. *Science* **2010**, *327*, 202-206.

(41) Ober, M.; Lippard, S.J. *J. Am. Chem. Soc.* **2008**, *130*, 2851-2861.

(42) Ober, M.; Lippard, S.J. *J. Am. Chem. Soc.* **2007**, *129*, 6278-6286.

(43) Freisner, E.; Sigel, R.K.O. *Coord. Chem. Rev.* **2007**, *251*, 1834-1851.

(44) Pyle, A.M. *J. Biol. Inorg. Chem.* **2002**, *7*, 679-690.

(45) Acharya, P.; Acharya S.; Cheruku, P.; Amirkhanov, N. V.; Foldesi A.; Chattopadhyaya J. *J. Am. Chem. Soc.* **2003**, *125*, 9948–9961.

(46) Legault P.; Pardi, A. *J. Am. Chem. Soc.* **1997**, *119*, 6621–6628.

(47) Takahara, P.M.; Rosenzweig, A.C., Fredrick, C.A.; Lippard, S.J. *Nature* **1995**, *377*, 649-652.

(48) Chapman, E.G.; DeRose, V.J. *J. Am. Chem. Soc.* **2010**, *132*, 1946-1952.

(49) Rijal, K.; Chow, C.S. *Chem. Comm.* **2009**, 107-109.

(50) Rhodes, D.; Piper, P.W.; Clark, B.F.C. *J. Mol. Biol.* **1974**, *89*, 469-475.

(51) Rubin, J.R.; Sabat, M.; Sundaralingham, M. *Nuc. Acids. Res.* **1983**, *11*, 6571-6586.

(52) Dewan, J.C. *J. Am. Chem. Soc.* **1984**, *106*, 7239-7244.

(53) Hostetter, A.H., Chapman, E.G.; DeRose, V.J. *J. Am. Chem. Soc.* **2009**, *131*, 9250-9257.

(54) Hägerlof, M.; Personn, J.; Aldag, J.; Elmroth, S.K.C. *J. Biol. Inorg. Chem.* **2006**, *11*, 974-990.

(55) Papsai, P.; Snygg, S.; Aldag, J. *Dalton Trans.* **2008**, 5225-5234.

(56) Dalbies, R.; Payet, D.; Leng, M. *Proc. Natl. Acad. Sci. U.S.A.*, **1994**, *91*, 8147-8151.

(57) Dalbies, R.; Boudvillian, M.; Leng, M. *Nucl. Acids Res.* **1995**, *23,* 949-953.

(58) Comess, K.M.; Costello, C.E.; Lippard, S.J. *Biochemistry*, **1990**, *29*, 2102-2110.

(59) Bombard, S.; Kozelka, J.; Favre, A.; Chottard, J.-C. *Euro. J. Biochem.* **1998**, *252*, 25-35.

(60) Valadkhan, S.; Manley, J.L. *Nature* **2001**, *413*, 701-707.

(61) Yu, Y.T.; Maroney, P.A.; Darzynkiewicz, E.; Nilsen, T.W. *RNA* **1995**, *1*, 46-54.

(62) Fabrizio, P.; Abelson, J. *Nuc. Acids Res.* **1992**, *20*, 3659-3664.

(63) Woodson, S.A. *Curr. Op. Chem. Biol.* **2005**, *9*, 104-109.

(64) Escaraffe, M.; Chottard, J.C.; Bombard, S. *Nucl. Acids Res.* **2002**, *30*, 5222-5228.

(65) Boudvillian, M.; Guerin M.; Dalbies, R.; Saison-Behoaras, T.; Leng, M.; *Biochemistry* **1997**, *36*, 2925-2931.

(66) Aupeix-Scheidler, K.; Chabas, S.; Bidou, L.; Rousset, J.P.; Leng, M.; Toulme, J.J. *Nuc. Acids Res.* **2000**, *28*, 438-445.

(67) Hägerlof, M.; Hedmann, H.K.; Elmroth, S.K.C. *Biochem. Biophys. Res. Comm.* **2007**, *361*, 14-19.

(68) Hägerlof, M.; Pasai, P.; Hedmann, H.K.; Jungwirith, V.; Elmroth, S.K.C. *J. Biol. Inorg. Chem.*, 2008, 13, 385–399.

(69) Thomas, J.R.; Hergenrother, P.J. *Chem. Rev.* **2008**, *108*, 1171-1224.

(70) Boer, J.; Blount, K.F.; Luedtke, N.W.; Elson-Schwab, L.; Tor, Y. *Angew. Chem. Int. Ed. Eng.* **2005**, *44*, 927-932.

(71) N'soukpoe-Kossi, C. N.; Descoteaux, C.; Asselin, E.; Bariyanga, J.; Tajmir- Riahi H. A.; Berube, G. *DNA and Cell Biology* **2008**, *27*, 337–343.

(72) Pascoe, J.M.; Roberts, J.J. *Biochem. Phamacol.* **1974**, *23*, 1345-1357.

(73) Akaboshi, M.; Kawai, H.; Maki, H.; Akuta, K.; Ujeno, Y.; Miyahara, T. *Jpn. J. Cancer Res,* **1992**, *83*, 522-526.

(74) Tornaletti, S.; Patrick, S.M.; Turchi, J.J.; Hanawalt, P.C. *J. Biol. Chem.* **2003**, *287*, 35791-35797.

(75) Jung, Y.; Lippard, S.J. *J. Biol. Chem.* **2006**, *281*, 1361-1370.

(76) Ang, W.H.; Myint, M.; Lippard S.J. *J. Am. Chem. Soc.* **2010**, *132*, 7429-7435.

(77) Damsma, G.E.; Alt, A.; Brueckner, F.; Carell T.; Cramer, P. *Nat. Struct. Mol. Biol.* **2007**, *14*, 1127-1133.

(78) Jordan, P.; Carmo-Fonseca, M. *Nucl. Acids Res.* **1998**, *26*, 2831-2836.

(79) Heminger, K.A.; Hartson, S.D.; Rogers, J.; Matts, R,L *Arch. Biochem. Biophys.* **1997**, *344*, 200-207.

(80) Smittigen, T.D.; Ju, J.-F.; Danenberg, K.D.; Danenberg, P.V. *Int. J. Oncol.* **2003**, *23*, 785-789.

(81) Danenberg, P.V.; Shea, L.C.; Danenberg, K.D.; Horikoski, T. *Nucl. Acids Res.*, **1991**, *19*, 3123-3128.

(82) Rosenberg, J.; Sato, P. *Mol. Pharmacology*, **1987**, *33*, 611-616.

(83) Rosenberg, J.; Sato, P. *Mol. Pharmacology*, **1993**, *43*, 491-497.

Chapter II:

(1) Jung, Y.; Lippard, S. J. *Chem. Rev.* **2007**, *107*, 1387–1407.

(2) Wang, D.; Lippard, S. J. *Nat. Rev. Drug Discovery* **2005**, *4*, 307–320.

(3) Reedijk, J. *Proc. Natl. Acad. Sci. U.S.A.* **2003**, *100*, 3611–3616.

(4) Akaboshi, M.; Kawai, K.; Maki, H.; Akuta, K.; Ujeno, Y.; Miyahara, T. *Jpn. J. Cancer Res.* **1992**, *83*, 522–526.

(5) Pascoe, J. M.; Roberts, J. J. *Biochem. Pharmacol.* **1974**, *23*, 1345–1357.

(6) Harder, H. C.; Rosenberg, B. *Int. J. Cancer* **1970**, *6*, 207–216.

(7) Jung, Y.; Lippard, S. J. *J. Biol. Chem.* **2006**, *281*, 1361–1370.

(8) Damsma, G. E.; Alt, A.; Brueckner, F.; Carell, T.; Cramer, P. *Nat. Struct. Mol. Biol.* **2007**, *14*, 1127–1133.

(9) Schmittgen, T. D.; Ju, J. F.; Danenberg, K. D.; Danenberg, P. V. *Int. J. Oncol.* **2003**, *23*, 785–789.

(10) Rosenberg, J. M.; Sato, P. H. *Mol. Pharmacol.* **1993**, *43*, 491–497.

(11) Rosenberg, J.; Sato, P. *Mol. Pharmacol.* **1988**, *33*, 611–616.

(12) Hagerlof, M.; Papsai, P.; Chow, C. S.; Elmroth, S. K. C. *J. Biol. Inorg. Chem.* **2006**, *11*, 974–990.

(13) Papsai, P.; Snygg, A. S.; Aldag, J.; Elmroth, S. K. C. *Dalton Trans.* **2008**, 5225–5234.

(14) Papsai, P.; Aldag, J.; Persson, T.; Elmroth, S. K. C. *Dalton Trans.***2006**, 3515–3517.

(15) Hagerlof, M.; Papsai, P.; Hedman, H. K.; Jungwirth, U.; Jenei, V.;Elmroth, S. K. C. *J. Biol. Inorg. Chem.* **2008**, *13*, 385–399.

(16) Danenberg, P. V.; Shea, L. C. C.; Danenberg, K. D.; Horikoshi, T. *Nuc. Acids Res.* **1991**, *19*, 3123–3128.

(17) Rijal, K.; Chow, C. S. *Chem. Commun.* **2009**, 107–109.

(18) DeRose, V. J.; Burns, S.; Kim, N.-K.; Vogt, M. *Comprehensive Coordination Chemistry II*; Elsevier: St. Louis, MO, 2003; pp 787-813.

(19) Pyle, A. M. *J. Biol. Inorg. Chem.* **2002**, *7*, 679–690.

(20) Klein, D. J.; Moore, P. B.; Steitz, T. A. *RNA* **2004**, *10*, 1366–1379.

(21) Wahl, M. C.; Will, C. L.; Luhrmann, R. *Cell* **2009**, *136*, 701–718.

(22) Smith, D. J.; Query, C. C.; Konarska, M. M. *Mol. Cell* **2008**, *30*, 657–666.

(23) Wachtel, C.; Manley, J. L. *Mol. Biosyst.* **2009**, *5*, 311–316.

(24) Valadkhan, S.; Manley, J. L. *Nature* **2001**, *413*, 701–707.

(25) Hagerlof, M.; Papsai, P.; Chow, C. S.; Elmroth, S. K. C. *J. Biol. Inorg. Chem.* **2006**, *11*, 974–990.

(26) Ourliac-Garnier, I.; Bombard, S. *J. Inorg. Biochem.* **2007**, *101*, 514– 524.

(27) Sigurdsson, S. T.; Eckstein, F. *Anal. Biochem.* **1996**, *235*, 241–242.

(28) Huggins, W.; Shapkina, T.; Wollenzien, P. *RNA* **2007**, *13*, 2000–2011.

(29) Behlen, L. S.; Sampson, J. R.; Uhlenbeck, O. C. *Nucleic Acids Res.* **1992**, *20*, 4055–4059.

(30) Butcher, S. E.; Burke, J. M. *Biochemistry* **1994**, *33*, 992–999.

(31) Davies, M. S.; Diakos, C. I.; Messerle, B. A.; Hambley, T. W. *J. Inorg. Biochem.* **2000**, *79*, 167–172.

(32) Bancroft, D. P.; Lepre, C. A.; Lippard, S. J. *J. Am. Chem. Soc.* **1990**, *112*, 6860–6870.

(33) Chifotides, H. T.; Koomen, J. M.; Kang, M. J.; Tichy, S. E.; Dunbar, K. R.; Russell, D. H. *Inorg. Chem.* **2004**, *43*, 6177–6187.

(34) Green, R.; Doudna, J. A. *ACS Chem. Biol.* **2006**, *1*, 335–338.

(35) Valencia-Sanchez, M. A.; Liu, J.; Hannon, G. J.; Parker, R. *Genes Dev.* **2006**, *20*, 515–524.

(36) Farazi, T. A.; Juranek, S. A.; Tuschl, T. *Development* **2008**, *135*, 1201– 1214.

(37) Serganov, A.; Patel, D. J. *Nat. Rev. Genet.* **2007**, *8*, 776–790.

(38) Montange, R. K.; Batey, R. T. *Annu. Rev. Biophys.* **2008**, *37*, 117–133.

(39) Bayne, E. H.; Allshire, R. C. *Trends Genet.* **2005**, *21*, 370–373.

(40) Mandal, M.; Breaker, R. R. *Nat. Rev. Mol. Cell Biol.* **2004**, *5*, 451–463.

(41) Strobel, S. A.; Cochrane, J. C. *Curr. Opin. Chem. Biol.* **2007**, *11*, 636–643.

(42) Mansfield, K. D.; Keene, J. D. *Biol. Cell* **2009**, *101*, 169–181.

(43) Grundy, F. J.; Henkin, T. M. *Crit. Rev. Biochem. Mol. Biol.* **2006**,*41*, 329–338.

(44) Lukong, K. E.; Chang, K. W.; Khandjian, E. W.; Richard, S. *Trends Genet.* **2008**, *24*, 416–425.

(45) Thomas, J. R.; Hergenrother, P. J. *Chem. Rev.* **2008**, *108*, 1171–1224.

(46) Hermann, T.; Tor, Y. *Expert Opin. Ther. Pat.* **2005**, *15*, 49–62.

(47) Legendre, F.; Kozelka, J.; Chottard, J. C. *Inorg. Chem.* **1998**, *37*, 3964–3967.

(48) Redon, S.; Bombard, S.; Elizondo-Riojas, M. A.; Chottard, J. C. *Nucl. Acids Res.* **2003**, *31*, 1605–1613.

(49) Monjardet-Bas, W.; Chottard, J. C.; Kozelka, J. *Chem. Eur. J.* **2002**, *8*, 1144–1150.

(50) Danford, A. J.; Wang, D.; Wang, Q.; Tullius, T. D.; Lippard, S. J. *Proc. Natl. Acad. Sci. U.S.A.* **2005**, *102*, 12311–12316.

(51) Ober, M.; Lippard, S. J. *J. Am. Chem. Soc.* **2008**, *130*, 2851–2861.

(52) Zhang, C. X.; Chang, P. V.; Lippard, S. J. *J. Am. Chem. Soc.* **2004**, *126*, 6536–6537.

(53) Garnier, I. O.; Bombard, S. *J. Inorg. Biochem.* **2007**, *101*, 514–524.

(54) Bombard, S.; Kozelka, J.; Favre, A.; Chottard, J. C. *Eur. J. Biochem.* **1998**, *252*, 25–35.

(55) Boer, J.; Blount, K. F.; Luedtke, N. W.; Elson-Schwab, L.; Tor, Y. *Angew. Chem., Int. Ed.* **2005**, *44*, 927–932.

(56) Yu, Y. T.; Maroney, P. A.; Darzynkiewicz, E.; Nilsen, T. W. *RNA* **1995**, *1*, 46–54.

(57) Fabrizio, P.; Abelson, J. *Nucl. Acids Res.* **1992**, *20*, 3659–3664.

(58) Manning, G. S. *Q. Rev. Biophys.* **1978**, *11*, 179–246.

(59) Hambley, T. W. *J. Chem. Soc., Dalton Trans.* **2001**, 2711–2718.

(60) Kozelka, J.; Legendre, F.; Reeder, F.; Chottard, J. C. *Coord. Chem. Rev.* **1999**, *192*, 61–82.

(61) Legendre, F.; Bas, V.; Kozelka, J.; Chottard, J. C. *Chem.*s*Eur. J.* **2000**, *6*, 2002–2010.

(62) Davies, M. S.; Berners-Price, S. J.; Hambley, T. W. *Inorg. Chem.* **2000**, *39*, 5603–5613.

(63) Davies, M. S.; Berners-Price, S. J.; Hambley, T. W. *J. Am. Chem. Soc.* **1998**, *120*, 11380–11390.

(64) Zou, Y.; Van Houten, B.; Farrell, N. *Biochemistry* **1994**, *33*, 5404–5410.

(65) Redon, S.; Bombard, S.; Elizondo-Riojas, M. A.; Chottard, J. C. *Biochemistry* **2001**, *40*, 8463–8470.

(66) Villanueva, J. M.; Jia, X.; Yohannes, P. G.; Doetsch, P. W.; Marzilli, L. G. *Inorg. Chem.* **1999**, *38*, 6069–6080.

(67) Brabec, V.; Vrana, O.; Boudny, V. *Prog. Biophys. Mol. Biol.* **1996**, *65*, PB113.

(68) Snygg, A. S.; Brindell, M.; Stochel, G.; Elmroth, S. K. C. *Dalton Trans.* **2005**, 1221–1227.

(69) Monjardet-Bas, V.; Elizondo-Riojas, M. A.; Chottard, J. C.; Kozelka, J. *Angew. Chem., Int. Ed.* **2002**, *41*, 2998–3001.

(70) Baik, M. H.; Friesner, R. A.; Lippard, S. J. *J. Am. Chem. Soc.* **2003**, *125*, 14082–14092.

(71) Mantri, Y.; Lippard, S. J.; Baik, M. H. *J. Am. Chem. Soc.* **2007**, *129*, 5023–5030.

(72) Yang, E.; van Nimwegen, E.; Zavolan, M.; Rajewsky, N.; Schroeder, M.; Magnasco, M.; Darnell, J. E. *Genome Res.* **2003**, *13*, 1863–1872. (73) (a) Measured turnover rates range from 0.034 to 0.0048 μmol/kg · day for rRNA and 0.46-0.88 μmol/kg · day for tRNA. On the basis of the calculation put forth by Petersen et al., this roughly corresponds to 12-29 days for rRNA and 17-29 days for tRNA in average adults. . (b) Schoch, G.; Topp, H.; Held, A.; Hellerschoch, G.; Ballauff, A.; Manz, F. *Eur. J. Clin. Nutr.* **1990**, *44*, 647–658. (c) Nakano, K.; Nakao, T.; Schram, K. H.; Hammargren, W. M.; McClure, T. D.; Katz, M.; Petersen, E. *Clin. Chim. Acta* **1993**, *218*, 169–183. (d) Marway, J. S.; Anderson, G. J.; Miell, J. P.; Ross, R.; Grimble, G. K.; Bonner, A. B.; Gibbons, W. A.; Peters, T. J.; Preedy, V. R. *Clin. Chim. Acta* **1996**, *252*, 123–135. (e) Sander, G.; Topp, H.; Hellerschoch, G.; Wieland, J.; Schoch, G. *Clin. Sci.* **1986**, *71*, 367–374.

Chapter III:

(1) Hambley, T. W. *Dalton Trans.* **2001**, 2711–2718.

(2) Jamieson, E. R.; Lippard, S. J. *Chem. Rev.* **1999**, *99*, 2467–2498.

(3) Reedijk, J. *Proc. Natl. Acad. Sci. U.S.A.* **2003**, *100*, 3611–3616.

(4) Wang, D.; Lippard, S. J. *Nat. Rev. Drug Discovery* **2005**, *4*, 307–320.

(5) Jung, Y. W.; Lippard, S. J. *Chem. Rev.* **2007**, *107*, 1387–1407.

(6) Fuertes, M. A.; Castilla, J.; Alonso, C.; Perez, J. M. *Curr. Med. Chem.***2003**, *10*, 257–266.

(7) Doma, M. K.; Parker, R. *Cell* **2007**, *131*, 660–668.

(8) Parker, R.; Song, H. W. *Nat. Struct. Mol. Biol.* **2004**, *11*, 121–127.

(9) Bellacosa, A.; Moss, E. G. *Curr. Biol.* **2003**, *13*, R482–R484.

(10) Kelly, S. M.; Corbett, A. H. *Traffic* **2009**, *10*, 1199–1208.

(11) Rosenberg, J.; Sato, P. *Mol. Pharmacol.* **1988**, *33*, 611–616.

(12) Schmittgen, T. D.; Ju, J. F.; Danenberg, K. D.; Danenberg, P. V. *Int. J. Oncol.* **2003**, *23*, 785–789.

(13) Hagerlof, M.; Hedman, H.; Elmroth, S. K. C. *Biochem. Biophys. Res. Commun.* **2007**, *361*, 14–19.

(14) Hagerlof, M.; Papsai, P.; Hedman, H. K.; Jungwirth, U.; Jenei, V.; Elmroth, S. K. C. *J. Biol. Inorg. Chem.* **2008**, *13*, 385–399.

(15) Rijal, K.; Chow, C. S. *Chem. Comm.* **2009**, 107–109.

(16) Papsai, P.; Aldag, J.; Persson, T.; Elmroth, S. K. C. *Dalton Trans.* **2006**, 3515–3517.

(17) Papsai, P.; Snygg, A. S.; Aldag, J.; Elmroth, S. K. C. *Dalton Tran.* **2008**, 5225–5234.

(18) Hagerlof, M.; Papsai, P.; Chow, C. S.; Elmroth, S. K. C. *J. Biol. Inorg. Chem.* **2006**, *11*, 974–990.

(19) N'Soukpoe-Kossi, C. N.; Descoteaux, C.; Asselin, E.; Bariyanga, J.; Tajmir-Riahi, H. A.; Berube, G. *DNA Cell Biol.* **2008**, *27*, 337–343.

(20) Boer, J.; Blount, K. F.; Luedtke, N. W.; Elson-Schwab, L.; Tor, Y. *Angew. Chem., Int. Ed.* **2005**, *44*, 927–932.

(21) Hostetter, A. A.; Chapman, E. G.; DeRose, V. J. *J. Am. Chem. Soc.* **2009**, *131*, 9250–9257.

(22) Houseley, J.; Tollervey, D. *Cell* **2009**, *136*, 763–776.

(23) Mendell, J. T.; Dietz, H. C. *Cell* **2001**, *107*, 411–414.

(24) Philips, A. V.; Cooper, T. A. *Cell. Mol. Life Sci.* **2000**, *57*, 235–249.

(25) Li, Z. W.; Wu, J. H.; DeLeo, C. J. *IUBMB Life* **2006**, *58*, 581–588.

(26) Tullius, T. D.; Lippard, S. J. *J. Am. Chem. Soc.* **1981**, *103*, 4620–4622.

(27) Inagaki, K.; Kasuya, K.; Kidani, Y. *Chem. Lett.* **1983**, 1345–1348.

(28) Asara, J. M.; Hess, J. S.; Lozada, E.; Dunbar, K. R.; Allison, J. *J. Am. Chem. Soc.* **2000**, *122*, 8–13.

(29) Gonnet, F.; Kocher, F.; Blais, J. C.; Bolbach, G.; Tabet, J. C.; Chottard, J. C. *J. Mass Spectrom.* **1996**, *31*, 802–809.

(30) Gonnet, F.; Reeder, F.; Kozelka, J.; Chottard, J. C. *Inorg. Chem.* **1996**, *35*, 1653–1658.

(31) Chifotides, H. T.; Koomen, J. M.; Kang, M.; Tichy, S. E.; Dunbar, K. R.; Russell, D. H. *Inorg. Chem.* **2004**, *43*, 6177–6187.

(32) Rao, L.; Bierbach, U. *J. Am. Chem. Soc.* **2007**, *129*, 15764.

(33) Reeder, F.; Guo, Z. J.; Murdoch, P. D.; Corazza, A.; Hambley, T. W.; Berners-Price, S. J.; Chottard, J. C.; Sadler, P. J. *Eur. J. Biochem.* **1997**, *249*, 370–382.

(34) Danckwardt, S.; Hentze, M. W.; Kulozik, A. E. *Embo J.* **2008**, *27*, 482–498.

(35) Garneau, N. L.; Wilusz, J.; Wilusz, C. J. *Nat. Rev. Mol. Cell Biol.* **2007**, *8*, 113–126.

(36) Poole, T. L.; Stevens, A. *Biochem. Biophys. Res. Commun.* **1997**, *235*, 799–805.

(37) Alguero, B.; de la Osa, J. L.; Gonzalez, C.; Pedroso, E.; Marchan, V.; Grandas, A. *Angew. Chem., Int. Ed.* **2006**, *45*, 8194–8197.

(38) Bombard, S.; Kozelka, J.; Favre, A.; Chottard, J. C. *Eur. J. Biochem.* **1998**, *252*, 25–35.

(39) Iannitti-Tito, P.; Weimann, A.; Wickham, G.; Sheil, M. M. *Analyst* **2000**, *125*, 627–633.

(40) Fichtinger-Schepman, A. M. J.; Van der Veer, J. L.; Den Hartog, J. H. J.; Lohman, P. H. M.; Reedijk, J. *Biochemistry* **2002**, *24*, 707– 713.

(41) Inagaki, K.; Kidani, Y. *Inorg. Chim. Acta Bioinorg. Chem.* **1985**, *106*, 187–191.

(42) Costello, C. E.; Nordhoff, E.; Hillenkamp, F. *Int. J. Mass Spectrom. Ion Process.* **1994**, *132*, 239–249.

(43) Nyakas, A.; Eymann, M.; Schurch, S. *J. Am. Soc. Mass Spectrom.* **2009**, *20*, 792–804.

(44) Lippert, B. *Prog. Inorg. Chem.* **1989**, *37*, 1–97.

(45) Lippert, B. *Coord. Chem. Rev.* **2000**, *200*, 487–516.

(46) Campbell, M. A.; Miller, P. S. *Biochemistry* **2008**, *47*, 12931–12938.

(47) Elizondo-Riojas, M. A.; Gonnet, F.; Chottard, J. C.; Girault, J. P.; Kozelka, J. *J. Biol. Inorg. Chem.* **1998**, *3*, 30–43.

(48) Kozelka, J.; Barre, G. *Chem.*s*Eur. J.* **1997**, *3*, 1405–1409.

(49) Mandel, C. R.; Bai, Y.; Tong, L. *Cell. Mol. Life Sci.* **2008**, *65*, 1099– 1122.

(50) Lau, P. W.; MacRae, I. J. *J. Cell. Mol. Med.* **2009**, *13*, 54–60.

(51) Thompson, D. M.; Parker, R. *Cell* **2009**, *138*, 215–219.

(52) Pace, C. N.; Heinemann, U.; Hahn, U.; Saenger, W. *Angew. Chem., Int. Ed. Engl.* **1991**, *30*, 343–360.

(53) Noguchi, S.; Satow, Y.; Uchida, T.; Sasaki, C.; Matsuzaki, T. *Biochemistry* **1995**, *34*, 15583–15591.

(54) Escaffre, M.; Favre, A.; Chottard, J. C.; Bombard, S. *Anal. Biochem.* **2002**, *310*, 42–49.

(55) Mantri, Y.; Lippard, S. J.; Baik, M. H. *J. Am. Chem. Soc.* **2007**, *129*, 5023–5030.

(56) Motorin, Y.; Muller, S.; Behm-Ansmant, I.; Brantant, C. In *RNA Modification*; Elsevier Academic Press Inc: San Diego, 2007; Vol. 425, p 21-53.

(57) Mortimer, S. A.; Weeks, K. M. *Nat. Protocols* **2009**, *4*, 1413–1421.

(58) Mundoma, C.; Greenbaum, N. L. *J. Am. Chem. Soc.* **2002**, *124*, 3525–3532.

(59) Maderia, M.; Horton, T. E.; DeRose, V. J. *Biochemistry* **2000**, *39*, 8193–8200.

(60) Costa, M.; Michel, F. *Embo J.* **1997**, *16*, 3289–3302.

(61) Reedijk, J. *Chem. Rev.* **1999**, *99*, 2499–2510.

(62) Ober, M.; Lippard, S. J. *J. Am. Chem. Soc.* **2007**, *129*, 6278–6286.

(63) Monjardet-Bas, V.; Bombard, S.; Chottard, J. C.; Kozelka, M. *Chem. Eur. J.* **2003**, *9*, 4739–4745.

(64) Wurtmann, E. J.; Wolin, S. L. *Crit. Re*V. *Biochem. Mol. Biol.* **2009**, *44*, 34–49.

(65) Ragas, J. A.; Simmons, T. A.; Limbach, P. A. *Analyst* **2000**, *125*, 575–581.

Chapter IV:

(1) Cruz, J.A.; Westhof, E. *Cell* **2009**, *136*, 604-609.

(2) Sharp, P.A. *Cell*, **2009**, *136*, 577-580.

(3) Harris, M.E.; Christian, E.L. *Methods Enzymol.* **2009**, *468*, 128-146.

(4) Lippert, B. In *Progress in Inorganic Chemistry, Vol. 37*; S.J. Lippard Ed. Wiley, New York **1989**, pp. 1-97.

(5) Redon, S.; Bombard, S.; Elizondo-Riojas, M-A.; Chottard, J-C. *Nucl. Acids Res*. **2003**, *31,* 1605-1613.

(6) Bombard, S.; Kozelka, J.; Favre, A.; Chottard, J.C. *Eur. J. Biochem.* **1998**, *252*, 25-35.

(7) Hostetter, A.A.; Chapman, E.G.; DeRose, V.J. *J. Am. Chem. Soc.* **2009**, *131*, 9250-9257.

(8) Rijal, K.; Chow, C.S. *Chem. Comm.*, **2009**, 107-109.

(9) Tukalo, M.H.; Kubler, M.D.; Kern, D.; Mougel, M.; Ehresmann, C.; Ebel, J-P.; Ehresmann, B.; Giegé, R. *Biochemistry* **1987**, *26*, 5200-5208.

(10) Rasmussen, N-J.; WIkman, F.P.; Clark, B.F.C. *Nuc. Acids Res.* **1990**, *18*, 4883-4889.

(11) Yusupova, G.; Reinbolt, J.; Wakao, H.; Laalami, S.; Grunberg-Manago, M.; Romboy, P.; Ehresmann, B.; Ehresmann, C.; *Biochemistry*, **1996**, *35*2987-2984.

(12) Strothkamp, K.G.; Lippard, S.J. *Proc. Natl. Acad. Sci. USA* **1976**, *73*, 2536-2540.

(13) Elmroth, S.K.C.; Lippard, S.J. *J. Am. Chem. Soc.*, **1994**, *116*, 3633-3634.

(14) Elmroth, S.K.C.; Lippard, S.J. *Inorg. Chem.* **1995**, *34*, 5234-5243.

(15) Kjellström, J.; Elmroth, S.K.C. *Inorg. Chem.* **1999**, *38*, 6193-6199.

(16) Chu, B.C.F.; Orgel, L.E. *Nucl. Acids Res.* **1989**, 17, 4783-4798.

(17) Chu, B.F.; Orgel, L.E. *Nucl. Acids Res.* **1990**,*18*, 5163-5171.

(18) Chu, B.F.; Orgel, L.E. *DNA and Cell Bio.* **1990**, *9*, 71-76.

(19) E. Gruff, L.E. Orgel, *Nucl. Acids Res.* **1991**, *19*, 6849-6854.

(20) Nelson, J.A.; Uhlenbeck, O. *RNA 14*, 605-615.

(21) Osborne, E.M.; Schaak, J. E.; DeRose, V.J. *RNA* **2005**, *11*, 187-196.

(22) Wang, S.; Karbenstein, K.; Peracchi, A.; Beigelman, L.; Herschlag, D. *Biochemistry,* **1999**, *38*, 14363-14378.

(23) Kim, N.-K.; Murali A.; DeRose, V.J. *J. Am. Chem. Soc.* **2005**, *127*, 14134-14135.

(24) Kratochwil, N.A.; Parkinson, J.A.; Sacht, C.; Murdoch, P.S.; Brown, T.; Sadler, P.J. *Euro J. Inorg. Chem.* **2001**, 2743-2746.

(25) Martick, M.; Lee, T-S.; York, D.M.; Scott, W.G. *Chemistry and Biology* **2008**, *15*, 332-342.

(26) Crabtree, R.H *The Organometallic Chemistry of the Transition Metals*, 3rd Ed.; Wiley and Sons, New York, 2001.

(27) Al-Hashimi, H.M.; Walter, N.G. *Curr. Op. Struct. Bio.* **2008**, *18*, 321-329.

(28) Pyle, A.M. *J. Biol. Inorg ,Chem.*, **2002**, *7*, 679-690.

(29) DeRose, V.J., Burns, S.; Kim, N.K.; Vogt M. in *Comprehensive Coordination Chemistry* I, Elsevier, St. Louis, **2003**, pp. 787-813.

(30) Frederiksen, J.K.; Piccirilli, J. *Methods Enzymol.* **2009**, *468*, 289-309.

(31) Chapman, E.G.; DeRose, V.J. *J. Am. Chem. Soc.* **2010**, *132*, 1946-1952.

(32) Weeks, K.M. *Curr. Op. Struct. Bio.* **2010**, *20*, 1-10.

Chapter V:

(1) Serganov, A.; Patel, D.J. *Nat. Rev. Genetics*, **2007**, *8*, 776-790.

(2) Sharp, P.A. *Cell*, **2009**, *136*, 577-580.

(3) Mattick, J.S. *Nat. Rev. Genet.*, **2004**, *5*, 316-323.

(4) Doudna, J.A.; Lorsch, J.R. *Nat. Struct. Mol. Bio.*, **2005**, *12*, 395-402.

(5) Strobel, S.A; Cochrane, J.C. *Curr. Op. Chem. Bio.*, **2007**, *11*, 636-643.

(6) DeRose, V.J. *Chem. Biol.*, **2002**, *9*, 961-969.

(7) Fedor, M.J. *Curr. Op. Struct. Bio.* **2002**, *12*, 289-95.

(8) Eckstein, F. *Ann. Rev. Biochem.* **1985**, *54*, 367-402.

(9) Houghland, J.L.; Kravchuk, A.V.; Herschlag, D.; Piccirilli, J.A. *PLOS Bio.* **2005**, *3*, 1537-1548.

(10) Herschlag, D.; Piccirlli, J.A.; Cech, T.R. *Biochemistry* **1991**, *30*, 4844-4854.

(11) Ora, M.; Peltomäki, M.; Oivanen, M.; Lönnberg, H. *J. Org. Chem.* **1998**, *63*, 2939-2947.

(12) Sigel, R.K.O.; Song, B.; Sigel, H. *J. Am. Chem. Soc.* **1997**, *119*, 744-755.

(13) DaCosta, C.P.; Okruszek, A.; Sigel, H. *ChemBioChem* **2003**, *4*, 593-602.

(14) Westheimer, F.H. *Acc. Chem. Res.* **1978**, *1*, 70-78.

(15) Oivanen, M.; Ora, M.; Almer, H.; Strömberg, R.; Lönnberg, H. *J. Org. Chem.* **1995**, *60*, 5620-5627

(16) Oivanen, M.; Kuusela, S.; Lönnberg, H. *Chem. Rev.* **1998**, *98*, 961-990.

(17) Lönnberg, T.; Ora, M.; Virtanen, S.; Lönnberg H. *Chem. Euro. J.* **2007**, *13*, 4614-4627.

(18) Chapman, E.G.; DeRose, V.J. *submitted*

(19) Lippert, B. *Prog. Inorg. Chem.* **1989**, *37*, 1–97.

(20) DeRose, V. J.; Burns, S.; Kim, N.-K.; Vogt, M. *Comprehensive Coordination Chemistry II*; Elsevier: St. Louis, MO, 2003; pp 787-813.

(21) Hindmarsh, K.; House, D.A.; Turnbull, M.M. *Inorg. Chim. Acta* **1997**, *257*, 11-18.

(22) Osborne, E. M.; Ward, W.L.; Ruehle, M.Z.; DeRose, V.J. *Biochemistry* **2009**, *48*, 10654-10664.

(23) Karikó, K.; Sobol, R.W. Jr.; Suhadolnik, L.; Li, S.W; Reichenbach, N.L.; Suhadolnik, R.J.; Charubala, R.; Pfeiderer *Biochemistry* **1987**, *26*, 7127-7135.

(24) Heemstra, J. M.; Liu, D. R. *J. Am. Chem. Soc.* **2009**, *131*, 11347-11349.

(25) Chapman, E.G.; DeRose, V.J. *J. Am. Chem. Soc.* **2010**, *132*, 1946-1952.

(26) Costello, C. E.; Nordhoff, E.; Hillenkamp, F. *Int. J. Mass Spectrom. Ion Process.* **1994**, *132*, 239–249.

(27) Nyakas, A.; Eymann, M.; Schurch, S. *J. Am. Soc. Mass Spectrom.* **2009**, *20*, 792–804

(28) Crabtree, R.H *The Organometallic Chemistry of the Transition Metals*, 3rd Ed.; Wiley and Sons, New York, 2001.

(29) Marchán, V.; Moreno, V.; Pedroso, E.; Grandas, A. *Chem. Euro. J.* **2001**, *7*, 808-815.

(30) Lau, J. K.-C.; Deubel, D.V. *Chem. Euro. J.*, **2005**, *11*, 2848-2855.

(31) Lax, P.M.; Añorbe, M.G.; Müller,B.; Bivián-Castro, E.Y.; Lippert, B. *Inorg. Chem.* **2007**, *46*, 4036-4043.

(32) Elmroth, S.K.C.; Lippard, S.J. *J. Am. Chem. Soc.*, **1994**, *116*, 3633-3634.

(33) Elmroth, S.K.C.; Lippard, S.J. *Inorg. Chem.* **1995**, *34*, 5234-5243.

(34) Kjellström, J.; Elmroth, S.K.C. *Inorg. Chem.* **1999**, *38*, 6193-6199.

(35) Mikkola, S.; Stenman, E.; Nurmi, K.; Yousefi-Salkdeh, E.; Strömberg, R.; Lönnberg H. *J. Chem. Soc. Perkin Trans.* **1999**, 1619-1625.

(36) Lyne, P.D.; Karplus, M.; *J. Am. Chem. Soc.* **2000**, *122*, 166-167.

(37) Frey, P.; Sammons, R.D. *Science* **1985**, *228*, 541-545.

(38) Deubel, D.V. *J. Am. Chem. Soc.* **2002**, *124*, 5834-5842.

(39) Rassolov V.; Pople J.A.; Ratner M.; Redfern P.C.; Curtiss L.A.; *J. Comp. Chem.* **2001**, *22*, 976-984.

(40) Miguel, P.J.S.; Roitzsch M.; Yin, L.; Lax, P.M.; Holland, L.; Krizanovic, O.; Lutterbeck, M.; Schürmann, M.; Fusch, E.C.; Lippert, B. *Dalton Trans.* **2009**, 10774-10786.

(41) Westheimer, F.H. *Science*, **1987**, *235*, 1173.

(42) Knowles, J.R. *Ann. Rev. Biochem.* **1980**, *49*, 877-919.

(43) Sigel, R.K.O.; Pyle, A.M. *Chem. Rev.* **2007**, *107*, 97-113.

(44) Freisinger, E.; Sigel, R.K.O *Coord. Chem. Rev.* **2007**, *251*, 1834-1851.

(45) Lönnberg, T.; Lönnberg, H. *Curr. Op. Chem. Biol.* **2005**, *9*, 665-673.

(46) Morita, H.; Bailar, J.C. Jr.; *Inorg. Syn.* **1983**, *22*, 124-125.

Chapter VI:

(1) Halcyon Molecular: http://halcyonmolecular.com/ (accessed November 5, 2010).

(2) Schradt, E.E.; Turner, S.; Kararsakis, A. *Human Mol. Gen.* **2010**, *19*, R227-R240.

(3) Krivanek, O.L.; Chisholm, M.F.; Nicolosi, V.; Pennycook, T.J.; Dellby, N.; Murfitt, M.F.; Own, C.S.; Szilagyi, Z.S.; Oxley, M.P.; Pantelides, S. T.; Pennycook, S.J. *Nature* **2010**, *464*, 571-574.

(4) Das, R.; Kudaravalli, M.; Jonikas, M.; Laederach, A.; Fong, R.; Schwans, J.P.; Baker, D.; Piccirlli, J.A.; Altman, R.B.; Herschlag, D. *Proc. Natl. Acad. Sci. U.S.A.* **2008**, *105*, 4144-4149.

(5) Mauger, D.M.; Weeks, K.M. *Nat. Biotech.* **2010**

(6) Ryder, S.P.; Strobel, S.A.; *Methods*, **1999**, *18*, 38-50

(7) Suydam, I.T,; Strobel, S.A. *Methods Enzymol.* **2009**, *468*, 3-30.

Appendix C:

(1) Cathala, G.; Brunel, C. *Nuc. Acids Res.* **1990**, *18*, 201.

(2) Kratochwil, N.A.; Parkinson, J.A.; Sacht, C.; Murdoch, P.S.; Brown, T.; Sadler, P.J. *Euro J. Inorg Chem.* **2001**, 2743-2746.

(3) Ross, S. A.; Lowe, G.; Watkin, D.J.; *Acta Cryst.* **2001** *C57*, 275-276.

(4) Takahara, P.M.; Rosenweig, A. C.; Frederick, C.A.; Lippard S.J. *Nature*, **1995**, *377*, 649-652.

(5) Martick, M.; Lee, T-S.; York, D.M.; Scott, W.G. *Chemistry and Biology* **2008**, *15*, 332-342.